University Of Oxford

D.Phil thesis

Study of two mouse mutants to identify novel neurodegenerative pathways

Mattéa J. Finelli

Linacre College/ Michaelmas 2010

Supervisor: Prof. Kay Davies
Department of Physiology, Anatomy, and Genetics

Mattéa J. Finelli/ Linacre College/ D.Phil/ Michaelmas 2010

Study of two mouse mutants to identify novel neurodegenerative pathways

Abstract:

Neurodegenerative disorders (NDD) are an ever-increasing burden on healthcare; consequently, elucidating the mechanisms underlying neurodegeneration (ND) is critical for the development of effective treatments for these diseases. In order to unravel the molecular pathways underlying movement disorders and identify new genes involved in ND, two ataxic mouse mutants characterised by cell death in the cerebellum were studied in detail using a combination of *in vitro* and *in vivo* techniques.

The *robotic* mouse demonstrated the key role of a transcription factor, Af4, in Purkinje cell (PC) survival and how only small changes in the levels of a single transcriptional cofactor could deleteriously affect normal cerebellum function. Expression array studies of the *robotic* PCs revealed the first confirmed targets of Af4-mediated transcription, including insulin-like growth factor 1 (*Igf-1*). It was demonstrated that Igf-1 is critical for PC survival, highlighting the role of the IGF-1 signalling pathway as a potential therapeutic target for the treatment of cerebellar ataxia in humans.

Detailed analysis of the *bella* mutant demonstrated that ataxia and apoptotic cerebellar degeneration is caused by loss of the oxidative resistance 1 (*Oxr1*) gene. *In vitro* modelling experiments went on to show that the levels of this previously uncharacterised gene are critical for controlling the sensitivity of neuronal cells to oxidative stress (OS). Moreover, this study showed that Oxr1 was up-regulated both in human and pre-symptomatic mouse models of amyotrophic lateral sclerosis (ALS), demonstrating that Oxr1 was an early marker of ROS defence, prior to pathology, and potentially a novel neuroprotective factor in NDD. Preliminary interaction studies show that Oxr1 is likely to be a multi-functional protein that forms complexes with proteins known to be mutated in NDD.

Thus, the study of both the *robotic* and the *bella* mouse has demonstrated the value of the phenotype-driven approach to investigate novel neurodegenerative pathways.

Declaration

The work in this thesis was performed in the Department of Physiology, Anatomy and Genetics. Except where acknowledgement is made, all of the work presented is my own and has not been submitted for any other degree in this or any other University or institute of learning.

Acknowledgements

Labor improbus omnia vincit.

Firstly, thanks to Kay for giving me the opportunity to work in her laboratory and for her support throughout.

Thanks go to Pete for his guidance and the countless discussions we had about the experiments. I also would like to thank him for his constant help for all the cloning, mouse work, and his patience and advice when correcting my manuscripts.

Thanks also go to Emmanuelle for her advice -on Life and Science- from the very beginning and for her help when I had given up hope and when everything seemed impossible.

I would also like to thank Alice and Alastair for all the nice dinners we shared and all the enjoyable conversations.

I sincerely thank all the current and former members of the Davies' lab for their help over the last three years.

And finally a very special thank go to my family for their love and their constant encouragement. *Unus omnes ligat*.

Table of contents

1. Introduction 1

1.1. Neurodegenerative diseases are governed by common mechanisms 1
1.2. Modelling neurodegeneration in vitro and in vivo 7
1.3. Cerebellar ataxia is an heterogeneous neurological disorder characterised by a lack of coordination of muscle movements 10

1.3.1. Classification of ataxias: 10
1.3.1.1. Inherited ataxias: 11
1.3.1.2. Sporadic and acquired non-hereditary ataxias: 13
1.3.2. Current therapies for ataxias: 13
1.4. Cerebellum dysfunction is observed in cerebellar ataxia 15
1.5. Spontaneous and targeted mutant mouse models of ataxia 17
1.5.1. Many mouse mutants of cerebellar ataxia to model an heterogeneous group of disorders 17

1.5.2. Common themes in ataxia: towards new therapies for neurodegenerative disease? 21
1.6. ENU mouse mutants are tools to model movement disorders 25
1.7. The robotic and bella mouse are two mouse models presenting ataxia and specific cerebellar neurodegeneration 27
Robotic 27
Bella 32

2. Material and methods 36

2.1. Material 36
2.1.1. Constructs 36
2.1.2. Antibodies 36
2.1.3. Culture medium 36
2.2. Methods 36
2.2.1. Animal and treatment 37
2.2.2. Laser-capture microdissection (LCM) and RNA extraction 38
2.2.3. Immunohistochemistry and immunofluorescence 39
2.2.4. Chromatin immunoprecipitation (ChIP) 40
2.2.5. Antisera production 41
2.2.6. Protein extraction, cell fractionation, western blotting 41
2.2.7. Cell Culture and treatment for N2As, HeLas, HEK293Ts 42
2.2.8. Primary cell culture and treatment for granule cells (GCs) and cortical cells (CCs) 43
2.2.9. Viral production and primary cell infection 44
2.2.10. Mass spectrometry 44
2.2.11. Tunel assay 45
2.2.12. Catalase assay 45
2.2.13. Thiobarbituric acid reactive substances (TBARS) assay 45
2.2.14. Picogreen assay 46
2.2.15. Statistical analysis 46

3. AF4 as a regulator of the IGF1 signalling pathway during Purkinje cell development 47

3.1. Study of Af4 expression pattern 50
3.1.1. Gene deregulation found by microarray could be confirmed by independently 50
3.1.2. Af4 mRNA level peaks at P14 and then is downregulated at P21 50
3.1.3. Levels of Af4 are dramatically higher in the anterior lobes compared to the posterior lobes and lobe X of the wt cerebellum 51
3.1.4. Af4 accumulates in robotic Purkinje cells at P21 52
3.2. Af4 in the robotic PCs and its role in deregulation of Igf1 gene expression and downstream pathways 54
3.2.1. Igf1 and IgfBP3 expression are downregulated in the organs affected in the *robotic* mouse 54
3.2.2. *Igf1* downregulation in the robotic mouse is conveyed by increased amounts of the Af4 transcriptional complex to *Igf1* gene 56
3.2.3. *Igf1* downregulation in the robotic mouse leads to deregulation of the ERK pathway 58
3.2.4. IGF1 treatment of robotic mouse can slow down Purkinje cell degeneration 59
3.3. Discussion 62
3.3.1. Compartmentalized Af4 expression pattern and regional PC degeneration are correlated 62
3.3.2. Af4 can be a positive or negative transcriptional regulator of a same gene in a tissue-dependent manner 63
3.3.3. Study of the robotic mouse confirmed the crucial role of IGF-1 for PCs survival and its role in non neuronal tissues 67
3.3.4. The mechanism of cell death in the *robotic* mouse is still unclear 70
3.3.5. The study of *robotic* mouse confirmed IGF-1 as a potential for therapy for ataxia 71

4. Investigating the function of Oxr1 in oxidative stress resistance 74

4.1. Study of the *bella* mouse phenotype 77
4.1.1. As a consequence of Oxr1 deletion in the *bella* mouse, *bella* GCs are more sensitive to OS than wild-type GCs 77
4.1.2. DNA damage specifically occurs in *bella* GCs 80
4.1.3. Deregulation of genes involved in the OS response occurs in the *bella* mouse 82
4.2. Role of OXR1 in the OS response in mammalian systems 83
4.2.1. Restoring OXR1 levels can rescue the *bella* phenotype both *in vitro* and *in vivo* 83
4.2.2. Over-expression of OXR1 protects cells against oxidative stress 84
4.3. Oxr1 expression and its functional regulation 85
4.3.1. Oxr1 is expressed under different isoforms in various tissues 85
4.3.2. OXR1 is induced by oxidative stress and is localised to the mitochondria 87
4.3.3. Oxr1 transcription may be regulated by Nrf2 87

4.4. Potential involvement of OXR1 in neurodegenerative disease 89
4.4.1. OXR1 is over-expressed in ALS 89
4.4.2. OXR1 is up-regulated in pre-symptomatic SOD1 mice 90
4.5. Discussion 91
4.5.1. GCs are more susceptible to ROS insults than other neuronal populations 91
4.5.2. Oxr1 may have a role in ALS pathology 92
4.5.3. The pathway in which Oxr1 plays a role is still unknown 93
4.5.4. Oxr1 has common features with key antioxidants linked to NDDs 96

5. The TLDc domain as a functional domain defining a conserved family of eukaryotic proteins 98

5.1. Study of general features of the TLDc domain and its involvement in protecting cells against OS 101
5.1.1. The conserved TLDc domain of Oxr1 is sufficient to confer protection against OS both in vitro and in vivo 101
5.1.2. Ncoa7 can protect cells against OS through its TLDc domain 102
5.1.3. Ncoa7 is induced by OS and is localised to the nucleus 104
5.1.4. A residue in Oxr1 TLDc domain is crucial for Oxr1 function 105
5.2. Study of Oxr1 regulation 106
5.2.1. Oxr1 regulation is not through phosphorylation or glycosylation 106
5.2.2. Oxr1 can form multimers through a residue in its TLDc domain 107
5.3. Study of Oxr1 novel functions 108
5.3.1. Oxr1-FL has many binding partners under OS 108
5.3.2. Oxr1-S has specific binding partners 109
5.3.3. NCOA7-FL and Oxr1-FL have common binding partners 110
5.4. Study of Oxr1 and FUS/TDP-43 interaction 111
5.4.1. Oxr1 binds to FUS and TDP-43 under OS 111
5.4.2. Oxr1 binds to FUS and TDP-43 not through RNA or through a conserved glutamic acid in Oxr1 TLDc domain 112
5.4.3. Oxr1, FUS and TDP-43 form a complex 113
5.4.4. Mutations linked with ALS alter FUS and TDP-43 binding to Oxr1 and their localisation under OS 114
5.5. Discussion 118
5.5.1. Oxr1 and DNA damage 120
5.5.2. Oxr1 and cell cycle 121
5.5.3. Oxr1 and protein folding 122
5.5.4. Oxr1 and RNA processing 122
5.5.5. Oxr1 and microRNA 123
5.5.6. Oxr1 and its shuttling between mitochondria and cytoplasm 124
5.5.7. Oxr1, a multifunctional protein 126

6. Discussion: 127

References 133
Appendix 148

List of figures

Figure 1. Common pathogenic mechanisms underlying many NDDs. 2
Figure 2. Simplified classification of ataxias. 11
Figure 3. The cerebellum, organ of motor coordination. 16
Figure 4. Common pathogenic mechanisms underlying cerebellar ataxias. 23
Figure 5. Progressive adult-onset regions specific Purkinje cell (PC) loss in the *robotic* cerebellum. 30
Figure 6. Af4 is mutated in the *robotic* mouse. 29
Aims for the *robotic* mouse study. 31
Figure 7. Progressive granule cell (GC) death in the *bella* granule cell layer (GCL) of the cerebellum. 33
Figure 8: *Oxr1* is deleted in the *bella* mouse. 35
Aims for the *bella* mouse study. 35
Aims for chapter 3. 49
Figure 9. *Af4* mRNA levels peak at P14 in wild-type cerebellum. 50
Figure 10. Af4 protein accumulates in *robotic* PCs. 53
Figure 11. *Af4* gene expression is not altered in *robotic* PCs. 52
Figure 12. *Igbp-3* gene expression is decreased in *robotic* PCs. 54
Figure 13. *Igf-1* gene expression is altered in neuronal and non-neuronal affected tissues of the *robotic* and *Af4* KO mice. 55
Figure 14. Primers used for ChIP are localised along the *Igf-1* gene. 56
Figure 15. The Af4 transcriptional regulatory complex binds to the *Igf-1* locus in the cerebellum. 57
Figure 16. The AF4 transcriptional regulatory complex binds to the *Igf-1* locus in the thymus and bone marrow at P42. 58
Figure 17. Activation of the IGF-1 signalling pathway is reduced in robotic PCs. 59
Figure 18. Rotarod performances show no difference in fall latency between mice treated with vehicle or IGF-1 at P70. 60
Figure 19. Treatment of *robotic* mice with IGF-1 slows down PC death. 61
Figure 20. Summary: Af4 accumulates in the *robotic* PCs leading to *Igf-1* transcription deregulation. 64
Figure 21. The IGF-1 pathway regulates cell survival. 69
Figure 22. A 193.5kb region is deleted in the *bella* mouse. 74
Aims for chapter 4. 76
Figure 23. Oxr1 regulates sensitivity of GC neurons to oxidative stress (OS) specifically. 78
Figure 24. Oxr1 regulates sensitivity of GC neurons to OS. 78
Figure 25. Primary cortical cells are less sensitive to loss of *Oxr1*. 79
Figure 26. Loss of *Oxr1* induces DNA damage. 80
Figure 27. *Bella* GCs present an increase in DNA damage. 81
Figure 28. Genes involved in the OS-response are deregulated in the *bella* mouse. 83
Figure 29. The *bella* phenotype can be rescued by an *Oxr1* transgene. 84
Figure 30. Oxr1 is highly expressed in the brain, cerebellum, heart and skeletal muscles as various isoforms 86
Figure 31. Oxr1 shuttles between the mitochondrial and cytoplasmic compartment. 88
Figure 32. *Oxr1* could be regulated by Nrf2. 89
Figure 33. OXR1 is overexpressed in ALS and in an ALS-mouse model. 90

Figure 34. Summary: Oxr1 has a role in the OS-response. 95
Aims for chapter 5. 100
Figure 35. Oxr1 confers resistance to OS *in vitro*. 101
Figure 36. The shortest Oxr1 isoform containing the TLDc domain is sufficient to confer resistance to OS *in vivo*. 103
Figure 37. Ncoa7 regulates sensitivity of GC neurons to OS. 103
Figure 38. *Oxr1* and *Ncoa7* are induced by OS. 104
Figure 39. Nco7 is localised to the nucleus under OS. 105
Figure 40. The TLDc domain confers Oxr1 OS-related function. 106
Figure 41. Oxr1 is not phosphorylated or glycosylated. 107
Figure 42. Oxr1 forms a dimer through its TLDc domain. 108
Figure 43. Oxr1 is involved in RNA processing and cell cycle regulation. 110
Figure 44. Targets identified by mass spectrometry analysis in N2A cells were confirmed in the brain (Br) and cerebellum (Cb). 109
Figure 45. Ncoa7-FL is involved in OS-response and RNA processing. 111
Figure 46. Oxr1 interacts with FUS and TDP-43 under OS. 112
Figure 47. Oxr1 does not interact with FUS and TDP-43 through RNA or a conserved glutamic acid residue in Oxr1 TLDc domain. 113
Figure 48. Oxr1-S, FUS and TDP-43 form a complex. 114
Figure 49. Mutations in FUS or TDP-43 alter their interaction with Oxr1. 115
Figure 50. Oxr1 can restore FUS and TDP-43 mutants' localisation. 117
Figure 51. Summary: Oxr1 is a multifunctional protein that can bind to FUS and TDP-43. 120
Figure 52. *Oxr1* is expressed in the adult mouse brain. 130

List of abbreviations

8-OHdG: 8-hydroxydeoxyguanosine
Abra: actin-binding Rho activating protein
AD: Alzheimer's disease
Aif: apoptosis-inducing factor
ALL: acute lymphoblastic leukaemia
ALS: amyotrophic lateral sclerosis
AREs: antioxidant response elements
ATLD: ataxia-telangiectasia-like disorder
ATM: ataxia-telangiectasia mutated gene
ATXN: ataxin
Aβ: β-amyloid
BDNF: brain-derived neurotrophic factor
Bel: bella
BME: basal medium eagle
CCND1: cyclin D1
CCs: cortical cells
CDK9: cyclin dependent kinase 9
CFTR: cystic fibrosis transmembrane regulator
CHD: C-terminal homology domain
ChIP: chromatin immunoprecipitation
CIC: capicua
CIP: alkaline phosphatase
complex I: NADH:ubiquinone oxidoreductase
CoQ10: Coenzyme Q10
dsDNA: double-stranded DNA
EAs: Episodic ataxias
EM: electron microscopy
Endo-H: endoglycosidase
ENU : N-ethyl N-nitrosourea
ER: estrogen receptors
ERK1/2: extracellular signal regulated kinases
ERαbd: estrogen-receptor binding domain
FRDA: Friedreich ataxia
FXN: frataxin
FXTAS: Fragile X-associated tremor/ataxia syndrome
GCL: granule cell layer
GCLC: glutamate-cysteine ligase
GCs: granule cells
GPX: glutathione peroxidise
GST: glutathione S-transferase
H_2O_2: hydrogen peroxide
HD: Huntington's disease
HDAC6: histone deacetylase 6
HEK293T: Human Embryonic Kidney 293T
HeLa: negroid cervix epitheloid carcinoma
Hq: Harlequin mouse
htt: huntingtin
Igf-1: insulin-like growth factor 1
ILOCA: idiopathic late-onset cerebellar ataxia
IRS-1: insulin receptor substrate 1
ISC: iron-sulfur cluster
LCM: Laser-capture microdissection
MEK1/2: MAP Kinases
Mitoch.: mitochondrial
ML: molecular cell layer
MLL (mixed lineage leukaemia)
MSA: multiple system atrophy
mtDNA: mitochondrial DNA
N2A: Neuro2a
Ncoa7: Nuclear receptor coactivator 7
ND: neurodegeneration
NDD: neurodegenerative disorders
NHD: N-terminal homology domain
NLS: nuclear localisation sequence
NLS: nuclear localisation sequence
NQO1:NAD(P)H:quinone oxidoreductase
Nrf2: NF- E2-related factor 2
NTFs: neurotrophins
OS: oxidative stress
Oxr1: oxidative resistance 1
PC: Purkinje cell
Pcd: Purkinje cell degeneration mouse
PD: Parkinson's disease
PI3K: phosphatidylinositol 3-kinase
PKB: Akt/protein kinase B
PKC: protein kinase C
Poly-Q: polyglutamine expansion
qRT-PCR: quantitative real time PCR
RA: retinoic acid
Rob: robotic
ROS: reactive oxygen species
SCAs: spinocerebellar ataxias
SGs: stress granules
Siah: ubiquitin E3 ligase
SMN: survival motor neuron
SOD: superoxide dismutases
Swl: sprawling mouse
TAD: transactivation domain
TBARS: thiobarbituric acid reactive substances
tBHQ: tert-butylhydroquinone
TBP: TATA binding protein
TFIIB: transcription factor
Tg: tottering mouse
Wv: weaver mouse

1. Introduction

Neurodegenerative disorders (NDD) are characterized by progressive and irreversible dysfunction and loss of neurons and synapses in selected areas of the nervous system. They are one of the major burdens on healthcare. Indeed, as the risk of developing these conditions generally increases with age, these diseases are becoming an increasing health issue in ageing populations of developed countries. NDDs including dementia currently cost the NHS more than £23 billion a year, which represents more than cancer and heart disease combined (Luengo-Fernandez, Leal et al. 2010). Therefore, the prevention and development of effective treatments for NDDs represent one of the critical challenges of medical research today.

1.1. Neurodegenerative diseases are governed by common mechanisms

Neurodegeneration (ND) is typically triggered by a combination of genetic, environmental and endogenous factors related to aging but the precise molecular mechanisms leading to ND are not fully understood (Skovronsky, Lee et al. 2006; Jellinger 2010). NDDs are currently classified according to known genetic mechanisms and/or to the major compounds of their protein deposits. Some of the principal pathways associated with the onset and progression of neuronal cell death are discussed below (**Figure 1**).

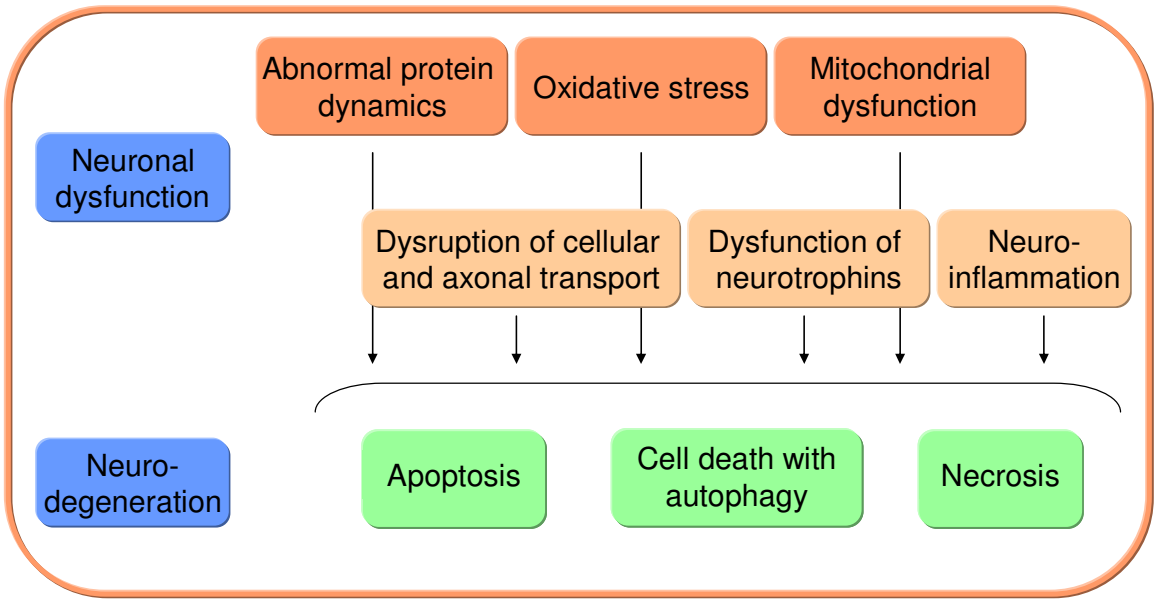


Figure 1. Common pathogenic mechanisms underlying many NDDs. Each mechanism is described in the text.

★ Abnormal protein dynamics

Converging lines of investigation have revealed that aggregation and deposition of misfolded proteins is one of the main common pathogenic mechanisms underlying NDDs. Under non-pathological conditions, newly synthesised proteins are usually folded by molecular chaperones, which also prevent the inappropriate interaction between non-native polypeptides, and promoting the refolding of misfolded proteins as a result of a cellular stress (Frydman 2001). Aberrant proteins may be produced due to production errors, cellular stress or acquired amino-acid substitution, but chaperones and intracellular proteases oversee the protein quality control and remove any misfolded proteins (Hayes and Dice 1996). These unwanted proteins are subsequently degraded through the ubiquitin-proteasome system and the autophagy-lysosome pathway (Reinstein and Ciechanover 2006). However, if aberrant proteins accumulate they are able to form interactions between other misfolded proteins leading to their abnormal deposition and aggregation via distinct precursors (Bauer and Nukina 2009). For example, β-amyloid (Aβ) oligomers are increased in Alzheimer's disease (AD) in brain and plasma (Xia, Yang et al. 2009). Aβ aggregates are ordered oligomers and Aβ oligomerization occurs via distincts

intermediates: oligomers of 3-50 Aβ monomers, annulor oligomers, protofibrils, fibrils and plaques; the most toxic species being the small oligomers (Finder and Glockshuber 2007). Aggregation may happen when a mutation occurs in its sequence or a change in the cellular environment that would lead to the partial unfolding of the protein native state (Zoghbi and Orr 2000; Orr 2004; Bauer and Nukina 2009).

★ Oxidative stress (OS)

OS occurs when the production of reactive oxygen species (ROS), by-products of oxygen metabolism, are produced in excess in the cell. ROS can initiate a cascade of events than can damage DNA, proteins or lipids. The link between OS and cell death/survival is still unclear, although there is still some debate whether ROS are a primary cause or a simply a result of ND (Andersson, Stahlberg et al. 2008; Halliwell 2006). Proteins are the initial targets of ROS, and protein radicals once generated can oxidize reduced gluthatione, which in turn triggers dysregulation of calcium homeostasis, observed in many NDDs (Ballatori, Krance et al. 2010). Oxidative damage to nuclear and mitochondrial DNA may also play a role in the mechanism of ND as they are amongst the earliest detectable signs of AD, Parkinson's disease (PD), and Huntington's disease (HD) (Beal 2006; Wang and Michaelis 2006). Similar observations have been made in normal aging brains implying that OS may have a direct role in the mechanisms of ND (Halliwell and Cutteridge 1985; Halliwell 2006; Halliwell 1992). OS in ND and in NDDs will be discussed in more detail in Chapter 4.

★ Mitochondrial dysfunction

Because mitochondria generate energy for the cell, they play vital roles in the function and survival of neurons. Firstly, deregulation in mitochondrial fission and fusion events have been associated with ND (Frank 2006; Chen and Chan 2009). Moreover, perturbation in the physiological function of mitochondria and mitochondrial DNA (mtDNA) damage are significant components in all NDDs (Mancuso, Orsucci et al. 2008). For example, in HD

and PD multiple mtDNA deletions are observed (Swerdlow, Parks et al. 1996; Banoei, Houshmand et al. 2007). In AD and PD, defects in energy metabolism are related to NADH:ubiquinone oxidoreductase (complex I) deficiency (Bubber, Haroutunian et al. 2005; Lin and Beal 2006; Mancuso, Orsucci et al. 2008; Distelmaier, Koopman et al. 2009). Both Cu/Zn superoxide dismutase (SOD), aggregates found in brains from patients with amyotrophic lateral sclerosis (ALS) and Aβ may contribute to cell death by triggering apoptosis when found in the mitochondria matrix (Borchelt, Davis et al. 1996; Stathopulos, Rumfeldt et al. 2003; Armstrong 2006; Devi, Prabhu et al. 2006).

Additional features of NDD that are likely to be secondary to the pathways outlined above include:

★ **Disruption of cellular and axonal transport**

There is growing evidence that defective neuronal and axonal transport play a mechanistic role in several NDDs (Roy, Zhang et al. 2005; Fischer and Glass 2007; De Vos, Grierson et al. 2008; Morfini, Burns et al. 2009; Vickers, King et al. 2009). For example, huntingtin (htt), the protein disrupted in HD, plays a role in protein trafficking and vesicle transport; thus a loss-of-function of the normal protein and a toxic gain-of-function of the mutant htt contribute to the disruption of multiple intracellular pathways (Gauthier, Charrin et al. 2004). Furthermore, in SOD1 G93A transgenic mice, a model of ALS, retarded transport of neurofilament proteins and deficits in the delivery of mitochondria to the axon were reported prior to the onset of behavioural symptoms (Rothstein 2009). However, it is still unclear if this is a consequence of ND or if it plays an active part in the process of ND.

★ **Dysfunction of neurotrophins (NTFs)**

Reduced levels of NTFs in many NDDs have been observed (Bossers, Meerhoff et al. 2008). As NTFs affect cell survival and influence neuronal plasticity and function, a

decrease in NTFs levels may induce apoptosis (Chao 2003). It is still unclear what is responsible for these reduced levels of NTFs; however, it has been hypothesised that changes in axonal transport may be responsible for the reduction in neuronal NTFs supplies, as NTFs require retrograde and anterograde transport to shuttle from and to targeting neurons (Blesch 2006; Schindowski, Belarbi et al. 2008). For example, in HD, the mutant htt induces a downregulation of brain-derived neurotrophic factor (BDNF) in the basal ganglia, leading to neuronal loss. The involvement of NTFs in ND is still under investigation. Nevertheless, it has already been proposed that NTFs and BDNF could be used as a treatment for HD and other NDDs; but while results have been promising in mouse models, it is still unclear if this strategy could be used in human (Ross and Shoulson 2009; Hathorn, Snyder-Keller et al. 2010; Wu, Hwang et al. 2010).

★ Neuroimmune processes

Many features in NDDs, such as glial cell responses, T-cell infiltration and blood-brain barrier dysfunction, suggest that neuroinflammatory processes may be part of the mechanisms of ND (Stolp and Dziegielewska 2009). Processes of inflammation have been studied in AD and conflicting results have shown that deposition of Aβ could be triggering neuroinflammation, or in the contrary could be useful to dampen the ND itself (Frank-Cannon, Alto et al. 2009; Salminen, Ojala et al. 2009). Thus, the role of neuroinflammation in ND is still unclear and further studies are required to understand the interplay between the nervous system and the local systemic immune system (Galimberti, Fenoglio et al. 2008; McAllister and Van de Water 2009; Piehl and Olsson 2009; Yong and Rivest 2009).

★ Final steps of the cell death cascades

In response to these potential ND pathways, neurons undergo cell death via one of three major mechanisms: apoptosis (gene-directed programmed cell death), necrosis (passive killing of the cell) or cell death with autophagy (Jellinger 2010).

Apoptosis presents nuclear fragmentation, chromatin condensation, cell shrinkage, and plasma membrane bebbling (Wyllie 1997; Elmore 2007). Apoptosis can affect cells locally without having any consequence on the whole tissue (Elmore 2007). The main pathway involved in apoptosis is a cascade of activation of proteases termed caspases (Wyllie 1997; Ribe, Serrano-Saiz et al. 2008).

Cell-death with autophagy is characterised by the formation of numerous autophagic vacuoles, endocytosis and enlargement of the Golgi apparatus that provides a source of lysosomes filled with hydrolytic enzymes that will engulf the endoplasmic reticulum (Gonzalez-Polo, Boya et al. 2005; Winslow and Rubinsztein 2008).

Necrosis is an accidental and uncontrolled cell death and can damage whole tissues and induce an inflammatory response (Golstein and Kroemer 2007). The main players in necrosis are calcium signalling and ROS (Vanlangenakker, Vanden Berghe et al. 2008).

One major factor that determines which type of cell death will be activated is the level of energy in the cell at the time of the insult (Roth and D'Sa 2001; Gorman 2008; Ribe, Serrano-Saiz et al. 2008). For example, apoptosis is favoured under conditions with mild insult and preserved ATP levels, while necrosis is often induced by spontaneous insults with depletion of ATP (Gorman 2008; Ribe, Serrano-Saiz et al. 2008). Mitochondria also play a central part in any mechanism of cell death; indeed, mitochondrial membrane potential is depolarised under stress conditions inducing the release of cytochrome c, which in turn can lead to depletion of energy reserves (which favours necrosis) or activation of the caspase cascade, Bcl-2 and p53 families, and the mitogen-activated protein (MAP) kinase pathway (which favours apoptosis) (Kroemer, Dallaporta et al. 1998; Gorman 2008; Ribe, Serrano-Saiz et al. 2008).

As illustrated by these examples, cell death in neurons is clearly moderated by a complex array of multiple pathways; yet some common themes emerge. However, some of the major questions in NDD research are still to be answered. For example, it is still unclear

why ND often occurs in a highly specific population of neurons despite ubiquitous expression of the disease protein and why there is a long pre-clinical phase in many NDDs although the mutant genes are expressed from birth. In addition, the primary trigger of NDDs, which is crucial in term of therapeutic intervention, is often still unknown (Roth and D'Sa 2001; Cotman 2005; Gorman 2008; Ribe, Serrano-Saiz et al. 2008; Franco 2009). Consequently, modelling ND in cells and in animal models has been utilised to investigate these questions.

1.2. Modelling neurodegeneration *in vitro* and *in vivo*

The analyses of the molecular mechanisms that underlie ND rely heavily on the use of model systems, both *in vitro* and *in vivo*. Cellular models present the advantage of being relatively rapid and low cost; large numbers of cells can be produced easily aiding the reproducibility and practicality of this approach; in addition, primary cell lines can be generated from neuronal tissues or a mutant mouse or human disease biopsy samples, that may be more relevant for the study of basic molecular mechanisms occurring in neurons. For example, cellular models have been a valuable tool for dissecting the molecular function of the genes and proteins implicated in PD such as the role of a novel mutation linked with PD on α-synuclein aggregation, as in this example the mutant α-synuclein was more prone to aggregation than the non mutated one (Moore, West et al. 2005; Pandey, Schmidt et al. 2006). However, one needs to interpret cellular studies with caution, since they can be prone to experimental artefacts. For instance, some cellular processes can be specific to a given cell line or a certain condition of culture and cellular stress or a given stage of cell differentiation, or the number of passages, these being only few of the parameters that can vary in cell culture and which may affect the experimental conclusions. Therefore, particularly when modelling diseases where multiple systems are involved or behaviour needs to be addressed, the ideal approach is to study these cellular

processes in the context of functional neuronal circuits in a whole organism (Dawson, Ko et al. 2010).

Many different model organisms have been used to study ND. Mutants in lower organisms like the fly *Drosophila melanogaster*, nematode worm *Caenorhabditis elegan*s and the zebrafish *Danio rerio* have already proven the importance of using model organisms to study basic biological mechanisms of ND, like protein aggregation and toxicity of misfolded disease-related proteins (Tenreiro and Outeiro; Benzer 1971; Nusslein-Volhard and Wieschaus 1980; Fernandez-Funez, Nino-Rosales et al. 2000; Kazemi-Esfarjani and Benzer 2002; Hirsch 2003; Thompson and Marsh 2003; Ghosh and Feany 2004; Morley and Morimoto 2004; Bonini and Fortini 2006; Kraemer, Schellenberg et al. 2007; Hamamichi, Rivas et al. 2008; Ichibangase, Saimaru et al. 2008; van Ham, Thijssen et al. 2008; Wang, Lao et al. 2009). For example, *C.elegans* worms expressing fluorescent labelled polyglutamine streches, involved in human NDDs like HD or various SCAs, showed a repeat-length dependent- and age-dependent aggregation and toxicity, capturing the inverse correlation between the onset-age of disease and length of repeat expansion seen in human polyglutamine diseases (Morley, Brignull et al. 2002; Morley and Morimoto 2004). Moreover, screens have been used to dissect the response of the fly brain to the insult posed by Aβ expression, and they reported that OS was a particularly significant contributor, which appeared to be true in human (Rival, Page et al. 2009; Moloney, Sattelle et al. 2010). Indeed, these small organisms share at least 30% of their genes with humans and show a strong evolutionary conservation of many complex cellular pathways (Van Ham et al. 2009). Furthermore, genomic manipulation and methods such as genetic modifier screens are faster and cheaper in lower organisms than mammalian systems.

However, to study mammalian gene function in a context of a whole organism, the mouse is frequently used due to its small size, its relatively short generation time as well as the

extensive range of genetic manipulation techniques available. Moreover, sequencing of the mouse genome demonstrated that it shares an average of 85% common genes with human (Denny, Bate et al. 2001). Mouse models have played a crucial role in the study of NDDs based on the introduction or deletion of normal or mutated disease genes (Heintz and Zoghbi 2000; Hafezparast, Ahmad-Annuar et al. 2002). Accurately modelling late-onset NDDs can still be problematic. In reality, the lifespan and developmental profile in mice are very different from humans, and aging studies in mice are time-consuming and expensive. However, one of the main advantages of using mouse models is that early, pre-symptomatic markers of disease can be identified and analysed, markers that could not be inferred by observations of human post-mortem tissues.

Considering the great similarity between human and mouse genomes, it has been predicted that engineering the same genetic defect in the mouse that causes a human neurological disorder is likely to result in a similar phenotype. For this reason, mice have been used to explore the pathological significance of a putative target gene in neurological disorders and to generate disease models that resemble the human pathological state. The SOD1 mouse models for ALS are good examples of such a successful strategy. They have been generated by overexpressing mutant G93A SOD1 present in ALS patients, and these mutants replicate many of the key features of the disease in humans (Gurney, Pu et al. 1994). This has been a popular disease model, although it is important to consider that the very early onset of pathology in this mutant is very different from the late-onset of SOD-related ALS; for example, in the high-copy G93A SOD1 mouse the first signs of the disease occurs at 3-4 months and continues for another 1-2 months (Gurney, Pu et al. 1994; Turner and Talbot 2008). Unfortunately, not all mouse ND mutants are able to replicate all the key aspects of human phenotype and therefore multiple models using differing approaches have been necessary (Dawson, Ko et al. 2010; Kokjohn and Roher 2009). Early models of Parkinson's disease (PD) were based on the administration of toxins that selectively degenerated dopamine neurons

(Hamre, Tharp et al. 1999; Dauer and Przedborski 2003; Bové, Prou et al. 2005; Banerjee, Starkov et al. 2010). These models have been then used to screen potential neuroprotective agents, but unfortunately none of the agents identified using these mutants has shown to be efficacious in PD patients (Dawson, Ko et al. 2010). This failure demonstrated that these PD-intoxication models could not be used reliably as PD models to screen for new therapeutics as they could not replicate the features and the complexity of the PD phenotype i.e. dopamine neuron loss combined with motor dysfunction, Lewy bodies and Lewy neurites that contain α-synuclein and ubiquitin-proteasomal proteins (Ravina, Fagan et al. 2003; Dawson, Ko et al. 2010). Since the discovery of genes linked to PD, more recent models have therefore been based on known pathogenic mutations (Beal; Dawson, Ko et al. 2010). Indeed, mouse models with mutations in LRRK2 and α-synuclein, (linked with autosomal-dominant PD) and mutations in parkin, DJ-1 and PINK-1, (responsible for autosomal recessive PD) have been generated, each model focusing on one aspect of the molecular mechanisms behind PD (Abeliovitch, Schmitz et al. 2000; Chandra, Fornai et al. 2004; Albrecht 2005; Forman, Lee et al. 2005; Savitt and Dawson 2006; Kitada, Pisani et al. 2007). The obvious complexity of NDDs means that generating a 'perfect' mouse model may be impossible, but combining data from a range of mutant lines, in concert with human and cellular data is crucial for the study of the molecular mechanisms involved in ND, and for the identification and testing of new therapeutic strategies.

1.3. Cerebellar ataxia is an heterogeneous neurological disorder characterised by a lack of coordination of muscle movements

One significant group of NDDs with no known treatment are the cerebellar ataxias. These are a group of heterogeneous conditions that can affect medial zone, intermediate zone or lateral zone of the cerebellum (Manto 2008). Ataxia results from the degeneration of the

cerebellum itself or from a combination of cerebellar and extra-cerebellar lesions. Ataxia is generally a highly debilitating disease; patients will usually become wheelchair bound and also need gastrostomy when swallowing difficulties worsen. There are many different types of ataxias, including inherited and sporadic forms, as summarised below (**Figure 2**).

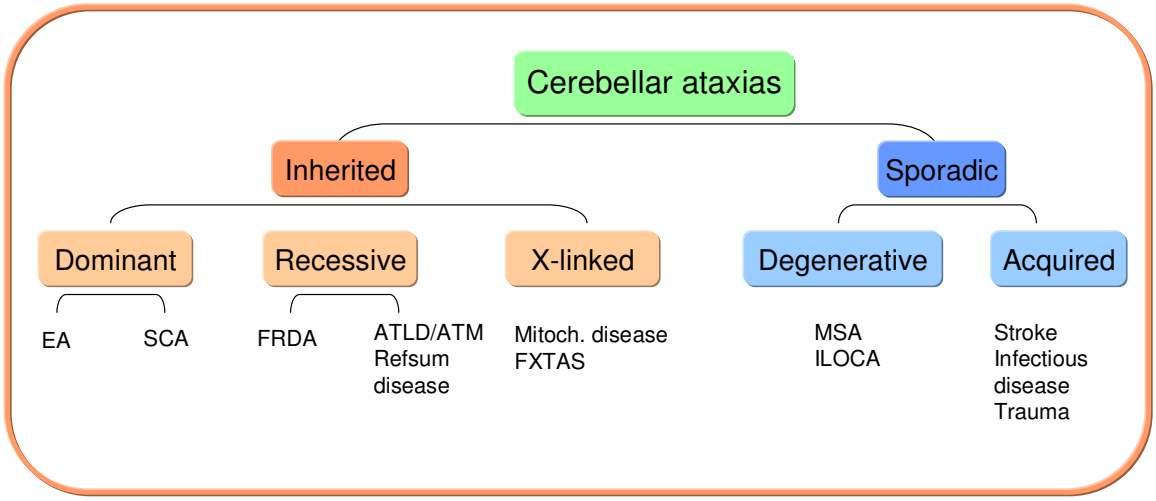


Figure 2. Simplified classification of ataxias. Ataxia, which means 'lack of order', is a neurological condition that consists of gross lack of coordination of muscle movements. Ataxia is due to dysfunction of the parts of the nervous system that coordinate movement, such as the cerebellum. Several possible causes exist for these patterns of neurological dysfunctions: it can be non-hereditary (or sporadic) due to drugs or exogenous substances or hereditary (inherited). Few examples are given for each type of cerebellar ataxia and they are discussed in the text. EA: Episodic ataxias**;** SCA: spinocerebellar ataxia; FRDA: Friedreich ataxia; ATLD/ATM: ataxia-telangiectasia-like disorder/ ataxia-telangiectasia mutated gene; Mitoch.: mitochondrial; FXTAS: Fragile X-associated tremor/ataxia syndrome; MSA: multiple system atrophy; ILOCA: idiopathic late-onset cerebellar ataxia.

1.3.1. Classification of ataxias

1.3.1.1. Inherited ataxias

★ Autosomal dominant ataxias are represented by a group of heterogeneous disorders, including **spinocerebellar ataxias (SCAs)**, affecting 1 to 4 people every 100,000 (Tsuji 2008). They are characterised by specific mutations, the majority of known mutations involving a sequence of CAG trinucleotide repeat expansions leading to progressive

ataxia (Manto and Marmolino 2009). These repeats are associated with abnormal polyglutamine accumulation and formation of nuclear aggregates (Chen, Tang et al. 2008).

Episodic ataxias (EAs) are a group of monogenic disorders. The onset of symptoms is generally in the childhood (Jen, Graves et al. 2007). Anxiety and fatigue increase the susceptibility to an attack (Brusse, Maat-Kievit et al. 2007). EA2 is the most common episodic ataxia and patients present ataxia and vertigo (Jen, Graves et al. 2007).

★ Autosomal recessive ataxias (ARCAs) present dysfunction in other organs like heart, bone, skin, kidney (Filla, De Michele et al. 2000; van de Warrenburg, Steijns et al. 2005). The most common ARCA is **Fredreich's ataxia (FRDA)** with an incidence of 1 in 40,000 (Delatycki, Williamson et al. 2000). Patients present ataxia, motor speech disorder, and an absence of neurologic reflexes such as the knee-jerk reaction. Patients are also usually diabetic and develop cardiomyopathy (Filla, De Michele et al. 2000). FRDA is caused by a GAA triplet in the first intron of the frataxin gene coding for the mitochondrial frataxin (FXN) protein (Campuzano, Montermini et al. 1997; Marmolino and Acqaviva 2009). Patients carrying two expanded GAA repeats show very low levels of mature frataxin mRNA and protein (Sakamoto et al. 2001). Indeed, it has been shown that the GAA expansion induces a heterochromatin state (termed sticky DNA) that decreases histone acetylation and increases methylation and resulting in a partial deficiency of *frataxin* transcription (Becker and Richardson 2001; Gakh, Park et al. 2006).

Coenzyme Q10 deficiency presents cerebellar atrophy, and ataxia and is due to deficiency in the coenzyme Q10 involved in the electron transfer in the mitochondria (Mollet, Giurgea et al. 2007; Montero, Pineda et al. 2007).

Ataxia-telangiectasia is frequent in children, first symptoms starting at 2-8 years old. It is due to a mutation in the Ataxia-telangiectasia mutated (*ATM*) gene involved in DNA repair (Gilad, Chessa et al. 1998; Smirnov and Cheung 2008).

Refsum's disease starts usually in patients in their 20s. It is characterised mainly by malfunction of peripheral nerves throughout the body, progressive blindness, and cerebellar ataxia (Leys, Petit et al. 1989). Other symptoms like deafness, cardiac arrhythmias, renal failure and bony and skin abnormalities have also been reported (Leys, Petit et al. 1989).

★ Mitochondrial ataxias are due to mutations in mitochondrial genes that alter mainly oxidative phosphorylation (Zeviani and Di Donato 2004).

★ X-linked ataxias are rare conditions and are due to a CGG repeat carried on the X-chromosome (Jacquemont, Orrico et al. 2005; Jacquemont, Hagerman et al. 2007). The two main X-linked ataxias are the **fragile X tremor ataxia syndrome** and **Rett syndrome**.

1.3.1.2. Sporadic and acquired non-hereditary ataxias

★ Degenerative ataxias include **multiple system atrophy (MSA)** and **idiopathic late-onset cerebellar ataxia (ILOCA)** (Gilman, Wenning et al. 2008).
★ Acquired ataxias can be mainly caused by stroke (infarction, hemorrhage), infectious diseases (cerebellitis), trauma, and induced by drugs; ethanol being the most common cerebellotoxic agent.

1.3.2. Current therapies for ataxias

Current strategies for treating ataxia are mainly based on addressing the associated symptoms such as altered skeletal muscle performance, Parkinsonism, uncontrolled sustained muscle contractions, bladder dysfunction, and hypotension (Soong and Paulson 2007; Manto and Marmolino 2009; Marmolino and Manto 2009; Mancuso, Orsucci et al.

2010). In the case of SCAs, no therapy has been found to stop the disease progression, although symptomatic improvements have been reported (Yabe, Sasaki et al. 2001; Dressler and Benecke 2005; Palau and Espinós 2006). For example, ataxic tremors may be decrease in SCA6 using acetazolamide; the mechanism of action of acetazolamide is still unclear (Jen, Yue et al. 1998; Yabe, Sasaki et al. 2001). For FRDAs, mainly the cardiomyopatic and diabetic symptoms are currently treated. For instance, drugs are used to reduce cardiac hypertrophy but unfortunately without acting on the progression of ataxia (Schulz, Di Prospero et al. 2009; Mancuso, Orsucci et al. 2010).

In ataxias linked with dietary deficiencies, oral supplementations in the missing element or dietary restrictions are usually sufficient to restore a normal condition: CoQ10 supplementation improves ataxia caused by CoQ10 deficiencies or dietary restriction of phytanic acid can improve Refsum's disease (Wills, Manning et al. 2001; Embiruçu, Martyn et al. 2009). High doses of CoQ10 and N-acetylcysteine were thought to be promising drugs for mitochondrial ataxias as one is part of the respiratory chain and the other is an antioxidant so this combination could potentially reduce oxidative stress accumulating in the cells (Schilling, Coonfield et al. 2001; Ferrante, Shefner et al. 2005; Oliver and Davies 2005; Oliver, Keays et al. 2007). But their efficacy has not yet been proven.

As described above, the treatments currently available for ataxias only relieve a specific subset of symptoms but do not treat the cause of the disease or even the disease progression. The lack of efficient therapies is due mainly to our lack of general knowledge of the molecular mechanisms and pathways involved in cell death in cerebellar ataxias. Therefore, understanding the molecular and developmental mechanisms underlying cell loss in the cerebellum needs to be addressed and may be used to find therapies that could improve the conditions of patients.

1.4. Cerebellum dysfunction is observed in cerebellar ataxias

The cerebellum acts as a coordination centre, using sensory inputs from the periphery to tune movement and balance (Wang and Zoghbi 2001). In mammals, the cerebellum consists of the outer cerebellar cortex, beneath which lies a mass of white matter containing the deep cerebellar nuclei (Inouye and Murakami 1980) (**Figure 3A**). The cerebellum of the mouse is composed of ten lobes consisting of three layers that are made up of distinct cell populations; from inner to outer, the granule (GCL), Purkinje (PCL), and molecular cell layers (MCL) (Ito 1998) (**Figure 3B**). The molecular cell layer (ML) consists of basket cells and outer stellate cells. The Purkinje cell (PC) layer is a monolayer of large PCs, and the granule cell layer contains mainly granule cells (GCs), in addition to Golgi cells. PCs provide the sole cerebellar output projecting their dendrites to the deep cerebellar nuclei (Kandel, Schwartz et al. 2000). PCs receive excitatory inputs from mossy fibres and climbing fibres. The mossy fibres originate from the spinal cord and brain stem, and synapse with GCs. The climbing fibres originate from the inferior olivary nucleus and synapse with PCs. The other cells present in the cerebellar cortex are inhibitory interneurons: basket cells and stellate cells forming synapses with PCs, Golgi cells with GCs (**Figure 3B**).

Importantly, dysfunction of the cerebellum is a feature of many other diseases; not only those that present with motor coordination problems (Manto and Pandolfo 2001; Schmahmann 2004). For example, in addition to ataxia, SCA patients, often present impaired executive functions, deficits in short-term memory, and mild, generalized cognitive impairment, and sometimes depression and personality changes (Geschwind 1999; Bürk, Bäsch et al. 2001; Bürk, Globas et al. 2003; Paulson 2009; Teive 2009). For example, 80 to 90% of patients with SCA17 present cognitive impairment (Fujigasaki,

Martin et al. 2001; Manto 2008). Defects in cerebellar structure have also been described in patients with early infantile autism; indeed they present enlarged IV ventricles, loss of PCs in the lateral and inferior cerebellar cortex, and abnormal or reduced numbers of neurons in the deep cerebellar nuclei (Bauman and Kemper 1985; Ritvo, Freeman et al. 1986; Courchesne, Piven et al. 1999; Allen 2005; Fatemi, Reutiman et al. 2008).

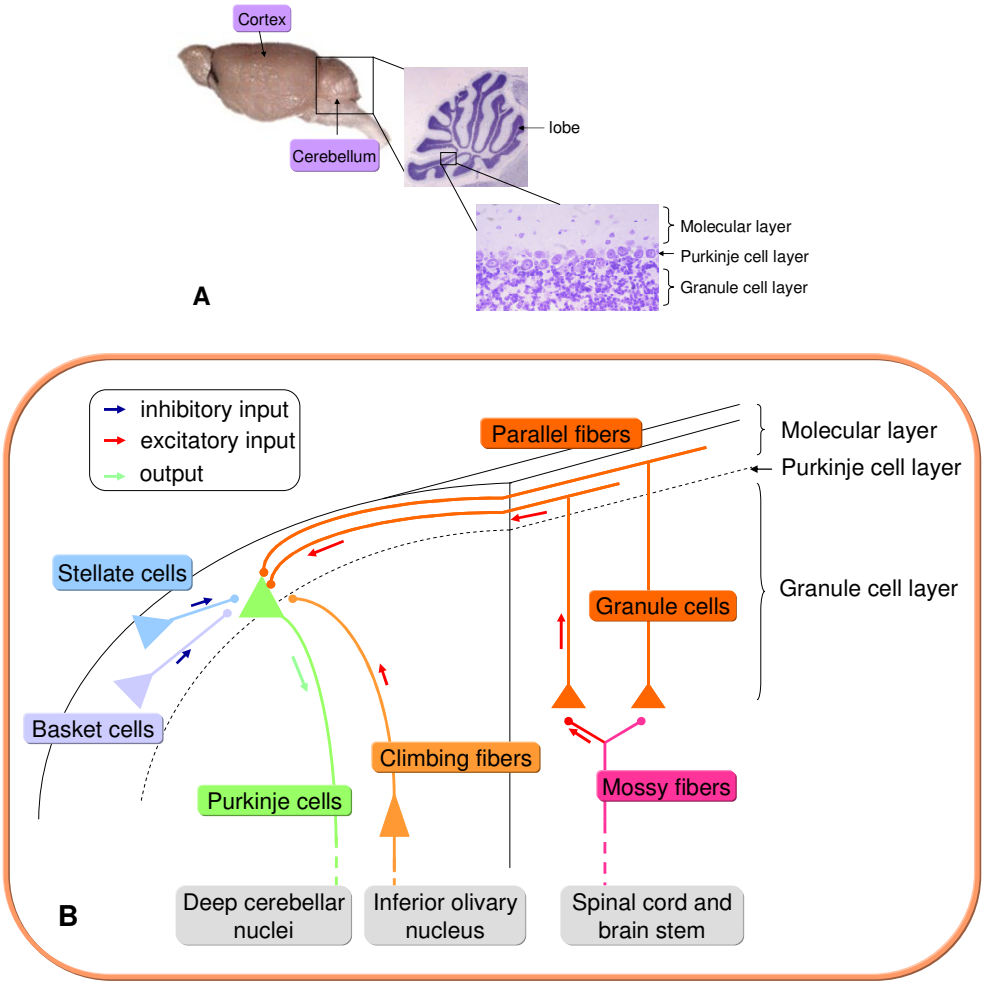


Figure 3. The cerebellum, organ of motor coordination. (**A**) The mouse cerebellum contains 10 lobes as showed on the parasagittal section stained with cresyl violet. The cerebellar cortex presents three layers: the molecular layer, the Purkinje cell (PC) layer, and the granule cell layer. (**B**) The schematic represents the cerebellar inputs and outputs. Inputs arrive from the brain stem and spinal cord and are modulated in the cerebellum before an output goes from the PC to the deep cerebellar nuclei. PCs receive excitatory inputs from mossy fibres and climbing fibres. The other cells present in the cerebellar cortex are inhibitory interneurons. Basket cells and stellate cells both synapse with PCs. The excitatory inputs are shown by red arrows, while inhibitory inputs are shown in blue.

Similarly, cerebellar vermal lobules VIII through X are smaller in patients with bipolar disorder who experienced multiple episodes of depression (Baldaçara, Borgio et al. 2008; Monkul, Hatch et al. 2008). Brain MRI scans of PD patients also show abnormal cerebellar structure (Bhattacharya, Saadia et al. 2002). Thus the cerebellum is not only for regulation of motor coordination but also for higher cognitive functions. The role of the cerebellum in the modulation of complex behaviour remains to be established, but the examples above emphasize that the study of the cerebellum development and function is relevant to not only ataxia but may help us understand some of the symptoms of complex behavioural disorders.

1.5. Spontaneous and targeted mutant mouse models of ataxia

1.5.1. Many mouse mutants of cerebellar ataxia to model an heterogeneous group of disorders

Initial studies of movement disorders in mouse models in the 1970s were based on spontaneous mutants that displayed ataxic phenotypes. At the time of discovery, these mutant lines were well characterized pathologically, but the genetic lesions responsible for the phenotypes have not been discovered until the advent of positional cloning and DNA sequencing (Harper et al. 2010).

The weaver (*wv*) mutant presents a defect in cerebellar GCs migration followed by a selective degeneration of dopaminergic neurons in the substantia nigra as well as PC abnormalities (Rezai and Yoon 1972; Rakic 1973; Marti, Santa-Cruz et al. 2009). The causative mutation (G953A) was eventually identified in the *Girk2* gene encoding for a subunit of a G-protein-activated inwardly rectifiying K^+ channel, leading to a gain-of-function of the channel. The mutant channel is characterised by loss of its cationic

selectivity, a constitutively active form and its inability to be activated by G-proteins (Patil, Cox et al. 1995; Kofuji, Hofer et al. 1996; Navarro, Kennedy et al. 1996; Liss, Neu et al. 1999). Moreover, it was demonstrated in *wv* mouse that the pathway leading to cerebellar GC death involved caspases both *in vitro* and *in vivo*, suggesting that ND in the *wv* mouse was through an apoptotic mechanism (Peng, Wu et al. 2002).

Another mutant, the tottering (*tg*) mouse, has seizures but a normal viability (Noebels and Sidman 1979). It also exhibits intermittent movement disorders similar to forms of epilepsy, and cerebellar ataxia (Noebels and Sidman 1979). The involvement of the cerebellum and PCs in the ataxic phenotype has been extensively studied (Hess and Wilson 1991; Abbott, Bump et al. 2000; Otis and Jen 2006; Chen, Popa et al. 2009). An allelic series of mutations in the gene coding for the calcium channel subunit α1A (Leaner tg^{la}, Ducky tg^{du}, Nagoya tg^{rol}, *tg-4J*, *Tg5J*) has been described (Barclays, Balaguero et al. 2001; Barclays 2001, Fletcher 1996). Comparison of the various phenotypes displayed by the tottering mutants, from subtle to severe degeneration of PCs of the cerebellum, can provide valuable comparative functional information (Tsuji and Meier 1971; Herrup and Wilczynski 1982; Heckroth and Abbott 1994; Fletcher, Lutz et al. 1996; Miki, Zwingman et al. 2008; Sawada, Kalam Azad et al. 2009). Indeed, the various *tg* mutants have been used as models of human ataxias, both spinocerebellar ataxia 6 (SCA6) and episodic-ataxia type-2 (EA2), and epilepsy to understand the molecular mechanisms underlying these disorders but more importantly to design and test therapeutics (Jouvenceau, Eunson et al. 2001; Strupp, Kalla et al. 2004; Weisz, Raike et al. 2005; Jen, Graves et al. 2007; Watase, Gatchel et al. 2007; Bauer and Nukina 2009). It should be noted that at the time when the first *tg* mouse was identified, no known mutations in human has been linked to SCA6 or epilepsy. It is only much later that similar mutations/disruptions in the same potassium channel involved in the *tg* mice were detected in human SCA6 and various forms of epilepsy, reviving the study of the *tg* mouse (Du, Bautista et al.; Noebels

and Sidman 1979; Ophoff, Terwindt et al. 1996; Riess, Schöls et al. 1997; Toru, Murakoshi et al. 2000; Jouvenceau, Eunson et al. 2001; Spacey, Hildebrand et al. 2004).

Another example, the Purkinje cell degeneration (*pcd*) mouse, displays a combined cerebellar and retinal degeneration (Mullen, Eicher et al. 1976). It exhibits normal development and structure of the cerebellum until a sudden and dramatic PCs degeneration, with almost total loss from P35, leading to a profound ataxic phenotype even though the mice present a normal lifespan (Mullen, Eicher et al. 1976). Several different *pcd* alleles (1J to 7J) have arisen and one transgene insertion allele (pcd^{JWG}) has occurred (Krumewski, Neumann et al. 1989; Fernandez-Gonzalez, Spada et al. 2002; Chakrabarti, Neal et al. 2006). Mutations in the *Nna1* gene have been linked to the *pcd* phenotype (Chakrabarti, Neal et al. 2006). The *Nna1* gene encodes for a putative protease -a zinc carboxypeptidase- that is highly conserved in various species, ranging from worms to humans, but its function is still unknown (Harris, Morgan et al. 2000; Fernandez-Gonzalez, Spada et al. 2002; Chakrabarti, Neal et al. 2006; Li, Gu et al. 2010). Interestingly, *in situ* hybridizations have shown that the pattern of *Nna1* expression corresponds to the pattern of ND (Harris, Morgan et al. 2000). Few groups have performed microarray analysis from *pcd* and wild-type whole cerebella at various time points, especially at the onset of PCs degeneration, in order to identify genes that may initiate ND (Ford, Ford et al. 2008; Chakrabarti, Eng et al. 2009; Chakrabarti, Zahra et al. 2010). Moreover, a recent study showed an increased in autophagy pathway activity in *pcd* PCs as well as mitophagy; it has been concluded that dysregulation of autophagy and increased or aberrant mitophagy may be responsible for PC death in *pcd* mouse (Chakrabarti, Eng et al. 2009; Chakrabarti 2009). Understanding the mechanisms leading to retinal-cerebellar degeneration may be of great interest as a number of neurological diseases are characterized by similar phenotypes (Martin, Krols et al. 1994; Gouw, Kaplan et al. 1995; Abe, Abe et al. 1997).

Taken together, the mouse mutants described above have shown that related phenotypes can be attributed to a range of neurodegenerative mechanisms like altered K^+ or Ca^{2+} channel function (*wv*, *tg*) or defects in neuronal bioenergetics (*pcd*). They also display common themes related to the mechanisms of cell death in the cerebellum, including morphologic abnormalities in mitochondria as well as activation of the Bcl-2 family members and caspases (Selimi, Doughty et al. 2000; Ebadi, Sharma et al. 2004; Bäurle, Kranda et al. 2006; Bawa and Abbott 2008; Chakrabarti, Zahra et al. 2010).

Since the identification of human mutations that cause movement disorders and advances in mouse genetics, it has been possible to generate targeted transgenic and knockout mouse models of ataxia; in addition to the spontaneous mutants, these engineered models have been powerful tools used to understand the mechanisms underlying NDDs. For example, this targeted approach has been used to generate mouse models for FRDA and SCA1. After the discovery of the triplet repeat expansions in the genes (*frataxin* and *ataxin-1*, respectively) (Chamberlain, Shaw et al. 1988; Kwiatkowski, Orr et al. 1993); mice were generated expressing these human disease sequences controlled by a promoter targeting expression specifically to the cells affected in patients (Orr, Chung et al. 1993; Cossée, Schmitt et al. 1997; Puccio, Simon et al. 2001). This SCA1 mouse has similar symptoms to human patients, including atrophy of PC dendrites, ataxin-1 (ATXN1) nuclear aggregates and an ataxic gait indicating it constitutes a good model for SCA1. Frataxin mouse mutants, however, do not accurately recapitulate the pathophysiology of FRDA, although they have been used to dissect the function of FXN, its role as a mitochondrial iron-chaperone and its involvement in iron-sulfur cluster (ISC) biogenesis (Calmels, Schmucker et al. 2009; González-Cabo, Espinós et al. 2009).

1.5.2. Common themes in ataxia: towards new therapies for neurodegenerative disease?

Ataxia is complex to study as it is a heterogeneous group of disorders. However, ataxias display similar ND pathways to more common NDDs (**Figure 4**); therefore models of ataxia can be used to understand more general neurodegenerative mechanisms. For example, it has been shown that SCA1, like HD, is caused by poly-Q repeat expansions (in ATXN1 or htt, respectively), leading to the misfolding of these proteins and subsequent neurotoxic effects. Consequently, the similarities between SCA1 and HD were used to infer that therapies that have been showed to be efficient in HD would be efficient in SCA1 (Xia, Mao et al. 2004; Huen, Wong et al. 2007). Prevention of protein aggregation in SCA1 was achieved by overexpressing chaperones such as heat-shock protein HSP70 or DNAJ1 *in vivo* in a mouse model of SCA1, as done previously in HD models (Smith, Whitesell et al. 1998; Cummings, Sun et al. 2001; Huen, Wong et al. 2007). This strategy suppressed neuropathology and improved motor function in SCA1 mice. Another strategy was to silence the mutant *ataxin-1* gene using AAV vectors injected at multiple sites in the midline cerebellar lobules of a SCA1 mouse expressing the human ataxin-1 disease allele in cerebellar PCs (Xia, Mao et al. 2004). This strategy using long lasting RNA interference (RNAi) -mediated gene silencing in viral vectors showed promising results in SCA1 model, with a successful target gene suppression and a significant improvement in motor performance (Xia, Mao et al. 2004; Farah 2007; Gonzales-Alegre 2007; Paulson 2009).

Other approaches target the mode of neuronal cell death that occurs. In the case of FRDA, pharmacological compounds such as antioxidants or iron chelators were proposed to improve FRDA condition in regard of what was known at the molecular level on the disease. Indeed, Fe-S enzyme deficiency followed by intra-mitochondrial iron deposits is observed in both FRDA patients and in mouse models of the disease (Puccio and Kaënig

2000; Schmucker and Puccio 2010). A small number of compounds are already in clinical testing after giving promising results in mouse models of FRDA (Cooper and Schapira 2003; Seznec, Simon et al. 2004; Hart, Lodi et al. 2005; Cooper and Schapira 2007; Pandolfo 2007).

As an example of the more general applicability of ataxic mutants for NDD research, the *tg* mouse has been used to find new drugs to treat human epilepsy (Heller, Dichter et al. 1983; Imbrici, Jaffe et al. 2004; Weisz, Raike et al. 2005; Kalla, Glasauer et al. 2007). Indeed, the study of the *tg* mouse highlighted the importance of Ca^{2+} flux in PCs survival (Otis and Jen 2006; Watase, Barrett et al. 2008; Teive 2009). These findings suggested that drugs targeting the calcium channel affected in the *tg* mouse could potentially restore the normal PC function and improve the ataxic phenotype, both in mouse and human cases of EA2. Drugs (e.g. 4-AP and aminopyridines) previously selected and tested in the *tg* mouse were then tried successfully in human (Jouvenceau, Eunson et al. 2001; Strupp, Kalla et al. 2004; Weisz, Raike et al. 2005; Jen, Graves et al. 2007). A similar approach has been used to find new drugs to treat human epilepsy (Heller, Dichter et al. 1983; Imbrici, Jaffe et al. 2004; Weisz, Raike et al. 2005; Kalla, Glasauer et al. 2007). Another advantage of such mouse mutant is that it can be used to optimise therapeutic treatment by dissecting the mechanisms of action of a given drug, mechanisms which are often unclear (Alvina and Khodakhah 2010).

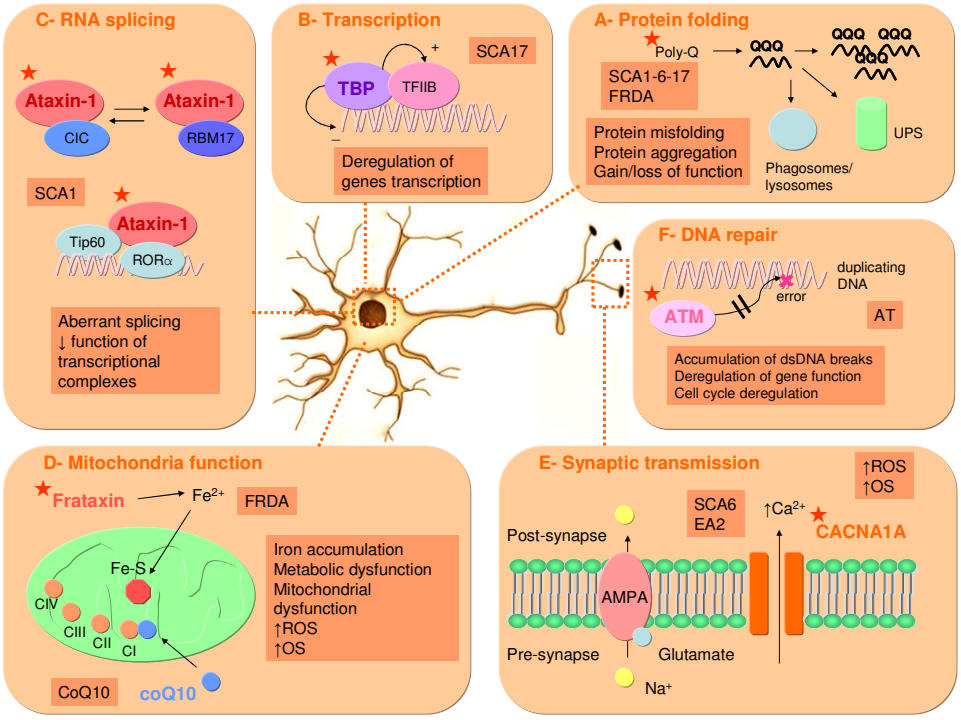


Figure 4. Common pathogenic mechanisms underlying cerebellar ataxias. All the examples showed on this figure are discussed in the text. (**A**) One common mechanism to almost all cerebellar ataxias is protein misfolding and aggregation due to a mutation occurring in a given gene or more frequently due to the addition of a polyglutamine expansion (poly-Q) to a protein. This protein misfolding leads to loss- or gain-of function of the protein and its aberrant function and neurotoxic effects. (**B**) The expression of genes can be deregulated in cerebellar ataxias. SCA17 is caused by polyglutamine expansion in the basal transcription factor TATA binding protein (TBP). Its expanded polyglutamine tract reduces the ability of TBP to dimerize (a regulation mechanism) and increases its binding to the general transcription factor (TFIIB), leading to gene expression deregulation, especially genes coding for neuroprotective factors. (**C**) Mutation or poly-Q tract can affect proteins involved in RNA splicing. The cellular function of ataxin-1 (ATXN1), the protein mutated in SCA1, remains unclear; however, research implicates ATXN1 in RNA splicing. In mouse, ATXN1 is stably associated into two different, large protein complexes: one containing the transcriptional repressor capicua (CIC) and one containing the mRNA splicing factor RBM17. *In vivo*, more wild-type ATXN1 is associated with CIC than with RBM17. By contrast, mutant ATXN1 preferentially associates with RBM17 leading to aberrant splicing of important genes affecting neuronal function and survival. Moreover, a decrease in ATXN1/CIC complexes may subsequently lead to reduced function of these transcriptional complexes within the cell. ATXN1 also transiently interacts in a complex with RORα, involved in PC development and maturation, and the transcription factor Tip60. However, expression of mutant ATXN1 leads to a decrease in both RORα levels and the transcription of a number of RORα regulated genes and cell death. (**D**) The gene associated with FRDA is a small mitochondrial protein called frataxin. The most common mutation in FRDA cases is a GAA triplet-repeat expansion within the *frataxin* gene leading to a reduced transcription of the gene. This leads to an accumulation of iron in the mitochondria, a deregulation of iron metabolism and Fe-S cluster biogenesis; enzymes found in Complex I and II of oxidative phosphorylation and involved in the oxidation-reduction reactions of mitochondrial electron transport. (**E**) Afferent inputs to PCs are mediated by glutamate stimulation of ionotropic AMPA-type glutamate receptors causing local depolarization of dendritic spines and activation of voltage gated calcium channels. However, in SCA6 and EA2, the poly-Q tract in the CACNA1A subunit of the voltage gated calcium channel type P/Q Cav2.1 leads to an increase in dendritic calcium spikes and downstream action potentials. (**F**) Mutations in the ataxia-telangiectasia (ATM) gene alters its function in protecting DNA from insults leading to an increase in DNA damage and cell death. EA: Episodic ataxias; SCA: spinocerebellar ataxia; FRDA: Friedreich ataxia; ATM: ataxia-telangiectasia mutated gene; AT: ataxia-telangiectasia; CoQ10: coenzyme deficiency disease.

Secondly, the *wv* mouse has be utilised as a model for PD and assisted in the selection of potential new therapeutics. Indeed, as the *wv* mouse presents a similar pattern of degeneration of a same subpopulation of dopaminergic midbrain neurons as in PD, it was inferred that the sequences of cellular events leading to selective neurodegeneration converged at a point downstream of an initial trigger mechanism and that the *wv* mouse could be used as a model for PD (Graybiel, Ohta et al. 1990). It was hypothesised that degeneration of dopaminergic neurons in *wv* was mediated via neuroinflammation, therefore *in vivo* administration of the anti-inflammatory agent minocycline was tested. This approach was deemed successful in that it attenuated nigrostriatal dopaminergic degeneration. These data suggested that similar methods targeting neuroinflammation in PD would be worth pursuing (Qian, Flood et al.; Hunot and Hirsch 2003; Gao, Sun et al. 2008; Hirsch and Hunot 2009). The *wv* has also been used as a model for PD to test potential transplantation of dopaminergic neurons to restore normal brain function (Triarhou 2002). A similar strategy has then been tested in two cases of human PD with very promising results as transplantation in the striatum and substantia nigra of PD patients of dopamine neurons provided specific dopaminergic reinnervation to the most affected striatal regions in the patients brain (Mendez, Sanchez-Pernaute et al. 2005). This mouse mutant is a good example of how a point mutant selected for its interesting phenotype can be subsequently used as a valuable model of a human neurological disease.

In conclusion, mouse mutants continue to provide vital insights into the function of the cerebellum and the pathological mechanisms of ataxia. More importantly, they also have been used to test and develop new therapeutic strategies to combat movement disorders.

1.6. ENU mouse mutants are tools to model movement disorders

The combination of spontaneous and targeted mouse mutants has been a valuable approach to identifying treatments for ataxia, although there are still many pathogenic genes that have no related mouse mutant line; in addition, a null allele may not always represent the most suitable model; this problem is not restricted to NDDs but being the case for all human diseases. Therefore, to close this apparent 'phenotype-genotype gap' between the number of genes and the number of mutant alleles available, several groups established random mutagenesis programmes in the late 1990s to generate large numbers of novel mouse mutants combined with an initial broad-based phenotyping screen (Nolan, Peters et al. 2000; Brown and Balling 2001). As mouse models of movement disorders are likely to display clearly observable phenotypes, this approach is a practical method of identifying new models of ataxia.

The mouse mutagenesis programme conducted at the MRC Mammalian Genetics Unit in Harwell, U.K., uses the alkylating agent N-ethyl N-nitrosourea (ENU) to induce germ line single random point mutations in male mice. These males are then bred with wild-type females resulting in offspring subsequently analysed directly for dominant mutations, or used for a second or third generation of breeding for the identification of inherited recessive traits (Nolan, Peters et al. 2000). The offspring is screened to identify neurological and behavioural phenotypes (Rogers, Fisher et al. 1997). When screening for neurological mutants, several parameters are assessed, including gait, posture, motor control and coordination. Once mendelian inheritance and penetrance of the trait of interest have been determined, the mutation is identified by genetic mapping and sequencing of candidate genes (Acevedo-Arozena, Wells et al. 2008). One advance of such strategy is that the mutation occurs in an endogenous copy of a gene so there are no issues with copy number or positioning as there are with an inserted transgene. In

addition, no assumptions are made about the type of mutations or genes that will be identified, leading to an unbiased search for phenotypes of interest (Oliver and Davies 2005). One of the main disadvantages of the ENU strategy is that it is time consuming to identify the mutation by positional cloning, and potentially only overt observational phenotypes will be identified using this strategy, potentially missing out more subtle or variable traits (Oliver and Davies 2005; Oliver, Keays et al. 2007; Acevedo-Arozena, Wells et al. 2008).

Another advantage of ENU mutants is that potentially different mutations can be generated in a same gene, producing an allelic series, as discussed previously with the spontaneous *tg* mouse. A combination of such mutants is more likely to provide information related to gene dosage, or to identify functionally important protein interacting domains, than a classical gene knockout (Oliver and Davies 2005; Oliver, Keays et al. 2007). They may be of particular interest for *in silico* drug designing to target specific residues of an active site of a disease protein or drug screening to find compounds that could improve the phenotype by altering the activity of proteins rather than eliminate their function (Russ, Stumm et al. 2002).

The focus of work in the Davies' group has been to identify new models of movement disorders. Because gait defects are a feature of the primary ENU phenotypic screen, new mutants are identified relatively easily by observation as opposed to relying on biochemical or detailed behavioural analyses. Once a new mutant is identified and inheritance has been confirmed, a pathological screen is carried out, including analysis of the central and peripheral nervous system. This is a vital additional step in the screening process that facilitates the selection of positional candidates as well as directing future work on the mutant. Initial studies in the Davies' group concentrated on an allelic series of mutations in peripheral myelin protein Pmp22, causing peripheral neuropathy (Isaacs, Davies et al. 2000). These mutants demonstrated that not only several ENU-induced

mutations in the same gene can provide valuable and directly comparable functional information, but also that mutations directly relevant to human disease can be identified (Isaacs, Davies et al. 2000). The work in this thesis focuses on two ENU mutant models of movement disorders, both with cerebellar ND.

1.7. The *robotic* and *bella* mouse are two mouse models presenting ataxia and specific cerebellar neurodegeneration

This project will focus on the dominant *robotic* and the recessive *bella* mouse models as both provide opportunities to dissect the molecular mechanisms underlying ND in relation to movement disorders. Both lines were originally identified from the Harwell ENU screen based on their jerky, ataxic gait. They also display cerebellar degeneration and general growth retardation; however they differ in the disease progression and cell type affected. The aim of the work presented in this thesis is to understand the neurodegenerative pathways that cause ataxia in these two mutants.

Robotic

The robotic mouse was identified as one of the earliest mutants from the Harwell mutagenesis screen in 1998. At that time, all offspring from the breeding of an ENU treated Balb/c male to C3H females were screened using the SHIRPA behavioural test battery to identify abnormal dominant phenotypes in the F1 population, in addition to information gathered from general observation by animal technicians (Rogers et al. 2000). The ataxia and the low body weight of the *robotic* mouse were clearly detectable without SHIRPA testing and importantly the penetrance of the phenotype was high, facilitating genetic mapping. The line was maintained by backcrossing male robotic (Rob/+) mice to wild-type C3H females (F2 population).

Further histological analysis of *robotic* brain sections performed in the Davies' group revealed degeneration of PCs in the cerebellar vermis from 3 to 4 weeks of age with progressive cell loss from 8 weeks (Isaacs, Oliver et al. 2003; Oliver, Keays et al. 2007) (**Figure 5**). Mice also display bilateral cataracts that are visible from 2-3 months of age (Isaacs, Oliver et al. 2003).

The initial genome scan was carried out using polymorphic microsatellite markers, followed by fine mapping on chromosome 5 using over 400 animals from the backcross population. In the absence of a completed genomic sequence, bacterial artificial chromosomes (BACs) spanning the critical region were identified by BAC library colony hybridiation and genes within these clones identified by exon trapping (Isaacs et al. 2003). Two new genes, *Klhl8* and *Hsd17b12* were identified in addition to *Af4*. After sequencing these three genes, the robotic mutation in *Af4* was the only mutation found; since completion of the mouse genome, the position and size of the candidate genes identified was confirmed. Thus, the gene responsible for the *robotic* mouse phenotype was identified as a T to C transition at nucleotide 839 of the *Af4* gene coding for the AF4/FMR2 family member 1, leading to a valine to alanine substitution at position 280 (V280A) in Af4 (Isaacs, Oliver et al. 2003). Af4 is characterised by a highly conserved ALF domain in which the *robotic* mutation lies. Af4 is part of the ALF (AF4/LAF4/FMR2/A5q31). AF4, LAF4 and AF5q31 were originally cloned due to their fusion with mixed lineage leukaemia (MLL) in different chromosomal translocations causing acute lymphoblastic leukaemia (ALL), whereas FMR2 is mutated in X-linked mental retardation (Hiwatari, Taki et al.; Taki, Kano et al. 1999; Gecz 2000; Chinen, Taki et al. 2007).

Despite their limited homology over their entire amino acid sequences, the ALF proteins share five highly conserved domains (**Figure 6A**): a N-terminal homology domain (NHD), a ALF domain, a acid serine-rich region (pSer), a consensus bipartite nuclear localisation sequence (NLS), and a C-terminal homology domain (CHD) (Nilson, Reichel et al. 1997).

Moreover, they all share a conserved minimal transactivation domain (TAD) establishing the potential function of the ALF family members as transcription factors (Prasad, Yano et al. 1995; Ma and Staudt 1996; Hillman and Gecz 2001; Estable, Naghavi et al. 2002). Af4 is expressed at very low levels in the CNS, although it is highly expressed in PCs in the cerebellum (Isaacs, Oliver et al. 2003). Af4 turnover is regulated by its binding to ubiquitin E3 ligase (Siah-1 and -2) proteins which catalyse Af4 ubiquitination and proteasome-dependent degradation. However, the *robotic* mutation lies in a conserved motif which alters the consensus binding motif for Siah proteins, resulting in a significant reduction of the proteasome-dependent turnover of mutant Af4 and its accumulation in the *robotic* PCs (Oliver, Bitoun et al. 2004) (**Figure 6B**).

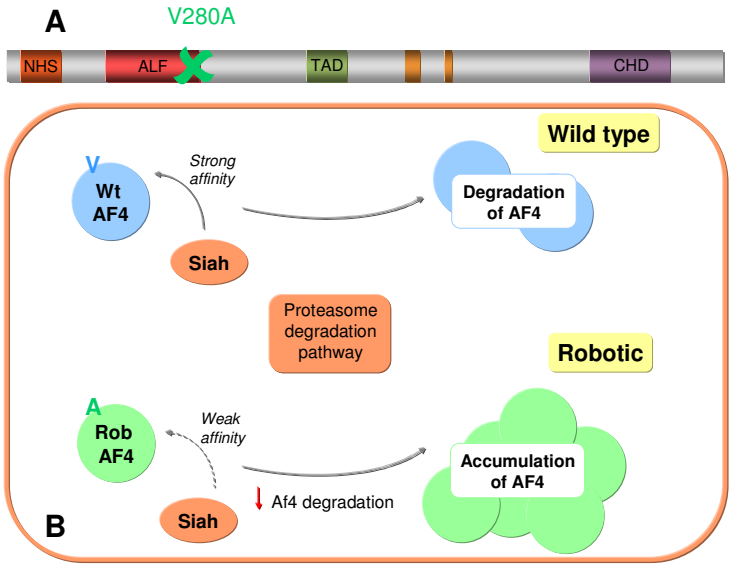


Figure 6. Af4 is mutated in the *robotic* mouse. (**A**) Representation of the Af4 protein structure. The *robotic* mutation occurs in the highly conserved ALF domain. (**B**) This mutation leads to the accumulation of Af4 due to a decreased affinity for the E3-ubiquin ligase Siah.

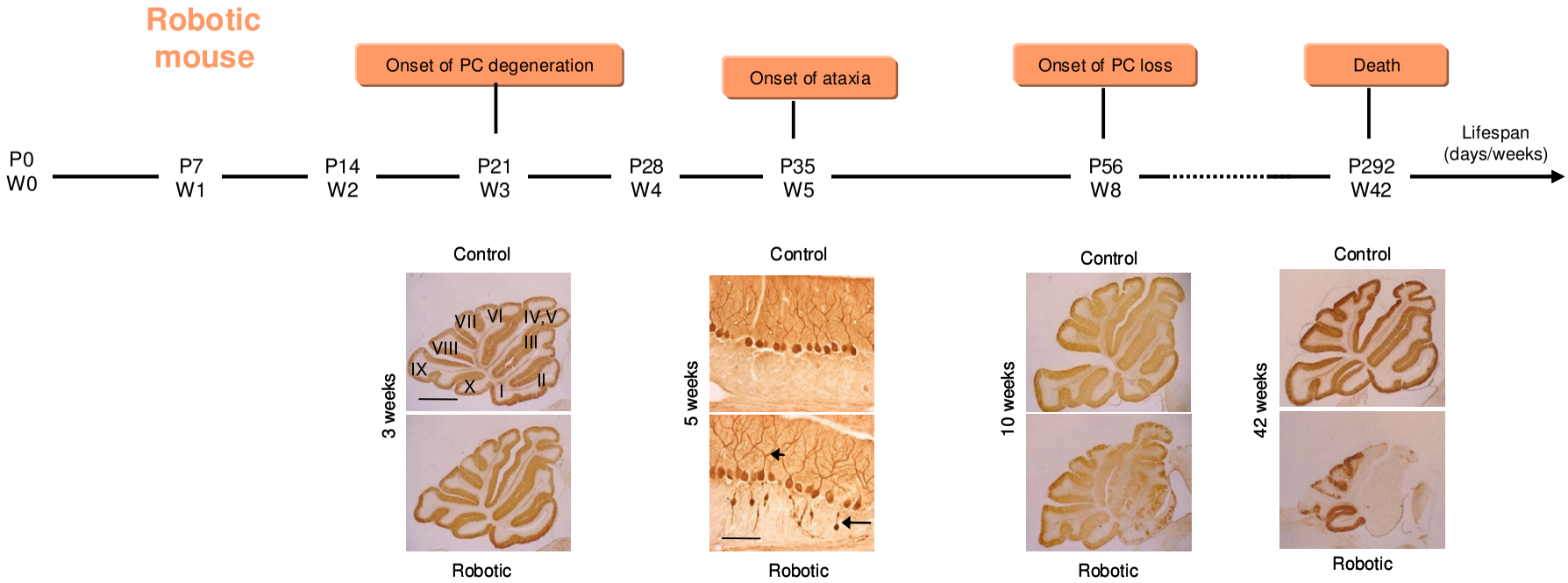


Figure 5. Progressive adult-onset regions specific Purkinje cell (PC) loss in the *robotic* cerebellum. Calbindin-stained parasagittal sections show that PC degeneration is first detected in the cerebellum around 21 days postnatally (P21) and is particularly evident at 5 weeks of age (W5) with swelling of cell bodies, dendrites (arrowhead) and axonal torpedoes (arrow); ataxia follows shortly after. From 8 weeks, a progressive region-specific PC death process takes place affecting most severely the anterior lobes (I to IV), whilst lobe X being spared throughout. Scale bars, 1mm and 100µm at 3, 10, 20, and 42 weeks, and 5 weeks respectively. Adapted from Isaacs et al, 2003.

Work in the Davies' group has since shown that Af4 is part of a large transcriptional activation complex, coordinating chromatin remodelling with RNA polymerase elongation factors (Bitoun, Oliver et al. 2007). However, nothing is known about the normal transcriptional targets of Af4 or about genes that might be influenced by the *robotic* mutation. In addition, although the PC-specific expression of Af4 provides some clue as to why the cerebellum is affected in *robotic* mice, the cause of cell death is still unknown.

Consequently, to understand the potential neurodegenerative mechanisms involved, a microarray experiment was performed in the Davies' group to compare gene expression patterns of PCs that had been isolated by laser capture microdissection (LCM) from *robotic* or wild-type mice aged P21 (see Chapter 3 for more details). This timepoint was chosen to reflect when the signs of degeneration first appear, in an attempt to find the genes deregulated in the *robotic* mouse that might be responsible for PC degeneration. Using Affymetrix GeneChip arrays, 498 differentially expressed genes were identified between *robotic* and *wild-type* PCs. For this study, it was decided to focus only one of these genes initially, insulin-like growth factor 1 (*Igf-1*), as it appeared from the literature to be highly relevant to PC survival and to other features observed in the *robotic* mouse such as growth retardation, cataracts and T-cell development defects.

The aims are therefore to:

1) Analyse the relationship between Af4 overexpression in the *robotic* cerebellum and cell death.
2) Confirm the regulation of *Igf-1* and Igf-1-related pathways by Af4.
3) Analyse the significance of Igf-1 in *robotic* ND.

Bella

The recessive *bella* mouse was also identified from the ENU screen based on its obvious ataxic gait. Indeed, in addition to screens for dominant traits, the Harwell mutagenesis programme also searched for recessive mutants, focusing on developmental phenotypes. To generate these lines, mice from an ENU F2 population were interbred. Embryos from this cross were scarified and subsequently analyzed at Harwell for morphological defects, although some litters were left to generate live mice. From one of these experiments, the *bella* ataxic phenotype was first identified. Like for the *robotic* mouse, the phenotype was highly penetrant with the expected Mendelian ratios for a recessive trait obtained in the first litters. In order to generate more *bella* (*bel/bel*) mice, littermates of the first mutants were subsequently interbred; those mice that produced *bella mice* being therefore heterozygous for the mutation. The bella mice generated are indistinguishable from their control littermates at P14; however they rapidly develop a severe ataxic gait, fail to gain weight as quickly as controls, and do not survive beyond P26 (**Figure 7**). Pathological analysis of the *bella* CNS revealed significant and increasing number of apoptotic cells in the GCL of the cerebellum from P18 onwards, although no cell death was observed in any other region of the brain in end-stage mutants or mice heterozygous for the *bella* deletion (**Figure 7**).

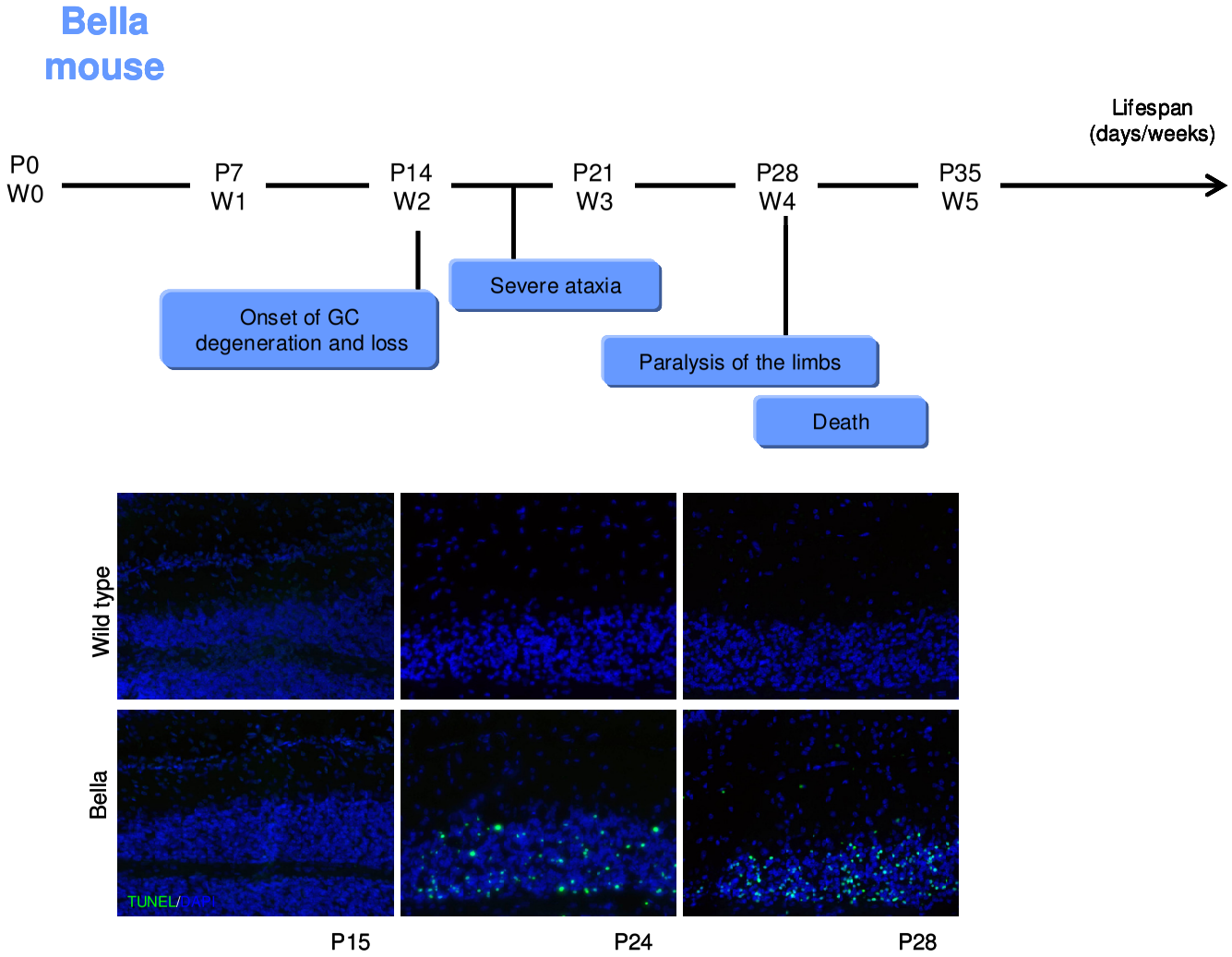


Figure 7. Progressive granule cell (GC) death in the *bella* granule cell layer (GCL) of the cerebellum. TUNEL staining showed specific GC death at P24 in the GCL of the cerebellum. The ataxic phenotype is detectable at P18. A very rapid progression of the disease occurs, and by P26-28 *bella* mice present paralysis of the limbs and die shortly after.

The initial genome scan was carried out using SNP markers on 13 *bella* mice, followed by further mapping using polymorphic microsatellites on 150 mice confirming linkage to chromosome 15. The marker *D15Mit229* co-segregated with the *bella* phenotype, suggesting the mutation was closest to this region. Candidate genes were prioritized for sequencing based on their known expression in the cerebellum and their proximity to this particular genetic marker. Surprisingly for an ENU mutant, which usually presents a point mutation, mapping and positional cloning showed that actually a deletion of a 193.5kb region occurred in *bella* mutants, the deletion spanning two genes: *Oxr1* (oxidation resistance 1 protein) and *Abra* (actin-binding Rho activating protein). It was confirmed that the *bella* deletion occurred in the Balb/c-derived ENU treated stock, as the closest polymorphic SNP markers flanking the deletion are from the Balb/c strain and not the background C3H strain. It is still unclear if this deletion is a consequence of the ENU strategy or a spontaneous deletion.

In situ hybridisation experiments carried in the Davies's group showed that *Oxr1* is highly expressed in the brain and spinal cord of wild-type mice while *Abra* is not detected, and that *Oxr1* expression is totally lost in bella mice, suggesting that the loss of *Oxr1* is responsible for the *bella* phenotype (**Figure 8A, B**). *In situ* results were confirmed by qRT-PCR (Dr Peter Oliver, unpublished data). Oxidative resistance 1 (*OXR1*) was originally identified as gene that was able to suppress DNA damage in *Escherichia coli* oxidative repair-deficient mutants (Volkert, Elliott et al. 2000). It was then discovered that the human protein, when localised to the mitochondria, was sufficient to prevent oxidative damage in *Saccharomyces cerevisiae* mutants lacking *OXR1* (Elliott and Volkert 2004). Indeed, the gene is found in all eukaryote genomes, although in lower organisms its sequence is restricted predominantly to the highly conserved C-terminal (TLDc) domain (Durand, Kolpak et al. 2007). The function of this TLDc domain has not been established, yet it was originally identified as a catalytic motif that is also shared by the highly-related protein, the nuclear receptor coactivator 7 (Ncoa7), in mammals (Durand, Kolpak et al.

2007) (**Figure 8C**). Studies have demonstrated that Oxr1 is induced under OS; however, virtually nothing is known about this obviously evolutionary significant gene in mammalian systems (Elliott and Volkert 2004).

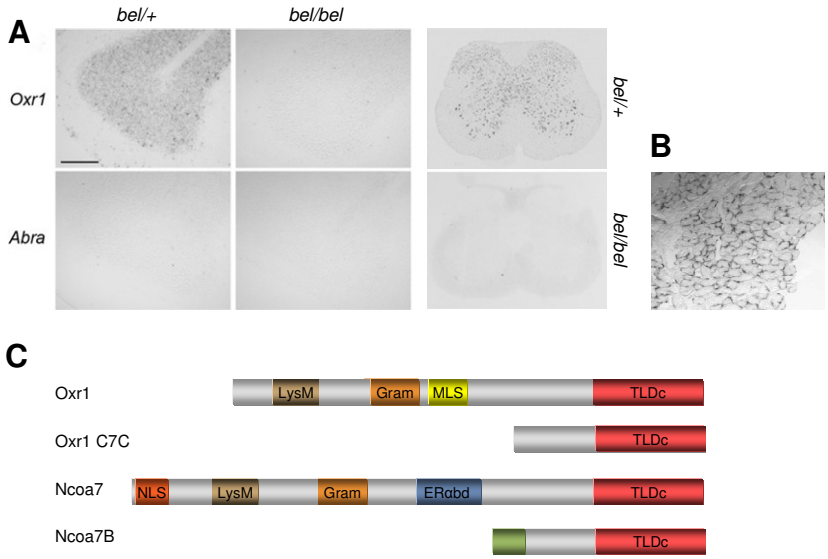


Figure 8. *Oxr1* is deleted in the *bella* mouse. (**A**) *In situ* hybridisations show the presence of *Oxr1* but not *Abra* in the GCL of the cerebellum (left panel) and spinal cord (right panel) in P24 heterozygous (*bel/+)* mice, whereas *bella* (*bel/bel*) mutants lack both genes. (**B**) *In situ* hybridisations show presence of *Abra* in skeletal muscle (transversal section of quadriceps). (**C**) Representation of Oxr1 and Ncoa7 full length (Oxr1-FL, Ncoa7-FL) and short versions (Oxr1-S or C7C and Ncoa7-S or B). Oxr1 and Ncoa7 have a highly homologous domain (TLDc).

As OS is a major component of many NDDs, it was decided to further characterize the *bella* mutant, the cause of the cerebellar ND and the function of this unknown family of proteins (Andersen 2004; Halliwell 2006; Jellinger 2010).

The aims are therefore to:

1) Further characterise the cell death in the *bella* cerebellum.
2) Investigate the significance of Oxr1 expression levels in relation to neuronal cell survival and protection.
3) Analyse the potential induction of OXR1 in biopsy samples from NDD.
4) Identify the function of Oxr1 and Ncoa7 by identifying protein binding partners.

2. Material and methods

2.1. Material

2.1.1. Constructs

Constructs were already available in the lab or made by Dr Peter Oliver. The list of constructs used in this study can be found in appendix 1.

2.1.2. Antibodies

Af4 antiserum was previously produced in the laboratory. Oxr1 and Ncoa7 antisera were produced in rabbits (see section 2.2.5). The list of antibodies used is shown in appendix 2. The secondary HRP antibodies anti-rabbit, anti-goat, anti-rat and anti-mouse were from Amersham Biosciences and were used at a 1:10,000 dilution for western blotting. Secondary antibodies Alexa Fluor used for immunofluorescence were from Invitrogen.

2.1.3. Culture medium

All culture medium (L-glutamine, DMEM medium, PBS, HBSS, antibiotics) were supplied by Gibco Invitrogen. Poly-ornithine, basal medium eagle (BME), Hepes, $MgSO_4$, $CaCl_2$, $NaHCO_3$ were from Sigma.

2.2. Methods

2.2.1. Animals and treatment

All the crossings and colony breedings were performed by Dr Peter Oliver.

For chapter 3: Experiments were carried out with the approval of the Home Office, University of Oxford, United Kingdom (PPL No 30/2306). Two groups of four *robotic* mice (C3H background) and four wild-types were injected subcutaneously with either IGF-1 (Cell Science) or with the vehicle only (0.1% DMSO), starting the injections at P7. After 4weeks of daily treatment at 1mg/kg, motor coordination of the mice at 5weeks was assessed using a rotarod device (Ugo Basile, Italy) consisting of a grooved plastic beam

of 5cm in diameter. Mice were placed on the beam and after 30sec the rod speed was gradually accelerated by electronic control of the motor to a maximum of 30rpm. The latency before falling was measured up to a maximum total time on the rod of 5min for three trials on three consecutives days. The rotarod test was performed again at 10 weeks of age and the mice were culled at 10 weeks old. Igf-1 levels were measured using an Igf1-Elisa kit (RayBio) in mice injected in parallel and culled straight after the end of treatment.

For chapter 4 and 5:

For Oxr1 knockout mice (*Oxr1* KO): These mice were generated at the Sanger centre. Gene-trap ES cell line RRR195 ($Oxr1^{Gt(RRR195)Byg}$) with a stop codon in *Oxr1* TLDc domain (common to all isoforms) was obtained from Bay Genomics and the correct identity of the insertion was confirmed by real time PCR (RT-PCR) from cultured cells prior to rederivation. RRR195 ES cells were injected into pre-implantation mouse embryos and chimeras were generated and bred with C57BL/6J mice.

For *Tg(Oxr1)* mice: The full-length mouse *Oxr1* coding sequence was cloned by Dr Peter Oliver into a pCAGGS-derived vector and injected into the pronuclei of superovulated CBAB6F1 mice at the Wellcome Trust Centre for Human Genetics. Founder mice were initially identified using *Oxr1* exon-spanning primers for subsequent breeding. Two independent founder females (*Tg(Oxr1)/+*) were bred to heterozygous *bel/+* males over two generations to generate mice homozygous for the *bella* deletion but also expressing the *Oxr1* transgene (*bel/bel*, *Tg(Oxr1)/+*) to determine genetic rescue.

2.2.2. Laser-capture microdissection (LCM) and RNA extraction

Sagittal cerebellum sections (10µm) were prepared using a cryostat at -19°C and mounted on PENmembrane slides (Zeiss, Germany) which were pretreated with RNase Zap (Sigma) and rinsed with DEPC-treated water. After sectioning, the slides were

hydrated through a series of 95, 75 and 50% ice-cold ethanol solutions prepared with DEPC–water (30s each) and stained with 1% cresyl violet acetate (Sigma) for 30s to 90s. Subsequently, slides were dehydrated in 75, 95 and 100% ethanol (30s each). Finally, sections were immersed in xylene for 30s, air-dried and subjected to LCM within the next hours. Purkinje cells from every lobe of the cerebellum were laser microdissected on a Leica AS LMD system (Leica Microsystems, Wetzlar, Germany). Cells were catapulted in RLT buffer (Qiagen) with β-mercaptoethanol (Sigma). Tubes containing 350 to 500 cells were frozen on dry ice and stored at -80°C until the RNA from all the samples collected was extracted simultaneously. RNA was extracted using Qiagen micro kit adding an extra step of treatment with proteinase K to the supplier's protocol. The RNA was eluted in 14µl of water and was used in a reverse transcription reaction using the sensiscript reverse transcriptase (Qiagen) designed for reactions using less than 50ng of RNA. The cDNA was subsequently used in a quantitative RT-PCR (qRT-PCR) reaction. mRNA level was quantified by qRT-PCR using SYBR Green PCR master mix (Applied Biosystems) and a Step One real time PCR machine (Applied Biosystems).

2.2.3. Immunohistochemistry and immunofluorescence

For paraffin sections: The paraffin embedded tissue was deparaffinised through two washes of xylene, and then hydrated through graded ethanol series (100%, 95%, 80%, 70%). Sections were treated for antigen unmasking in hot sodium citrate during 20min and subsequently rinsed four times in water and three times in PBS and treated 10min with 1% hydrogen peroxide (H_2O_2) diluted in methanol. Sections were rinsed three times in PBS and blocked for one hour at room temperature with (0.3% Triton, 2% goat serum) in PBS. The primary and secondary antibodies were both incubated between 1h to one/three overnight(s) at 4°C depending on the antibody used.

For frozen sections: The sections were dried one hour at room temperature and then treated with 4% paraformaldehyde (PFA) for 30min at room temperature. They were blocked with 10% fetal calf serum (FCS), 0.3% Triton 100-x in PBS for one hour at room temperature. Both the primary and the secondary antibodies were incubated overnight at 4℃.

For 8-OHdG: The coverslips were fixed in cold methanol and cold acetone for 10min each. After being washed in PBS, coverslips were treated with 0.05mM HCl for 5min on ice, and washed with PBS. RNA was digested by incubating the coverslips in 100µg/ml RNase in 150mM NaCl /15mM sodium citrate for 1h at 37℃. Coverslips were then washed in PBS, and incubated in increased concentration of ethanol for 2min each. DNA was denatured by incubating the coverslips with 0.15 mM NaOH in 70% ethanol for 5min. A serie of washes was performed starting with 70% ethanol containing 4% vol/vol formaldehyde and then 50% ethanol, 35% ethanol, and finally PBS for 2 min each. Proteins were digested with 5µg/ml proteinase K in TE, pH 7.5, for 10min at 37℃. After several PBS washes, coverslips were incubated with anti-8-oxo-dG antibody in 1× PBS/1% BSA/0.1% Tween 20 for 1h at room temperature. After several washes with PBS, coverslips were incubated with mouse secondary antibody for 2h at room temperature. Coverslips were mounted in DAPI medium.

2.2.4. Chromatin immunoprecipitation (ChIP)

The ChIP-IT™ Enzymatic kit (Active Motif, Carlsbad, CA) was used for ChIP assay. The samples were processed simultaneously. Briefly, various tissues were finely minced with a razor blade. The cross-linking of the proteins in the tissues was performed by incubating the minced tissue with 20ml of 37% formaldehyde solution (Aldrich) for 10min on a rocking shaker at room temperature. The cross-linking reaction was stopped by adding 5ml of glycine stop-fix solution (3ml of 10x glycine buffer; 3ml 10x phosphate-buffered saline and 24ml water) followed by homogenization, using a PRO200 homogenizer (Proscientific) in

2ml of ice-cold PBS supplemented with protease inhibitor (Roche) followed by centrifugation for 10min at 572 x g at 4°C and processed further as mentioned in the kit protocol. 50µl of the chromatin obtained by enzymatic shearing of the nuclei was incubated with 3µg of antibody (Af4 antiserum or pre-immunisation antibody) or with water together with 2 µl of the magnetic beads provided in the kit, and was placed on a rotator at 4°C for 4h. The cross-linking between the DNA and the antibody was then reversed, the proteins were cleared using proteinase K treatment and finally the DNA was purified using a DNA extraction mini kit (Qiagen). 5 set of primers used for qRT-PCR were designed to amplify DNA fragments of 150-250bp from the 5'UTR region, coding region or 3'UTR region. The data obtained were normalised by substracting the noise determined with the different negative controls and the enrichment was expressed as percentage of input (% input).

2.2.5. Antisera production

For production of Oxr1 antiserum: C7 domain 3 (amino acids 520–778), which is a highly conserved domain, common to all Oxr1 isoforms both in human and mouse, was generated by PCR using a full-length *Oxr1* cDNA plasmid as template. PCR primers were C7F3-NdeI and C7R3-Xho.

For Ncoa7 antiserum: A region (amino acids 304-559) region differing from Oxr1 sequence and still similar between mouse and human Ncoa7 sequence was chosen to produce antisera. This region was amplified by PCR using a full-length Ncoa7 cDNA plasmid as template. PCR primers were Ncoa7#1_NdeI-F and Ncoa7#1 _6xHis-XhoI-R. PCR fragment sfor both Oxr1 and Ncoa7 were digested with *NdeI* and *Xho* and were ligated into the *NdeI* and *Xho* sites of a pET22b vector (Amersham Pharmacia Biotech) to produce a Hisx6-*C7*d3 or Hisx6-Ncoa7#1 fusion construct.

For both Oxr1 and Ncoa7 antisera, the constructs were verified by sequencing and were transformed into BL21 (DE3) cells (Invitrogen). The expression of the fusion protein was induced overnight at 18°C (for Oxr1) or 4h at 37°C (for Ncoa7) with 0.5 mM (for Oxr1) or

0.1mM (for Ncoa7) IPTG (Sigma). Fusion proteins were purified from sonicated cells by affinity for BD Talon affinity resin (BD Biosciences Clontech) and the protein was eluted using increasing concentrations of imidazole (from 10 to 500mM, Fluka Sigma). The imidazole was subsequently removed from the fractions containing the purified proteins using a PD10 column (Amersham Biosciences) and replaced by PBS. Antisera were raised in rabbits (Eurogentec). Antisera were affinity purified against the fusion protein.

2.2.6. Protein extraction, cell fractionation, western blotting

The organs of interest were homogenised with a PRO200 homogeniser (Proscientific) or with a sonicator only for spinal cord samples (10/20 amplitude, 3x5s) in cold lysis buffer (50mM Tris-HCl (pH=7.4), 150mM NaCl, 1% Triton X-100) supplemented with a mixture of protease inhibitors (Sigma) and phosphatase inhibitor cocktail 1 and 2 when required (Sigma). After 30 min incubation on ice, the samples were centrifuged at 14,324 x g for 20 min at 4°C.

For cell fractionation: N2A cells were separated into the nuclear, mitochondrial and cytoplasmic fractions using Qproteome Mitochondria Isolation Kit according to the manufacturer's protocol (Qiagen) using the buffers provided in the kit.

For immunoprecipitation: 500µg-1mg of protein were pre-cleared with 30 µl of protein G–Sepharose beads (GE Healthcare) for 1h at 4°C. 2-3µg of antibody was then added to the pre-cleared protein extract overnight at 4°C on a wheel. The following day, 40µl G–Sepharose beads were added for 1h at 4°C. Immunoprecipitated proteins were washed three times with lysis buffer and resuspended in 20µl of sample loading buffer. For immunoprecipitation of HA, MYC and FLAG-tagged proteins, cleared protein extracts were incubated overnight at 4°C with EZview™ Red Anti-HA, MYC or FLAG Affinity Gel beads (Sigma), with no pre-clearing step.

For co-immunoprecipitation: A similar protocol was used using a milder buffer (50mM Tris (pH=7.5), 150mM NaCl, 1%Chaps) in place of the lysis buffer described above.

For RNAse, alkaline phosphatase (CIP) and Endoglycosidase (Endo-H) treatment: Co-immunoprecipitated proteins (≤500µg) were incubated for 1h30 at 37°C with 1mg/ml of RNAse (Roche), 3,500U of CIP (phosphorylated myelin basic protein was used as a control), or 200,000U of Endo-H (NEB) (RNase B was used as a control). Immunoprecipitated proteins were subsequently washed 3 times with PBS.

In all cases, lysates were quantified using the BCA assay kit (Pierce Thermo Scientific). For western blotting, equal amounts of protein were directly loaded on 7.5%, 10% or 12% SDS-PAGE or 4-12% Bis-Tris NuPAGE gels (Invitrogen) depending on the protein studied, or were first precipitated overnight with 5 volumes of cold acetone. Proteins once run on the gels, were transferred from few hours to overnight at 4°C depending on the protein size on PVDF membranes. Non-specific binding was blocked using 5% dried milk in PBSt. Membranes were then incubated with primary and secondary antibodies specific for the protein studied. Primary and secondary antibodies are listed in appendix 2. Proteins were visualized by enhanced chemiluminescence detection (Amersham Biosciences) following the manufacturer's instructions.

2.2.7. Cell Culture and treatment for N2As, HeLas, HEK293Ts

Negroid cervix epitheloid carcinoma (HeLa), Neuro2a (N2A), and Human Embryonic Kidney 293T (HEK293T) cells were grown in DMEM supplemented with 10% FBS, 2mM L-glutamine, 1mM non essential amino acids, and 1% ampicillin–streptomycin. Cells were transiently transfected for 24h to 48h (for shRNA experiments) with the different constructs using FuGENE 6 (Roche Diagnostics) as a transfecting reagent. One day after transfection, cells were treated for 4h with 150 µM of H_2O_2 (Sigma) or 30 min with 1mM H_2O_2 and let recover for various durations.

2.2.8. Primary cell culture and treatment for granule cells (GCs) and cortical cells (CCs)

Cerebella were dissected from P2-P7 mice for cortical or granule cell cultures respectively. Cerebella were cleared of any meninges. Usually 5-6 cerebella were pulled together and processed at the same time. Cerebella were washed twice with 10ml cold sterilized dissection solution (HBSS, 10mM $MgCl_2$, 7mM Hepes, 10mM L-glutamine, pen/strep), centrifuge cerebella at 94 x g for 5min. Dissection solution was replaced with 1.5ml trypsin (Gibco) and cerebella were incubated for 25min in a 37°C waterbath. Cerebella were centrifuged at 94 x g for 5min and tryspin was removed. Tryspin was replaced with 1.5ml trypsin inhibitors (0.8mg/ml) (Sigma) diluted in dissection solution and incubated for 5min at room temperature. Solution was removed and cerebella were washed twice with 5ml warm culture medium I (DMEM, 10%FCS) and triturated for 30 times with 1.5ml culture medium, and centrifuged for 5min at 94 x g. Supernatant was removed and cells were resuspended in 1ml culture medium I. Cell number was determined. Cells were plated at a confluence of $2.5\text{-}3.5.10^5$ cells/cm². Cells transfected with Amaxa were processed straightaway and 4.10^6 cells were used per reaction by mixing cells with 100µl Basic Neuron SCN Nucleofector (Lonza) and 2µg/5µg/10µg of GFP-control vector/pCX vector /shRNA vector constructs respectively into an electroporation cuvette (Lonza) and program O-005 was selected on the Nucleofector II. Cells were then resuspended in warm culture medium II (same as culture medium I with pen/strep). 24h after plating, cells were treated with 5µM ara C (Calbiochem) to inhibit the proliferation of glial cells. Cells transfected using Fugene 6 were processed similarly than in 2.2.7 for 72h after cells have been cultured for 11-18days.

2.2.9. Viral production and primary cell infection

Viral constructs were transfected into HEK293T cells with packaging vectors and virus-containing supernatants were collected 3 days later. GCs were infected after 11 days in culture by adding lentivirus-containing medium (1:50 dilution) for 24h followed by 48h incubation in fresh medium prior to cell survival estimation as in 2.2.7.

2.2.10. Mass spectrometry

To study interactors of Oxr1 and Ncoa7 (both full length and short isoforms), N2A cells were transfected with the appropriate pCX vector, HA-tagged at the C-terminus. Cells were transfected for 24h. After the appropriate treatment, cells were washed twice with cold PBS and lysed with 600µl gentle buffer (50mM Tris (pH=7.5), 150mM NaCl, 1% Chaps) complemented with a cocktail of protease inhibitors (Roche) per one confluent 63cm² dish, and incubated for 30min on ice. After lysates being cleared by centrifugation (30min, 4℃, 91 x g), 50ul of EZview™ Red Anti-HA (Sigma) were added to the lysates and incubated overnight at 4℃. Immuprecipitated proteins were then washed 5 to 10 times with gentle buffer. Proteins were resuspended in NuPAGE buffer and boiled for 5min. Samples were run through the stacking gel of a NuPAGE gel (Invitrogen) and the entire band was cut and sent for trypsin digestion and analysis by LC-MSMS sequencing identification at the Dunn School of Pathology (central proteomics facility). The list of protein targets were analysed using Ingenuity software. The *p*-values calculated by the software are a measure of the likelihood that the association between the set of proteins identified in the experiment and a given process or pathway is due to random chance. The *p*-value for a given function is calculated by considering the number of functional analysis molecules that participate in that function and the total number of molecules that are known to be associated with that function in the Ingenuity Knowledge Base.

2.2.11. Tunel assay

Tunel staining on cells were processed as per the manufacturer's protocol. Tunel staining on paraffin sections was processed after a step of antigen retrieval as in 2.2.3.

2.2.12. Catalase assay

Cells or tissues were homogenised in reaction buffer (0.05M Na_3PO_4, pH=7.4) on ice. 25µl of standard (catalase from Molecular Probes diluted in the range of 0mU/ml to 1000mU/ml) and samples were mixed with 40µM H_2O_2 in a 96-well black microplate and incubated for 30min at 37°C. 50µl of 100µM Amplex Red (Molecular Probes)/0.4U/ml horseradish peroxidise (Invitrogen) were then added. Fluorescence was measured every 15min with a fluorescence plate reader using 544/590 filter pairs. Catalase activity was calculated as followed: Catalase (U/L)=[(F sample blank - F sample) x n] / [slope(μM^{-1}) x time], F being the fluorescence intensity, n the sample dilution factor, slope being determined from the standard curve, time is the reaction time (30, 45, 60, 75min). One unit is the amount of catalase that decomposes 1µmole of H_2O_2 per min at pH 7.0 at room temperature.

2.2.13. Thiobarbituric acid reactive substances (TBARS) assay

TBARS levels are an index of lipid peroxidation under OS. One confluent 63cm² dish of treated/untreated cells was lysed with 300µl RIPA buffer and sonicated (10/20 amplitude, 3x5s) and incubated on ice for 30min. Cells were centrifuged for 10min at 3,000 x g at 4°C. 100µl of cell lysate was mixed with 200µl ice cold 10% trichloroacetic acid to precipitate protein and incubated 15min on ice. Samples were centrifuged for 15min at 2,200 x g at 4°C. 200µl of supernatants and standards (tetramethoxypropane from Sigma diluted at a concentration ranging from 0µM to 100µM) were mixed with 200µl of 0.67% (w/v) thiobarbituric acid (Sigma) and incubated for 10min at 100°C. 150µl were loaded in triplicate in a 96-well glass plate. Absorbance was read at 532nm. Hydroperoxide values

(HP) were calculated using the equation obtained from the linear regression of the standard curve substituting the corrected absorbance values for each sample (A sample), as indicated: HP (nmol) = (A sample – y-intercept) / slope.

2.2.14. Picogreen assay

Genomic DNA from one 63cm² dish of treated/untreated cells was extracted using the DNA extraction kit from Qiagen and the protocol designed for tissues (and not for cells as this protocol requires isolation of nuclei and hence loose of mitochondrial DNA (mtDNA)) provided by the manufacturer. Double-stranded DNA (dsDNA) was quantified using Picogreen (Thermo Scientific) as per manufacturer's instructions. A 2µg/ml stock of λ/HindIII DNA was diluted at different concentrations ranging from 1.25 to 20ng/ul to generate a standard curve. Fluorescence was measured with a microplate fluorescence reader using the following parameters: excitation and emission wavelengths 485 nm and 530 nm respectively. Strand scission factor was calculated as –ln(A treated / A control); A being the absorbance.

2.2.15. Statistical analysis

Results were analyzed using Prism software. The difference between wild type and mutant or between the various treatments was compared using a 2way ANOVA test. *P*-values <0.05 were considered significant. Data were expressed as mean -/+ S.E.

3. AF4 as a regulator of the IGF-1 signalling pathway during Purkinje cell development

The *robotic* mouse harbours a point mutation in *Af4*, a member of the *Alf* (*Af4/Laf4/Fmr2/Af5q31*) gene family. These proteins are now known to act as transcriptional co-factors via a large protein complex involving both histone modification and RNA polymerase activation (DiMartino, Ayton et al. 2002; Estable, Naghavi et al. 2002; Okada, Feng et al. 2005; Bitoun, Oliver et al. 2007). However, despite knowing that accumulation of Af4 occurs in *robotic* mouse due to disruption of the Siah binding domain, the cause and timing of PC death is still unclear. Furthermore, no transcriptional targets of any of the ALF proteins have been identified. The *robotic* mouse therefore provides an opportunity to identify transcriptional pathways that may lead to PC-specific ND in human movement disorders and ataxia. In addition, the identification of genes that are regulated by Af4 may shed light on the role of the ALF family in other diseases, such as leukaemia.

Consequently, to identify the genes deregulated in the *robotic* mouse caused by the accumulation of Af4 and to find potential neurodegenerative pathways, microarray analysis was performed on PCs obtained by laser-capture microdissection (LCM) at P21. This time point was chosen as it corresponds to when signs of ND (ataxia and axonal swelling) first appear but a considerable time prior any cell death. It was therefore hypothesised that this time point would reflect causative gene changes as opposed to those that were simply a result of PCs death. Microdissection and RNA extraction from PCs were optimised by Dr Emmanuelle Bitoun in the Davies' group and RNA samples from 2,500 PCs for each of 4 wild-type and *robotic* littermates were collected. Gene expression changes were then analysed by Sheena Lee (OXION) using Affymetrix GeneChip Mouse Genome arrays. Data were normalized by Sheena using GCRMA software with a cut-off *p*-value of 0.05 ($p \leq 0.05$) and cut-off fold expression score of 1.5

(fold change in *robotic* PC ≥1.5). A total of 498 differentially expressed genes were identified between wild-type and *robotic* PCs, of which one third were downregulated. The gene list obtained was further examined based on a combination of expression changes (≥2.0-fold), PC-specific cerebellum expression pattern, known link to ataxia or ND and/or relevance to PC function and a shortlist of 22 genes was selected (**Figure 5**, **Appendix 3**). The gene expression of these 22 genes was confirmed by qRT-PCR from microdissected PCs, independently from the samples used for the microarray (**Appendix 3**).

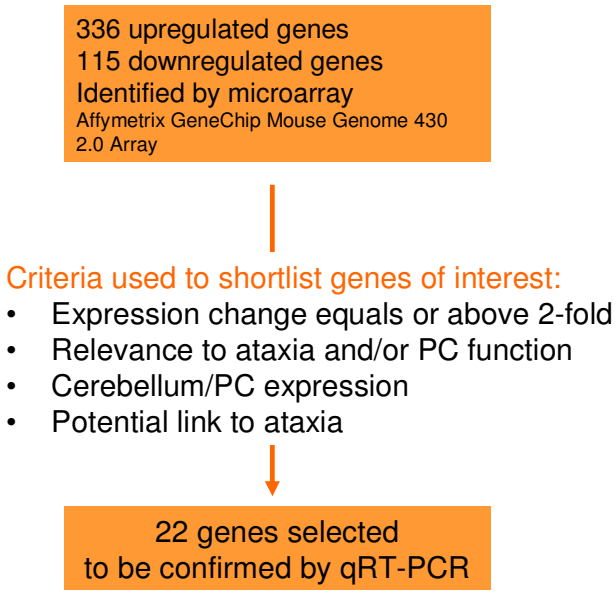


Figure 5: Analysis of the microarray results: This analysis was performed by Dr Emmanuelle Bitoun. The 451 genes found by microarray to be deregulated in the *robotic* PCs were analysed using the criteria described above and a shortlist of 22 genes was selected.

From this list of genes, *Igf-1 (*downregulated ≥2.7-fold in *robotic*) was selected as a promising gene that warranted further investigation. Indeed, it fulfils all the selection criteria mentioned above, bears functional relevance to the other non-neurological features of the *robotic* phenotype (growth retardation, T-cell development defects and cataracts) and is a well known factor in PC development and survival (Torres-Aleman, Pons et al. 1992; Baker, Jeh-Ping et al. 1993; Liu 1993; Powell-Braxton, Hollingshead et al. 1993; Walker, Liping et al. 2002; Welniak, Sun et al. 2002; Fukudome, Tabata et al. 2003; Ebong, Chepelinsky et al. 2004; Ruberte, Ayuso et al. 2004; Gatchel, Watase et al.

2008). In addition, the known expression pattern of *Igf-1* relates to the pattern of neurodegeneration in the *robotic* cerebellum; Igf-1 is specifically expressed in the soma of PCs with reduced levels in lobe X (Bondy, Werner et al. 1990; Lee, Javedan et al. 1992).

This chapter describes the detailed analysis of *Igf-1* transcriptional regulation in the *robotic* mouse via the interaction with the Af4-mediated transcriptional complex and how its deregulation leads to the *robotic* phenotype.

Aims:

- **Independently confirm the LCM microarray** results by qRT-PCR.
- **Determine the normal temporal pattern of Af4 expression.** Exploiting the LCM technology, Af4 expression in groups of cerebellar lobes will be determined in an attempt to find a correlation between Af4 expression levels and the pattern of *robotic* ND.
- **Study IGF-1 involvement in the *robotic* mouse phenotype** and determine if *Igf-1* gene expression could be regulated directly by Af4 using chromatin immunoprecipitation (ChIP) in the various organs affected.
- **Test whether Af4 accumulation in *robotic* PCs leads to a deregulation of downstream pathways** by investigating by immunofluorescence activation of various downstream proteins of the Igf-1 pathway that were described previously in the literature.
- **Compare the data from the *robotic* mouse to the *Af4* KO mutant** to determine whether the effects of the gain-of-function *robotic* mutation are reverse in mice lacking *Af4.*

3.1. Study of Af4 expression pattern

3.1.1. Gene deregulation found by microarray could be confirmed independently

22 genes shown to be deregulated by microarray were selected and their expression changes in *robotic* PCs were validated by qRT-PCR at P21 from independent laser microdissected samples from 2,500 of PCs (**table appendix 3**). This confirmed that the microarray data are reproducible using another quantification method combined with the processing of LCM samples by a different experimentor.

3.1.2. *Af4* mRNA level peaks at P14 and then is downregulated at P21

The first aim was to understand why the accumulation of Af4 in PCs triggers degeneration at P21 and whether this related to specific developmental fluctuations in *Af4* gene expression at this time point. To answer this question, the relative temporal expression of *Af4* was determined using LCM PCs and qRT-PCR. Approximately 500 PCs from the whole cerebellum were collected and *Af4* mRNA levels were determined using β-actin as an internal control. Five specific time points were selected: P7, P14, P21 (onset of PC degeneration in *robotic* mouse), P35 (onset of ataxia in *robotic* mouse) and P56 (onset of PC death). The results show that *Af4* mRNA levels peaks at P14 with a 2-fold increase compared to the level in P7 and P21 (**Figure 9A**). Thus, P21 could possibly be a key regulatory point of Af4 in PCs.

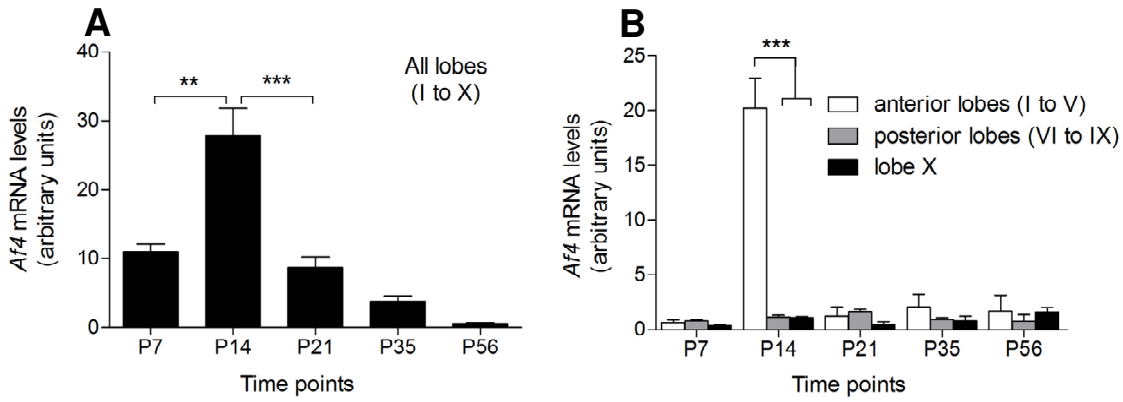


Figure 9. *Af4* mRNA levels peak at P14 in wild-type cerebellum. *Af4* transcript levels were determined by qRT-PCR from PCs of wild-type mice obtained by LCM (*n*=3). Analysis was performed from all 10 lobes (**A**), or from individual cerebellar regions (**B**). Results are shown+/-SD. The asterisks indicate significant differences between time point expression values (**p<0.01, ***p<0.001).

3.1.3. Levels of Af4 are dramatically higher in the anterior lobes compared to the posterior lobes and lobe X of the wild-type cerebellum

It was observed previously that the pattern of PC degeneration in the *robotic* mouse occurs first in anterior lobes then in posterior lobes, the lobe X being unaffected throughout (Isaacs 2003). It was investigated whether *Af4* expression could correlate with spatial pattern of PCs degeneration using PCs microdissected selectively from the anterior lobes (I toV), the posterior (VI to IX) and the lobe X of wild-type cerebella. *Af4* mRNA levels were subsequently determined by qRT-PCR. *Af4* mRNA levels peaks at different times for each lobe: at P14 for anterior lobes, at P21 for the posterior lobes, and P140 in the lobe X (**Figure 9B**). More importantly, the levels of *Af4* were dramatically different from one lobe to another. Indeed, this data revealed that *Af4* was expressed 20-times more in the anterior lobes than in lobe X at P14. These data suggest that lobes with high levels of Af4 expression are more susceptible to ND.

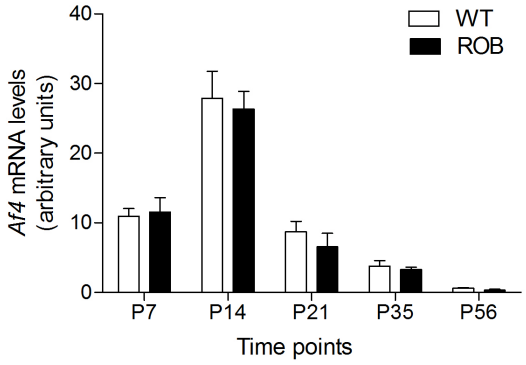


Figure 11. *Af4* gene expression is not altered in *robotic* PCs. *Af4* transcript levels were determined by qRT-PCR from PCs of wild-type (WT) and *robotic* (ROB) mice obtained by LCM (*n*=3). Results are shown+/-SD.

3.1.4. Af4 accumulates in *robotic* Purkinje cells at P21

To compare Af4 protein levels in wild-type and *robotic* mouse, immunohistochemistry was used on sections of frozen cerebella from a range of postnatal time points. Immuno-staining showed that the levels of expression were generally lower in wild-type than *robotic* mice, with a marked increase at P21 and P35 in mutants (**Figure 10**). No significant difference was observed between *Af4* mRNA levels in *robotic* and wild-type PCs at any time points analysed (**Figure 11**). These data combined with the qRT-PCR results suggest that AF4 accumulates in PCs at P21 due to a decrease in turnover of mutant Af4, *Af4* transcription being unaffected by the *robotic* mutation; this accumulation occurs at a potentially critical stage of PC development where levels of Af4 are usually very low in the wild-type.

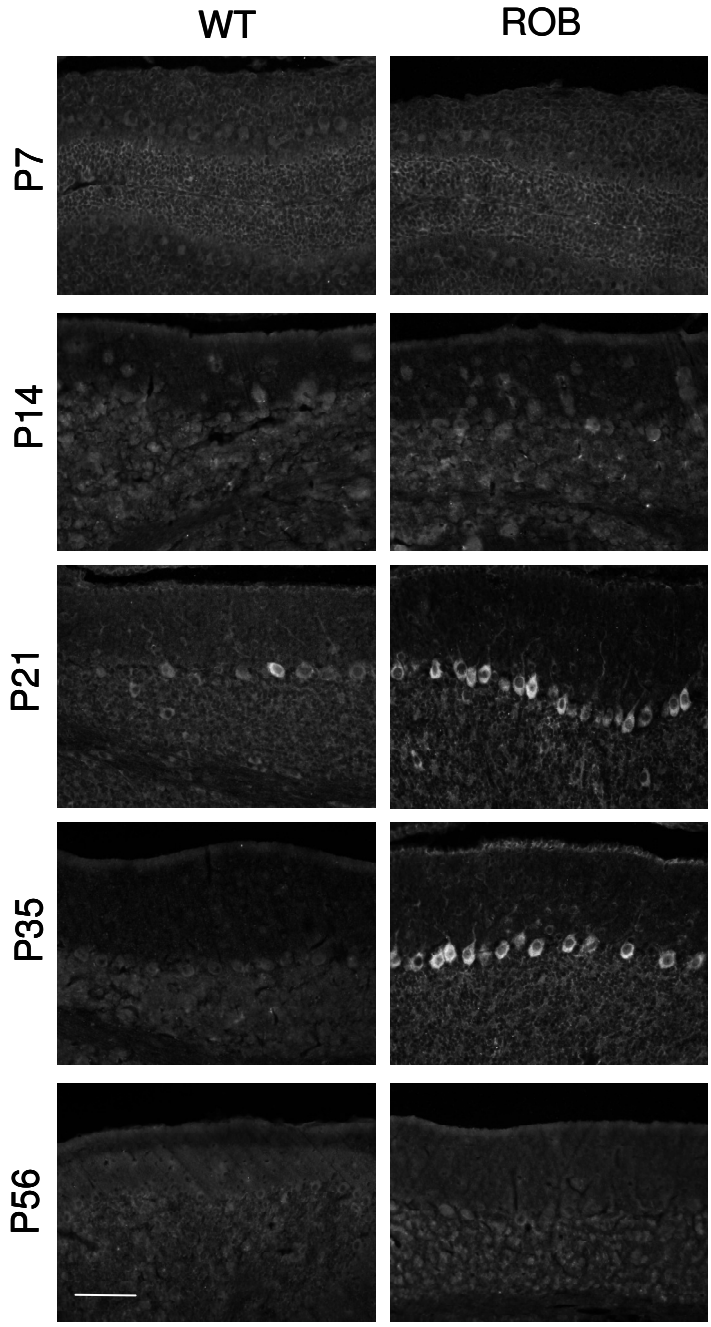


Figure 10. Af4 protein accumulates in *robotic* PCs. Immunostaining of Af4 in parasagittal cerebellum sections from wild-type (WT) and *robotic* (ROB) mice. To enable a direct comparison, pictures were taken using the same exposure time. The localization of Af4 to PCs was confirmed by double staining for calbindin (data not shown). Images show lobe III only and are representative of the results obtained for WT and ROB littermates from three independent litters. Scale bar, 100µm.

3.2. Af4 in the *robotic* Purkinje cells and its role in *Igf-1* gene expression and downstream pathways deregulation

3.2.1. *Igf-1* and *Igbp-3* expression are downregulated in the organs affected in the *robotic* mouse

IGF-1 function is regulated by its binding to IGFBP-3 which presents a striking similar spatiotemporal PC expression as to IGF-1, suggesting that IGF-1 also regulates *Igfbp-3* gene expression in PCs (Ye 2003). Indeed, *Igfbp-3* transcript levels are downregulated 2.3-fold in *robotic* PCs at P21 both by microarray and qRT-PCR (**Figure 12**). To provide further evidence of a direct correlation between *Igf-1* and *Igfbp-3* levels in *robotic* PCs, *Igfbp-3* mRNA levels were determined by qRT-PCR from cells obtained by LCM at earlier and later time points (**Figure 12**). *Robotic* expression levels were indeed significantly reduced by over two- to three-fold between P7 and P21. Based on the observations above, it seems that the reduction in *Igf-1* levels in *robotic* PCs leads in turn to a reduced *Igfbp-3* gene expression.

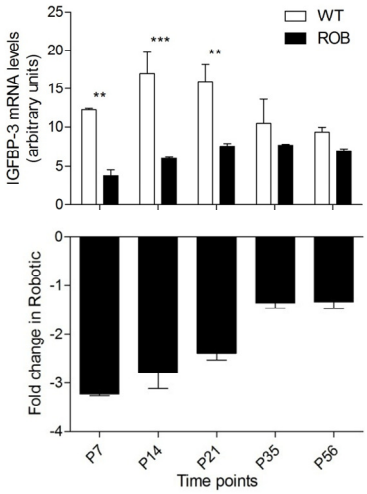


Figure 12. *Igbp-3* gene expression is decreased in *robotic* PCs. *Igfbp-3* transcript levels were determined by qRT-PCR from PCs of wild-type (WT) and *robotic* (ROB) mice obtained by LCM (n=3). Results are shown +/- SD. The asterisks indicate significant differences between WT and ROB expression values (**p<0.01, ***p<0.001).

As the IGF-1 signaling pathway is also a key regulator of general body growth, lymphoid development and lens differentiation, deregulation of *Af4* and *Igf-1* levels was determined in the other organs accounting for the non-neurological features observed in the *robotic* mouse i.e. growth retardation, T-cell maturation defects and cataracts. As in PCs, *Af4* transcript levels were not affected in the thymus, bone marrow, or lens of *robotic* mutants (data not shown). To investigate whether Af4 also regulates *Igf-1* gene expression in these tissues, the transcript levels of *Igf-1* in *robotic* and *Af4* KO mice were determined in the cerebellum, thymus, and bone marrow at P21, and in the lens at P70 when the symptoms have previously been observed and characterized (Isaacs, Oliver et al. 2003). Data showed statistically significant differences in the levels of *Igf-1* expression in both *robotic* and *Af4* heterozygous ($Af4^{-/+}$) and homozygous *Af4* KO tissues featured in the *robotic* phenotype compared with wild-type samples (**Figure 13**). The small intestine, in which *Af4* is not expressed, was used as a negative control and *Igf-1* levels were determined. As expected, *Af4* expression was not detected and no variations in the levels of *Igf-1* expression were observed (data not shown). It should also be noted that *Igf-1* gene expression changes were in opposite directions in *robotic* and *Af4* KO mice, strongly correlating with the levels of Af4 present in the various genotypes.

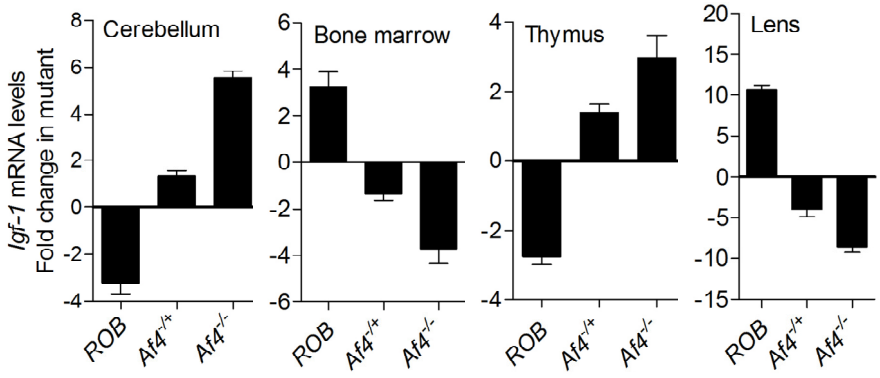


Figure 13. *Igf-1* gene expression is altered in neuronal and non-neuronal affected tissues of the *robotic* and *Af4* KO mice. *Igf-1* transcript levels were determined by qRT-PCR from tissues of robotic (ROB), and *Af4* heterozygous ($Af4^{+/-}$) and homozygous ($Af4^{-/-}$) KO mice (*n*=3). Analysis was performed in the cerebellum, thymus, and bone marrow at P21, and in the lens at P70. Results are shown in fold change of wild-type in robotic or KO mutants +/- SD.

3.2.2. *Igf-1* downregulation in the *robotic* mouse is conveyed by increased amounts of the Af4 transcriptional complex to *Igf-1* gene

To investigate if *Igf-1* was a direct transcriptional target of the Af4 transcriptional complex in the cerebellum, chromatin immunoprecipitation (ChIP) was performed from fresh wild type and *robotic* cerebella. The immunoprecipitated DNA was used in a qRT-PCR reaction using primer sets designed within the *Igf-1* sequence (**Figure 14**).

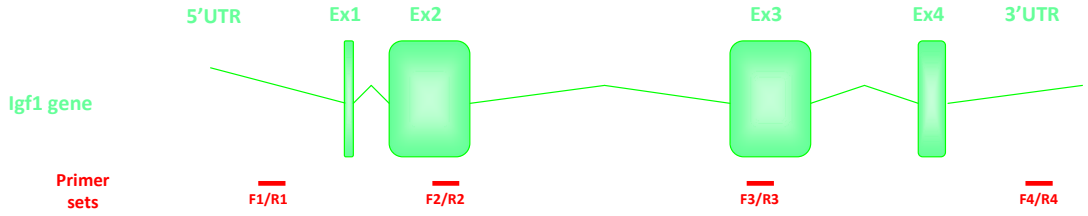


Figure 14. Primers used for ChIP are localised along the *Igf-1* gene. One primer was designed in the 5'UTR region (F1/R1), two in the coding region (F2/R2 and F3/R3) and one in the 3'UTR (F4/R4).

The results were first expressed in %Input (see Material and Methods for details) previously corrected by subtracting the noise present in the different negative controls using a similar approach as Haring et al, 2007, and then in fold change in *robotic* (Haring, Offermann et al. 2007). These data suggest first that Af4 has a direct interaction with *Igf-1* sequence at all time points for both wild-type and *robotic* as %Input values were all between 8 to 78% (**Figure 15A**). Moreover, the %Input is generally much higher in the *robotic* compared to the wild-type highlighting that Af4 transcriptional complex has a stronger interaction with *Igf-1* gene in the *robotic* than the wild-type (**Figure 15B**); At P14 especially, a 10- to 40-fold increase was observed for all set of primers. This is consistent with the downregulation of *Igf-1* occurring at P14 found in the previous section. Furthermore, a 40-fold increase was seen for the primer set F2/R2 designed in the coding region of *Igf-1* confirming the implication of Af4 transcriptional complex in regulating the elongation process (Bitoun, Oliver et al. 2007).

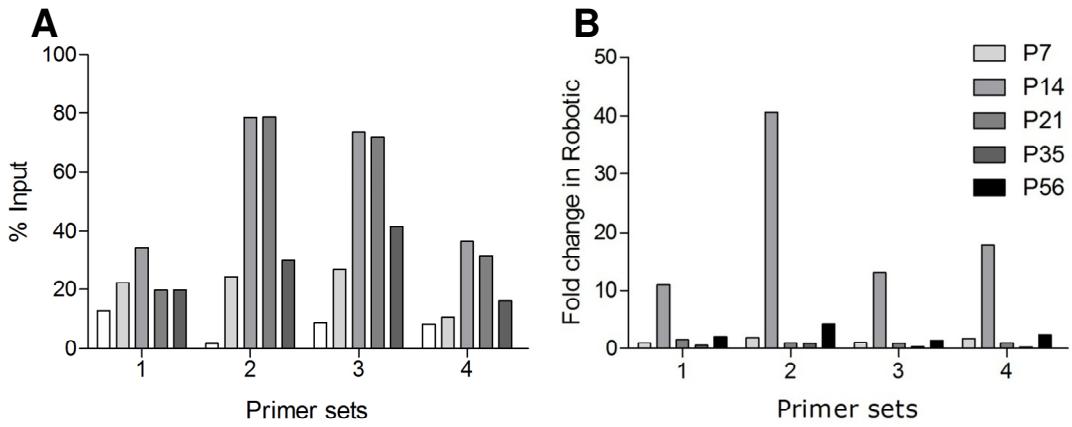


Figure 15. The Af4 transcriptional regulatory complex binds to the *Igf-1* locus in the cerebellum. Cerebellum from wild-type and *robotic* mice at the indicated age (*n*=3 in each group) were subjected to ChIP analysis using the AF4 antiserum. The isolated chromatin was used as a template for qRT-PCR with 4 primer sets designed within the 5'- UTR (1), coding (2 and 3), and 3'- UTR (4) regions of the *Igf-1* genomic sequence. Non-specific binding was determined through the use of negative ChIP controls and was subtracted, as described in Materials and Methods. The %Input for the indicated time points were calculated for both wild-type (**A**) and *robotic* samples and the difference was expressed in fold change in *robotic* (**B**). The percentage input was corrected by subtracting the noise from the various negative controls.

Then to confirm that *Igf-1* is also a direct transcriptional target of the Af4 regulatory complex in the thymus, bone marrow and lens, ChIP assays were performed from these tissues using P42 wild-type, *robotic* mice and *Af4* KO mouse. At P42, defects are strongly detectable in all the organs studied. Binding to the proximal coding region of *Igf-1* (detected with primer set F2/R2) was observed both in the thymus and bone marrow, with a six- and four-fold greater complex occupancy in *robotic* samples, respectively (**Figure 16**). However, a similar regulation of *Igf-1* gene expression by the Af4 transcriptional complex in the lens could not be confirmed due to the limiting amounts of starting material and the low levels of Af4 expression in this tissue (data not shown). These data show that altered *Igf-1* gene expression also occurs in the non-neuronal tissues affected in the *robotic* mouse, strongly suggesting that deregulation of the Igf-1 signalling pathway is also responsible for the lymphoid developmental defects and cataract formation in the *robotic* mouse.

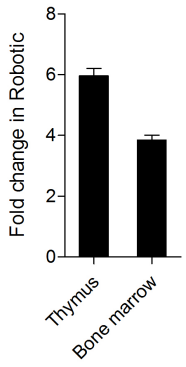


Figure 16. The Af4 transcriptional regulatory complex binds to the *Igf-1* locus in the thymus and bone marrow at P42. Thymus and bone marrow from wild-type and *robotic* mice at the indicated age (*n*=3 in each group) were subjected to ChIP analysis using the Af4 antiserum. The isolated chromatin was used as a template for qRT-PCR with 4 primer sets designed within the coding regions of the *Igf-1* genomic sequence. Non-specific binding was determined through the use of negative ChIP controls and was subtracted, as described in Materials and Methods. Results are expressed as %Input, in fold change of wild-type in *robotic*.

3.2.3. *Igf-1* downregulation in the *robotic* mouse leads to deregulation of the Erk pathway

To confirm the functional implication of reduced levels of Igf-1 in the pathogenesis of the *robotic* cerebellum, it was investigated if the activation of known signalling molecules downstream of Igf-1 including type 1 Igf receptor (Igf-1R), and the extracellular signal-regulated kinases Erk1 and Erk2 were also affected in *robotic* PCs (Torres-Aleman, Pons et al. 1992). Levels of phosphorylation of Igf-1R and p44/p42 MAP (Erk1/2) were studied in the *robotic* mouse and wild-type by immunohistochemistry. Results suggest that phosphorylation of Igf-1R was strongly decreased at P14 in the *robotic* mouse compared to wild-type (**Figure 17A, B**). As a consequence, phospho-Erk1/2 levels were decreased in the *robotic* at P14 confirming that deregulation of the Igf-1 signalling pathway occurs in *robotic* PCs at the onset of cell degeneration. Moreover, as the activation of IGF-1R and downstream pathways were strongly activated at P14 in the wild-type, these data suggest that Igf-1 has a role in normal PC development, especially at P14.

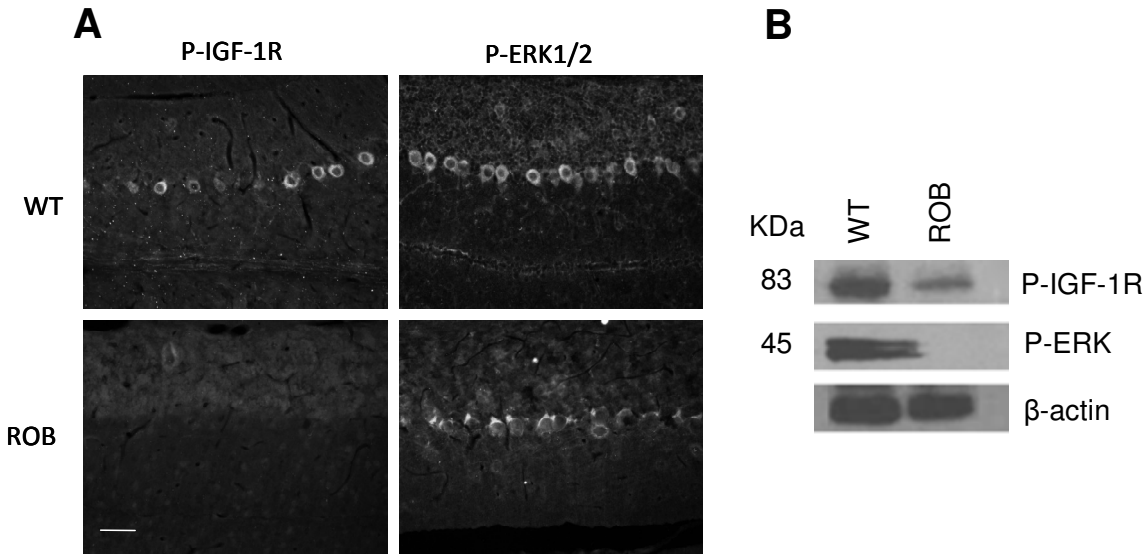


Figure 17. Activation of the Igf-1 signalling pathway is reduced in *robotic* PCs. (**A**) Immunostaining of parasagittal cerebellum sections of P21 wild-type (WT) and *robotic* (ROB) mice for p-IGF-1R and p-ERK1/2. To enable a direct comparison between WT and ROB, pictures were taken using the same exposure time. Pictures show lobe III only and are representative of the results obtained for WT and ROB littermates from three independent litters. Scale bar, 100µm. (**B**) Western blot presenting levels of P-IGF-1R and P-ERK in cerebella from wild-type (WT) and *robotic* (ROB) mice.

3.2.4. IGF-1 treatment of *robotic* mouse can slow down Purkinje cell degeneration

Then to confirm *in vivo* that it was indeed the reduced levels of Igf-1 and deregulation of its downstream targets that were responsible for the onset of *robotic* PCs degeneration, pre-symptomatic P7 mutant and control mice were injected daily with recombinant IGF-1 or vehicle for 4 weeks as this treatment will encompass the duration when *Igf-1* transcription levels were previously shown to be deregulated (assisted by Dr Peter Oliver). Mice were subcutaneously injected as previous reports have shown efficient delivery of IGF-1 to the mouse cerebellum using this route of administration (Fernandez, de la Vega et al. 1998; Nahm, Frank et al. 2003). Following treatment, motor coordination of IGF-1- and vehicle-injected groups was assessed using an accelerating rotarod and a static rod (assisted by Dr Peter Oliver). At P42, no significant difference was observed in the performance of the two groups of *robotic* mutants. It should be noted that in a previous

study no statistical difference in the rotarod performances between wild-type and *robotic* mice was detected until P70, although ataxia was already clearly noticeable by visual observation from P28 (Oliver, Keays et al. 2007). Therefore, animals were aged to P70 and locomotor activity analysis was repeated. Again, no significant difference was observed between IGF-1 and vehicle-treated *robotic* animals (**Figure 18**). As at both P42 and P70, the ataxic gait of IGF-1-treated mice was visually indistinguishable from that of vehicle-treated *robotic* littermates; this indicates that the delivery of exogenous IGF-1 to PCs at P7 is not sufficient to prevent PC dysfunction and its progression into ataxia.

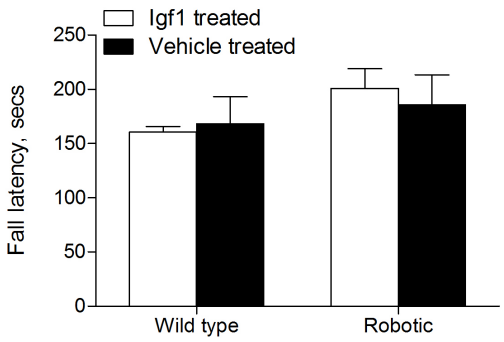


Figure 18. Rotarod performances show no difference in fall latency between mice treated with vehicle or IGF-1 at P70. Mice were injected for 4 weeks from P7.

P70 mice were then killed and the cerebellum was examined for signs of PC degeneration and death by immunohistochemical staining for calbindin (performed by Dr Peter Oliver). As expected, vehicle-treated *robotic* mice presented a small but significant loss of PCs in the anterior lobes, the surviving cells presenting the typical signs of degeneration with swelling of bodies and dendrites, and thickening of axonal torpedoes (**Figure 19A**). The efficiency of IGF-1 delivery by subcutaneous injection was confirmed: levels of IGF-1 in cerebella from *robotic* mice injected with IGF-1 were restored to a normal level (**Figure 19C**). Interestingly, the cerebellum of IGF-1-treated mice showed little or no cell loss, with a marked reduction in the early signs of degeneration, indicating that administration of IGF-I had effectively slowed down the degenerative process, in particular the progression of cell death, even if it did not prevent ataxia from occurring. Upregulation of the IGF-1 signaling pathway was confirmed as increased levels of p-IGF-1R and p-ERK1/2 were

detected on sections from IGF-1-treated *robotic* mice, IGF-1R and ERK1/2 phosphorylation being restored to a similar level than in wild-type (**Figure 19B**).

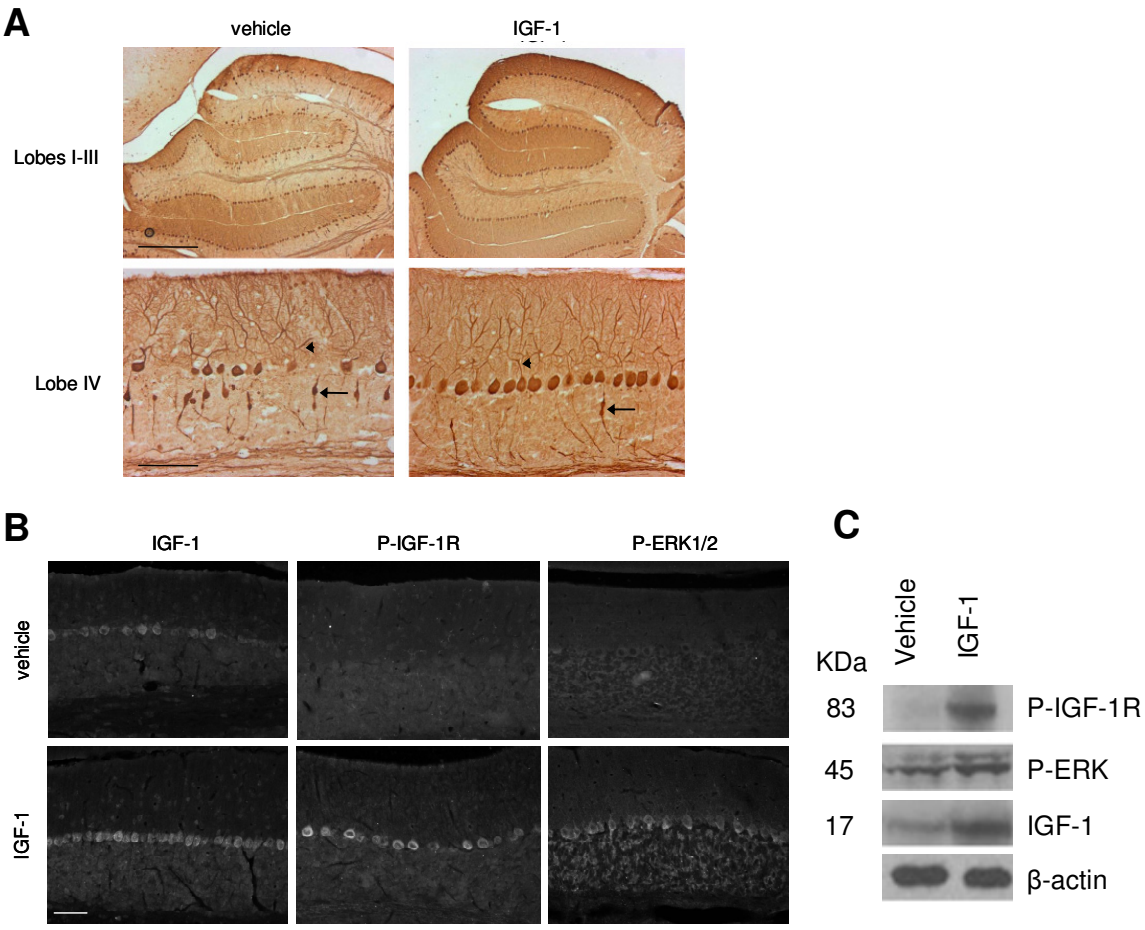


Figure 19. Treatment of *robotic* mice with IGF-1 slows down PC death. P7 robotic mice were injected daily for 4 weeks with IGF-1 at 1 mg/kg or the vehicle (n=7 in each group). (**A**) Analysis of PC degeneration in the cerebellum following IGF-1 treatment at P70. Parasagittal sections were immunostained for calbindin (performed by Dr Peter Oliver). Typical signs of PC degeneration including swelling of PC dendrites (arrow) and axonal torpedoes (arrowhead) can be observed. Scale bars, 1mm (lobes I–III); 100µm (lobe IV). (**B**) Analysis of IGF-1 pathway activation in the cerebellum following IGF-1 treatment at P70. Parasagittal sections were immunostained for IGF-1, p-IGF-1R, and p-ERK1/2. To enable a direct comparison, pictures were taken using the same exposure time. Scale bar, 100µm. In **A** and **B**, images are representative of the results obtained for three animals from each group. (**C**) Western blots representative of 3 independent experiments showing the levels of IGF-1, P-IGF-1R, P-ERK in cerebella from *robotic* mice treated with vehicle or IGF-1.

3.3. Discussion

In this study Af4 was discovered as the first negative transcriptional regulator of the Igf-1 pathway in the cerebellum. Deficits in activation of the Igf-1 pathway were shown to be involved in the early pathogenesis of PCs degeneration that takes place in the cerebellum of the ataxic *robotic* mouse (**Figure 20**).

3.3.1. Compartmentalized *Af4* expression pattern and regional PC degeneration are correlated

An accurate spatiotemporal expression of *Af4* during normal postnatal PC development was determined by exploiting LCM technology. *Af4* levels of expression differed between the anterior and posterior lobes and lobe X, highlighting the structural and functional patterning of the cerebellum, which is divided in subsets of PCs with different mRNA expression profiles, potentially underlying synaptic circuit formation and refinement (Herrup and Kuemerle 1998; Oberdick, Baader et al. 1998; Attwell, Rahman 2001; Armstrong and Krueger-Naug 2001; Abteen, Holtzman et al. 2010). These data showed that *Af4* expression remarkably coincides with the regional susceptibility of a specific lobe to degenerate, suggesting that the accumulation of Af4 protein becomes toxic for PCs above a certain threshold. Indeed, the onset of degeneration at P21 correlates with the first detection of increased levels of *robotic* Af4 in PCs. This argument is also consistent with 1) *Af4* KO mouse presenting no sign of neurological impairment (Isnard, Core et al. 2000, Dr Peter Oliver, unpublished observations) and 2) the toxic mechanism occurring in the *robotic* mouse is a gain-of-function. Moreover, the *robotic* mouse presents a compartmentalized pattern of regional PC degeneration, a common feature in many ataxic mouse mutants (Isaacs, Oliver et al. 2003; Sarna and Hawkes 2003). For example, a recent study has investigated such specific pattern of PC in the *Lurcher* mutant and

showed that the pattern of PC survival reflected the expression of the constitutively expressed small heat shock protein HSP25 in the wild-type cerebellum, suggesting that HSP25 may play a neuroprotective role in the regions not affected by the degeneration (Duffin, McFarland et al. 2010). This study, with others, can be interpreted as different lobes may have a different gene expression and a different function but so far no study has confirmed this hypothesis (Herrup and Kuemerle 1998; Oberdick, Baader et al. 1998; Attwell, Rahman 2001; Armstrong and Krueger-Naug 2001; Abteen, Holtzman et al. 2010). Significantly, the *robotic* mouse is the first reported model of cerebellar ataxia in which the regional expression of the causative gene in the cerebellum determines the susceptibility of expressing cells to degeneration.

3.3.2. Af4 can be a positive or negative transcriptional regulator of a same gene in a tissue-dependent manner

In this study, the first confirmed transcriptional target of Af4, *Igf-1*, was discovered. A previous study in the Davies' group was the first to characterise the role of Af4 function as part of a transcriptional complex with the positive transcriptional elongation factor b, P-TEFb via interaction with both the Cdk9 catalytic (cyclin dependent kinase 9) and cyclin T1 positive regulatory subunits (Estable, Naghavi et al. 2002; Bitoun, Oliver et al. 2007). Af9 and Af10, two potent transcriptional activators, are also part of this complex (Shibuya, Taki et al. 2001; DiMartino, Ayton et al. 2002; Okada, Feng et al. 2005; Bitoun, Oliver et al. 2007). This complex then links RNA polymerase II to histone H3 and mediates Dot1-dependent methylation of H3-K79 which allows localised changes in chromatin structure and facilitates transcription. Surprisingly, the microarray study suggested that Af4 could function not only as a positive regulator of transcription, but also as a negative regulator. In accordance with this finding, other studies have shown that methylation of H3K79 by Dot1, which is typically associated with transcriptionally active chromatin, could also be

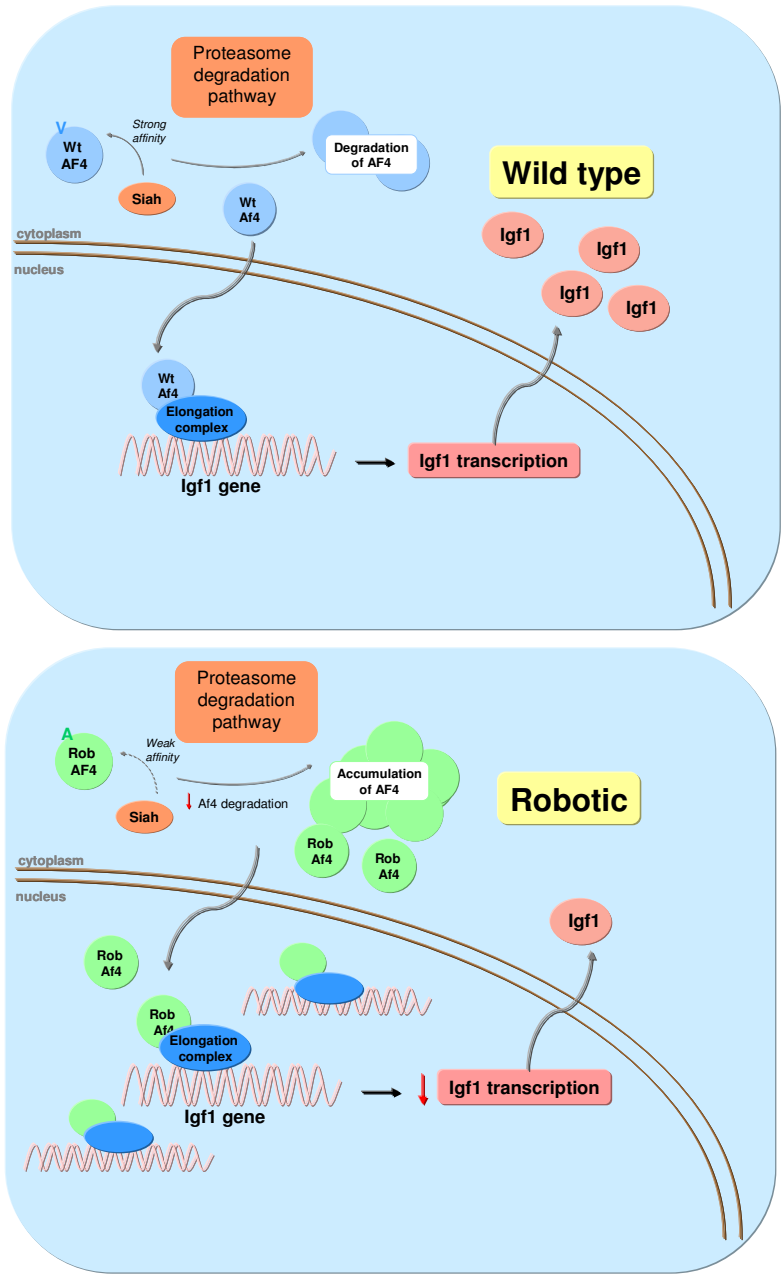


Figure 20. Summary: Af4 accumulates in the robotic PCs leading to *Igf-1* transcription deregulation. In the *robotic* mouse, mutated Af4 is not degraded as efficiently as wild-type Af4 and accumulates in PCs. This in turn enhances *Igf-1* regulation by Af4 transcriptional complex and leads to downregulation of *Igf-1* transcription.

found in repressed genes (Zhang, Xia et al. 2006; Steger, Lefterova et al. 2008). In addition, Af5q31 which is the closest ALF family member to Af4 was previously shown to repress transcription of HIV-I (Niedzielski, Hopewell et al. 2007). Moreover, ChIP studies found that binding of Af4 was identified across the *Igf-1* locus but predominantly localised within the proximal transcribed region of the gene implying that Af4 transcriptional

complex may be involved in transcription elongation. This is consistent with a previous study that described a similar distribution of P-TEFb and Dot1 across actively transcribed loci (Ni, Schwartz et al. 2004; Bitoun, Oliver et al. 2007; Steger, Lefterova et al. 2008).

This study also showed that the Af4-containing transcriptional complex mediates contrasting effects in a tissue-specific manner: repression of *Igf-1* transcription occurs in the cerebellum and thymus while activation of *Igf-1* transcription occurs in bone marrow and lens. This tissue-specific gene expression is probably regulated by a combination of transcription factors that work together to achieve tissue specificity (Yu, Lin et al. 2006). Thus, Af4 is likely to binds to other transcription factors dependent on the tissue, which will orientate its activity toward a positive or negative transcriptional regulation.

This study of Af4 also shed some light on the function of the additional members of the ALF family LAF4, FMR2 and AF5q31; indeed, they have all been predicted to be transcription factors due to the transactivation domain (TAD) they all share with AF4 (Bitoun, Oliver et al. 2007). However, no functional studies have been published to date. Moreover, the ALF proteins share four other highly conserved domains ranging from 60 to 88% homology (Bitoun, Oliver et al. 2007). This high homology between the family members let us hypothesised that they may also share some common functions. To support this argument, *Af4* and *Af5q31* KO mice present no neurological symptoms, while *Fmr2* KO mouse shows mild learning and memory deficiency but no evidence of PC death or ataxia; the hippocampus being more specifically affected (Isnard, Core et al. 2000; Gu and Nelson 2003; Urano, Endoh et al. 2005). These observations imply that the other family members may compensate for the missing member, and thus that they may have similar roles. Moreover, it was shown in the laboratory that Laf4 and Fmr2 are both expressed in the same nuclear compartment and bind to the same transcriptional protein complex (Af9, Enl, P-TEFb, and Dot-1) as Af4 (Monroe, Jo et al. 2010; Simon D'Alton and Justin Moore, unpublished data). These data suggest that the ALF members are

transcriptional factors with overlapping roles. It would be interesting to test if both Fmr2 and Laf4 regulate *Igf-1* gene transcription. If that was the case, and as they are both expressed in the hippocampus, the subventricular zone and upper layer of cortical plate, it would imply that Igf1 could also have a role, not only in PCs survival in the cerebellum which is well established, but in cortical cell proliferation and survival as suggested previously (Wilkins, Chandra et al. 2001). Indeed, preliminary data in the laboratory suggested that loss of *Laf4* in brain slices from wild-type brains electroporated with shRNA *Laf4*, impaired cortical cell division and migration in the cortex (Justin Moore, unpublished data). Interestingly, two recent studies showed that Laf4 binds to Af9 and that the cortex of *Af9* KO mice presented similar impaired pattern of cortical cell division and migration as in knock-down Laf4 brain slices (Büttner, Johnsen et al. 2010; Monroe, Jo et al. 2010). Taken together, this confirms that 1) ALF family members have common binding partners 2) ALF family members may potentially have a role in cortical cell development (Büttner, Johnsen et al. 2010; Monroe, Jo et al. 2010).

Moreover, a recent study showed that Af4 and Fmr2 co-localised with transcription factor Af9 in PCs of the cerebellum, the hippocampus and cortical subventricular zone (Vogel and Gruss 2009). Interestingly, a loss-of-function mutation in AF9 has been reported in a patient with similar symptoms as described in the *robotic* mouse and/or FRAXE patients, i.e neuromotor development delay, cerebellar ataxia, mental retardation, severe delay in language acquisition and communication skills, and epileptic seizures (Pramparo, Grosso et al. 2005). Thus, ALF proteins may have a functional relation to the developing ceberellum as well as other regions of the brain.

Finally, members of the ALF family might also have a role in non-neuronal cells and may be involved in the abnormal development of hematopoietic cells in leukemia. Indeed AF4, LAF4 and AF5q31 were originally cloned due to their fusion with MLL (mixed lineage leukaemia) in different chromosomal translocations causing acute lymphoblastic

leukaemia (ALL) (Hiwatari, Taki et al.; Taki, Kano et al. 1999; Chinen, Taki et al. 2007). Moreover, a recent study showed that fusing the pTEFb-interacting domain of AF4 family members to MLL was necessary and sufficient for leukemic transformation and they hypothesised that these MLL fusion protein complexes have a crucial histone methyl transferase activity that leads to aberrant expression activation of genes critical for leukemia (Monroe, Jo et al. 2010). Thus, studying the pathways occurring in the bone marrow of the *robotic* and *Af4* KO mouse may be beneficial as it may unravel the role of AF4 (and other ALF family members) in the onset and progression of leukemia.

3.3.3. Study of the *robotic* mouse confirmed the crucial role of IGF-1 for PCs survival and its role in non neuronal tissues

It is well known that IGF-1 stimulates neurogenesis and synaptogenesis in many parts of the CNS, and specifically promotes differentiation and survival of PCs in the cerebellum (Croci, Barili et al. 2010; Torres-Aleman, Pons et al. 1992; O'Kusky, Ye et al. 2000; Fukudome, Tabata et al. 2003). This study confirmed the crucial role of IGF-1 in PCs survival. Similarly, a recent publication demonstrated the link between *Igf-1* gene deregulation and PCs degeneration in a knockout mouse for another transcription factor, Ebf2 (Croci, Barili et al. 2010). In this *Ebf2* KO mouse, the EBbf2 loss-of-function led to *Igf-1* transcription downregulation which in turn inhibited the pro-survival PI3K signalling pathway (Croci, Barili et al. 2010). As mice died at birth no defects in their motor coordination could be assessed; however, similar to our *in vivo* findings, treatment of mutant brain slices with IGF-1 prevented PCs death confirming the importance of accurately regulating *Igf-1* to facilitate PCs survival (Croci, Barili et al. 2010).

IGF-1 pathway has been extensively studied and IGF-1 protective effect on cell survival originates from the interaction of the IGF-1R with one of its major substrates, insulin

receptor substrate 1 (IRS-1), which activates phosphatidylinositol 3-kinase (PI3K) and Akt/protein kinase B (PKB) (Torres-Aleman, Pons et al. 1992; Basergaa, Hongoa et al. 1997). Another alternative cascade involves serine/threonine kinase Raf, MAP Kinases (MEK1/2), and extracellular signal regulated kinases (ERK1/2) (Peruzzi, Prisco et al. 1999; Shelton 2004). IGF1R also acts as modulator of ion channels and IGF-1 binding to IGF-1R also leads to activation of voltage-dependent calcium channels; thus, causing large transient increases in the Ca^{2+} levels which have been suggested to activate the ERK1/2 pathway (**Figure 21**) (Torres-Aleman, Pons et al. 1992; Schmidt, Goebeler et al. 2000). The activation of the AKT pathway has been shown to inhibit apoptosis in most cell types while the ERK1/2 pathway is primarily known for mitogenic signaling and for modulating cell survival in most model systems (Torres-Aleman, Pons et al. 1992; Myers, Grammer et al. 1994; Dudek, Datta et al. 1997; Kulik, Klippel et al. 1997; Lawlor and Alessi 2001; Johnson and Lapadat 2002; Chang, Steelman et al. 2003; Brazil, Zhong-Zhou et al. 2004).

In this study, we focussed only on the ERK pathway as it is supposedly involved in cell death (Chang, Steelman et al. 2003). In accordance with this potential signalling pathway for IGF-1, it was showed that downregulation of *Igf-1* transcription leads to deregulation of ERK1/2 activation. ERK1/2 deregulation was also confirmed in the non-neuronal tissues affected in the *robotic* mouse (data not shown) confirming the role of IGF-1 in other organs.

IGF-1 has also been shown to have a crucial role in many other non-neuronal tissues. As an anabolic factor, IGF-1 is essential for embryonic and postnatal growth and development, as illustrated by a severe growth deficiency in the various *Igf-1* null mice (Baker, Jeh-Ping et al. 1993; Liu 1993; Powell-Braxton, Hollingshead et al. 1993). Moreover, IGF-1 plays important regulatory roles in the early stages of both B- and T-cell maturation as well as lens development (Landreth, Narayanan et al. 1992; Walker, Liping

et al. 2002; Welniak, Sun et al. 2002; Ebong, Chepelinsky et al. 2004). In addition, a number of studies have reported deregulation of the IGF-1 signalling pathway in both cases of ALL and cataract formation (Blatt 2000; Khatib, Levi et al. 2004; Ruberte, Ayuso et al. 2004; Kubo, Singh et al. 2005). The *robotic* mouse allow the confirmation of IGF-1 crucial role in non-neuronal tissues as its deregulation could explain the non-neurological features of the *robotic* mouse (growth retardation, impaired T-cell development, and

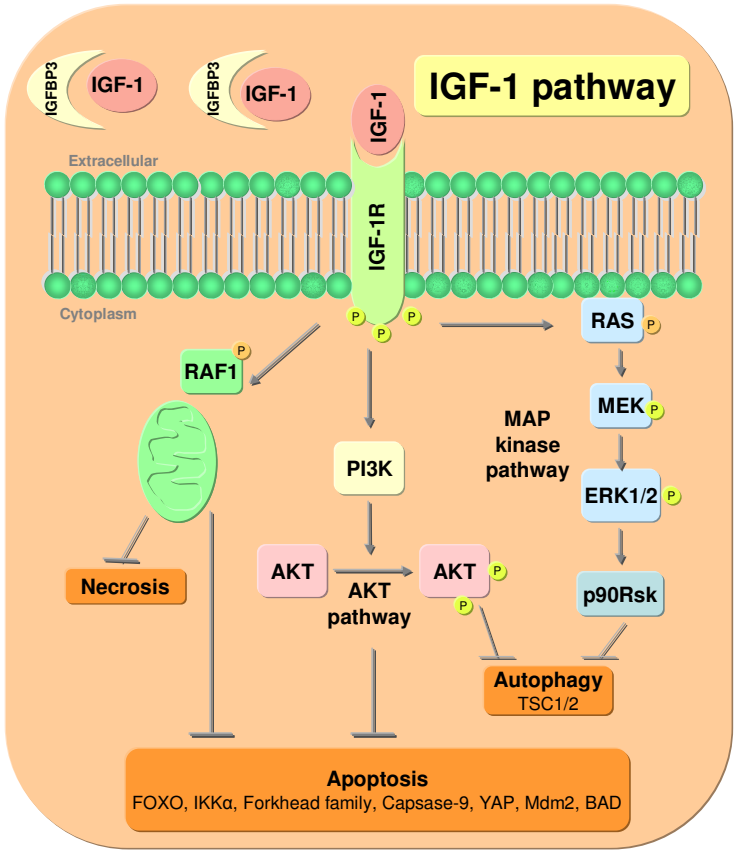


Figure 21. The IGF-1 pathway regulates cell survival. IGF-1 and IGF-1R provide a potent proliferative signalling system that stimulates growth in many different cell types and blocks apoptosis, autophagy and necrosis. IGF-1R activates three main signalling pathways: AKT, ERK and interaction of RAF1 with mitochondria.

cataracts) and the *Af4* KO mouse (impaired B-cell development). Similar signalling cascades may occur in non-neuronal tissues; however, further studies would be required to investigate the transcriptional regulatory roles of the Af4 complex on *Igf-1* gene expression specifically in these non-neurological tissues.

3.3.4. The mechanism of cell death in the *robotic* mouse is still unclear

Igf-1 deregulation occurs in the *robotic* mouse throughout the PC degenerative process but also before its onset suggesting that the deregulation of the Igf-1 pathway is an important primary causative event in the pathogenesis of the *robotic* cerebellum. Moreover, treatment of P7 pre-symptomatic *robotic* mice with IGF-1 markedly delayed the progression into PC death; and although IGF-1 treatment could not restore the phenotype entirely, it still provides *in vivo* evidence that the Igf-1 pathway is implicated in the pathological cascade that leads to PC death. However, the final pathway leading to cell death is still unclear. As discussed in Chapter 1, the last step of the cell death cascade can occur through apoptosis, autophagy and necrosis, three mechanisms that can be activated through IGF1 pathway (**Figure 21**). Previous studies in the Davies group excluded an apoptotic mechanism occurring in PCs of the *robotic* mouse based on the lack of DNA fragmentation or activation of the pro-apoptotic key markers caspase-3 and Bcl-2 (Isaacs, Oliver et al. 2003, unpublished observations). The swelling of PC bodies and dendrites observed in the early stages of the degeneration process, however, tends to suggest autophagic or necrotic pathways. Indeed, recent studies have shown that IGF-1 regulates autophagic vesicles turnover and that their accumulation leads to PC death (Bains, Florez-McClure et al. 2009). Moreover, decreased levels of IGF-1 have previously been associated with neuronal cell death by necrosis (Villalba, Bockaert et al. 1997). Ultrastructural analysis of *robotic* PCs by electron microscopy could not detect any autophagic vesicles (unpublished data), suggesting that autophagy may not be responsible for PCs death even if it appeared to be the most plausible hypothesis, as autophagy is regulated by the ERK1/2 cascade following IGF-1 deregulation (Cagnol and Chambard 2010) (**Figure 21**). The difficulty in detecting the cell death pathway is amplified by the fact that the cell death in the *robotic* cerebellum occurs over a long time

period; it is therefore very unlikely that ultrastructural analysis on a single PC in a brain section would catch a cell in the process of degenerating.

3.3.5. The study of *robotic* mouse confirmed IGF-1 as a potential therapeutic target for ataxia

No mutation in *AF4* has been identified in ataxic patients so far; however the IGF-1 deficiency degenerative pathway that takes place in the *robotic* mouse model may prove directly relevant to one of the many forms of human cerebellar ataxias as well as forms of mental retardation (Fernandez, Carro et al. 2005).

Interestingly, a *Mecp2* KO mouse model of Rett mental retardation syndrome has illustrated the function of the MeCP2 transcription factor in both activation and repression of transcription, similar to Af4 (Amir, Van den Veyver et al. 1999; Guy, Hendrich et al. 2001; Chahrour, Jung et al. 2008). Mecp2 was shown to couple DNA methylation-mediated chromatin remodelling to transcriptional regulation (Chahrour, Jung et al. 2008). A microarray performed from *Mecp2* KO and wild-type cerebella identified *Af4* gene as one of the genes to be upregulated (2-fold) in *Mecp2* KO. Moreover, using ChIP, *Af4* expression was shown to be directly repressed by Mecp2 (Urdinguio, Lopez-Serra et al. 2008). This finding raises the possibility that MeCP2 and Af4 may be part of the same pathway and that any deregulation of this pathway, either by AF4 accumulation or loss/dysfunction of the upstream MeCP2, can lead to neuronal degeneration and ataxia. Consistent with this hypothesis, PCs loss occurs in the cerebellum of Rett patients and IGF-1 treatment of MeCP2 mutant mice also partially rescued Rett syndrome symptoms including a marked improvement in locomotor activity (Oldfors, Sourander et al. 1990; Tropea, Giacometti et al. 2009).

Deregulation of the IGF-1 signaling pathway secondary to disease-specific mutations is a recurrent finding in mouse models and human patients with cerebellar ataxia, and thus represents a common pathological cascade in neuronal cell death that may be targeted for treatment (Fernandez, Carro et al. 2005; Gatchel, Watase et al. 2008). Moreover, many human disorders presenting IGF-1 deficiency were also characterized by growth retardation and mental retardation suggesting that the IGF-1 pathway also plays an important role in cognitive function, especially in learning and memory (Sonntag, Lynch et al. 2000; Bonapace, Concolino et al. 2003; van Nieuwpoort and Drent 2008).

As shown in our study, injection of IGF-1 subcutaneously may not be sufficient to restore a normal phenotype, even if the treatment was started early in the ataxia process i.e. before any ataxic symptoms occur. Higher doses of IGF-1 and injections performed directly in the organ affected in the ND process may have better effects (Fernandez, de la Vega et al. 1998). However, the reduction of PCs death observed in *robotic* cerebella treated with IGF-1 confirmed that IGF-1 could still be used as a potential therapy for ataxia. To follow-up these interesting findings, the next step would be to investigate whether IGF-1 treatment would prove to be beneficial if delivered late in the disease process, i.e. after the *robotic* mouse would have developed demonstrable ataxia. Indeed, such an approach would be more relevant for future application in human, as the treatment usually starts only after onset of the first symptoms. An adeno-associated virus (AAV) vector bearing IGF-1 would have to be administrated in the CNS as described previously (McBride, Ramaswamy et al. 2006; Ridet, Bensadoun et al. 2006; Dodge, Haidet et al. 2008). Indeed, injection of AAV-IGF-1 vectors in the deep cerebellar nuclei reduced ALS neuropathology and significantly extended life span in ALS mice (Dodge, Haidet et al. 2008). As the direct injection of AAV-IGF-1 in the part of the brain affected may be quite challenging technically and hard to translate readily for human treatment, systemic AAV-IGF-1 administration through the tail vein may also be tested; this method

was used in a promising study utilising a diabetic mouse model in which hypoalgesia as well as mouse mobility were improved (Chu, Moreland et al. 2008).

With the identification of Af4 as a negative regulator of *Igf-1* gene expression in the cerebellum, and possibly in other regions of the brain, this work opens new avenues of research into the manipulation of the IGF-1 signaling pathway for the treatment of a whole range of human NDDs, in particular for cerebellar ataxias (Fernandez, Carro et al. 2005; Zhong, Deng et al. 2005; Vig, Subramony et al. 2006; Ebert, Beres et al. 2008; Palazzolo, Stack et al. 2009). Importantly, this work has also demonstrated that the use of LCM combined with microarrays is a practical approach to identify the transcriptional profile of small sub-sets of neurons.

4. OXR1 as a protector against oxidative stress-induced neurodegeneration

The *bella* mouse was identified as part of the Harwell ENU mutagenesis screen based on its obvious ataxic gait. *Bella* mice are indistinguishable from their control littermates at P14; however they rapidly develop a severe ataxic gait, fail to gain weight as quickly as controls, and do not survive beyond P26 (**Figure 7**). Pathological analysis of the *bella* CNS revealed significant and increasing number of apoptotic cells in the granule cell (GC) layer (GCL) of the cerebellum from P18 onwards (**Figure 7**), although no cell death was observed in any other region of the brain in end-stage mutants or mice heterozygous for the *bella* deletion.

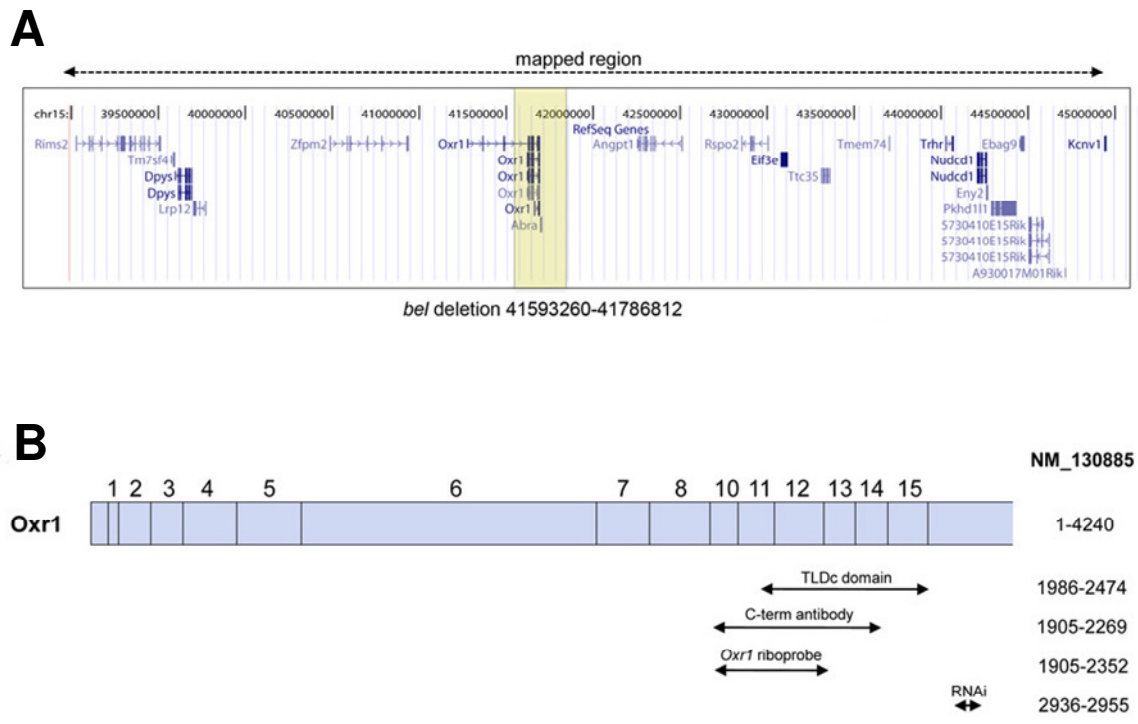


Figure 22. A 193.5kb region is deleted in the *bella* mouse. (**A**) Annotation of mouse chromosome 15 showing the critical mapped genetic region for the *bella* phenotype. (**B**) Schematic diagram of the full-length mouse *Oxr1* exonic structure and relative positions of regions used for production of antibodies and probes.

Positional cloning was carried out in the Davies' group to determine the potential mutation introduced by the ENU strategy. Surprisingly, a spontaneous deletion of a 193.5kb region was indentified, spanning two genes: the oxidation resistance 1 (*Oxr1*) and the striated muscle activator of Rho signalling (*Abra* or *Stars*) (**Figure 22**). To rule out any potential effects on promoter sequences, the expression of neighbouring genes (5Mb downstream or upstream of *Oxr1*) was assessed in the Davies' group and no changes were detected. A previous study showed by Northern blot that *Oxr1* was most abundant in brain and skeletal muscle, although it was also detected in placenta, lung, liver, kidney, and pancreas tissues, and was expressed under three different isoforms (2.9 and 4.9 kb and 5.1kb) (Elliott and Volkert 2004). The mouse *Abra* gene is much smaller than *Oxr1* (1kb) coding for predominantly one transcript form (381 amino acids) and is expressed in adult skeletal muscle and heart tissue only (Arai, Spencer et al. 2002; Arai, Spencer et al. 2002). These data were confirmed by *in situ* hybridizations performed in the Davies' group: *Oxr1* is expressed in all major regions of the brain, including the cerebellar GC layer affected in the *bella* mouse while *Abra* is not detected, suggesting that loss of *Oxr1* is responsible for the *bella* phenotype (**Figure 8**).

Oxr1 was first identified in a screen for genes that could confer resistance against oxidative stress (OS); indeed *Oxr1* was able to suppress DNA damage in *Escherichia coli* oxidative repair-deficient mutants (Volkert, Elliott et al. 2000). Moreover, it was found that, when the human protein localised to the mitochondria, it could prevent oxidative damage in *Saccharomyces cerevisiae* mutants lacking *Oxr1* (Elliott et al. 2004). *Oxr1* is found in all eukaryote genomes; however, nothing is known in mammalian systems about this obviously significant gene.

As OS is a major component of many NDDs and the link between OS and ND is still unclear, it was decided to further characterise the *bella* mutant and the function of Oxr1;

particularly as the widespread expression of the gene suggests that it may play a more general role in neuronal function outside of the cerebellum. This chapter describes the analysis of Oxr1 role in the *bella* mouse and its involvement in GCs survival and how its deletion leads to the *bella* phenotype. It is also investigated if OXR1 could be involved in ALS, a NDD that has been reported to display an increase in OS in the regions affected.

Aims:

- **Confirm that loss of cerebellar neurons in the *bella* mouse is due the deletion of *Oxr1*** using primary cell culture in which the levels of Oxr1 are modulated.

- **Determine spatiotemporal expression and cellular localisation of Oxr1 in mammalian cells** using western-blotting, cell fractionation, and immuno-cytochemistry.

- **Study Oxr1 function and its potential role as a general neuro-protector factor** by assessing cell survival in correlation with Oxr1 expression levels both *in vitro* and *in vivo.*

- **Investigate the potential involvement of OXR1 in the ALS pathology** by determining OXR1 levels in biopsy samples from patients with ALS and in a mouse model of ALS, the SOD-1 G93A transgenic mouse.

4.1. Study of the *bella* mouse phenotype

4.1.1. As a consequence of *Oxr1* deletion in the *bella* mouse, *bella* granule cells are more sensitive to oxidative stress than wild-type granule cells

Pathological analysis of *bella* cerebella revealed significant and increasing number of apoptotic granule cells in the *bella* granule cell layer from P18 onwards; to model this phenomenon using primary cells, GCs from P7 mice were cultured for 14 days to ensure that results were obtained at a time point relevant to the *in vivo* situation. Hydrogen peroxide (H_2O_2) treatment (150µM for 4h) was used to simulate OS. Optimisations of the duration and amount of stress were first carried out to ensure that cell death was detectable but not too severe. GC cultures were confirmed to be composed of 90% GCs using GABA(A) Receptor α6 as a marker specific for GCs (data not shown). Comparing *bella* and wild-type GCs under these conditions it was confirmed that *bella* mutant GCs were significantly more susceptible to exogenous peroxide-induced apoptosis than wild-type (**Figure 23A**). To demonstrate that loss of *Oxr1* rendered neurons from *bella* mice more susceptible to OS, *Oxr1* was knocked-down using a shRNA in wild-type GCs, and cell sensitivity to H_2O_2 was assessed as previously. The shRNA construct was selected to knock-down all *Oxr1* isoforms and qRT-PCR was used to confirm that less than 10% of Oxr1 endogenous levels were consistently obtained (**Figure 22 and 24A**). This level of *Oxr1* knock-down resulted in almost twice the level of cell death compared to neurons transfected with control constructs (**Figure 24B**).

To confirm the specific role of Oxr1 in OS-mediated cell death, a serum starvation treatment was used in place of H_2O_2. No difference was detected between *bella* and wild-

type GCs, suggesting that the role of Oxr1 is specific to OS-related cell death (**Figure 23B**).

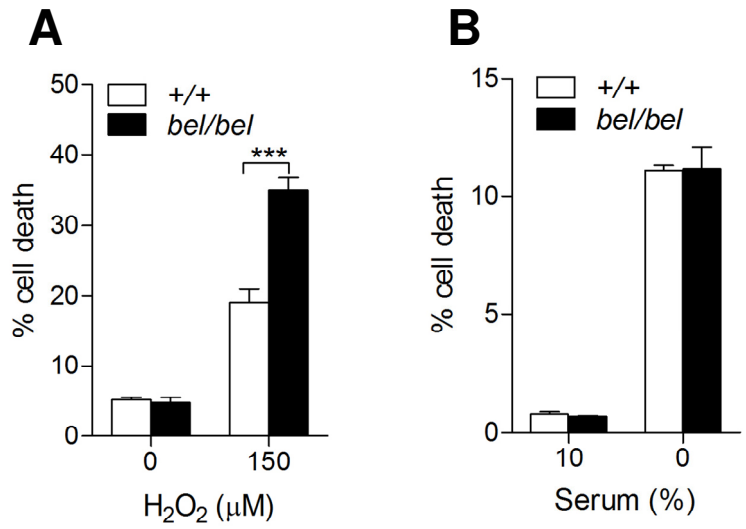


Figure 23. Oxr1 regulates sensitivity of GC neurons to OS specifically. (**A**) GCs from P7 *bella* (*bel/bel*) mice cultured for 14 days show a significant increase in apoptotic cell death compared to wild-type (*+/+*) when subjected to peroxide treatment. (**B**) Similar experiments were carried out using serum, and no difference is detected between *bella* (*bel/bel*) and wild-type (*+/+*) GCs. Asterisks indicate statistical significance (***$p < 0.001$; ANOVA).

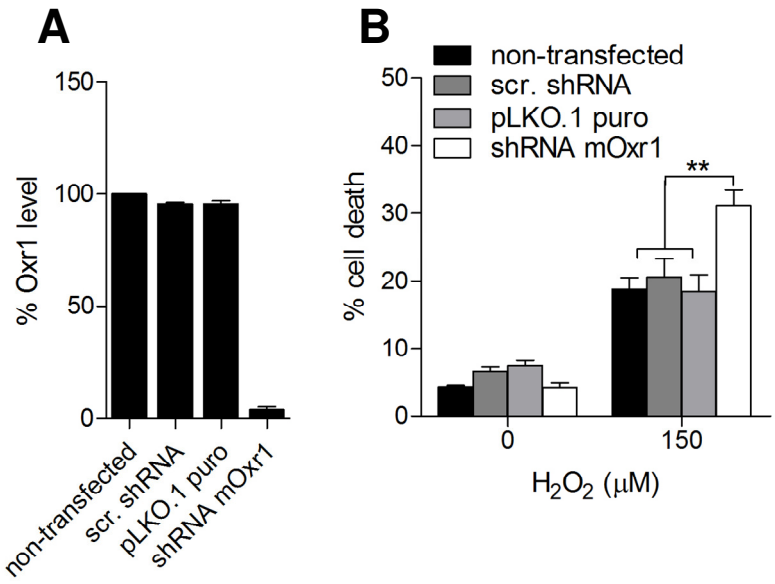


Figure 24. Oxr1 regulates sensitivity of GC neurons to OS. (**A**) qRT-PCR of relative total *Oxr1* expression level after knock-down from 3 independent experiments. (**B**) Wild-type GCs transfected with an *Oxr1* shRNA knock-down construct show a significant increase in apoptotic cell death compared to cells with the mock vector (pLKO.1puro) and scrambled shRNA transfected (scr. shRNA). Asterisks indicate statistical significance (**p < 0.01 ; ANOVA)

Then it was investigated whether loss of *Oxr1* would also render non-cerebellar neurons susceptible to OS. Indeed, end-stage mice only presented apoptotic cells in the cerebellar GCL despite *Oxr1* being expressed in high levels in other brain regions including the cortex as shown by *in situ* hybridisations (**Figure 8**). Sensitivity to OS was assayed in wild-type cortical cells (CCs) in which *Oxr1* was knocked-down by shRNA as above. Only a small but still significant increase in peroxide-induced cell death was observed in knocked-down CCs compared to cells infected with control vectors, suggesting that in cerebellum Oxr1 levels play a more defining role in neuronal survival than in other parts of the brain, consistent with the specificity of ND in *bella* mice (**Figure 25**).

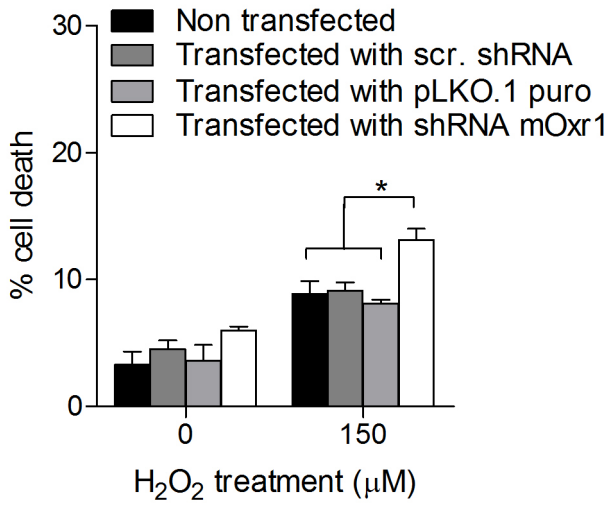


Figure 25. Primary cortical cells are less sensitive to loss of *Oxr1*. Wild-type cortical cells treated with H_2O_2 and transfected with the *Oxr1* shRNA result in a small but significant increase in apoptotic cell death compared to mock transfected (pLKO.1 puro) and scrambled shRNA (scr. shRNA) transfected controls (*$p < 0.5$; ANOVA).

4.1.2. DNA damage specifically occurs in *bella* granule cells

To understand more about the cause of GC degeneration in the *bella* mouse, it was decided to further characterise the *bella* cerebellum. Indeed, as discussed in chapter 1, increases in OS in cells can affect proteins, lipids or DNA, therefore specific markers representing by-products of cellular damage were used to assess *bella* and wild-type GCs. No difference in protein or lipid damage was detected between *bella* and wild-type GCs by immunofluorescence, while an increase in 8-hydroxydeoxyguanosine (8-OHdG) staining, a marker for DNA damage, was clearly detectable (**Figure 26**). Quantification of lipid peroxidation from *bella* and wild-type GCs treated with H_2O_2 confirmed that no difference in the levels of lipid degradation was observed in *bella* or wild-type mouse (**Figure 27A**). Moreover, the increase in DNA damage in *bella* mouse was also confirmed using immunohistochemistry on *bella* and wild-type cerebellar sections (**Figure 27B**).

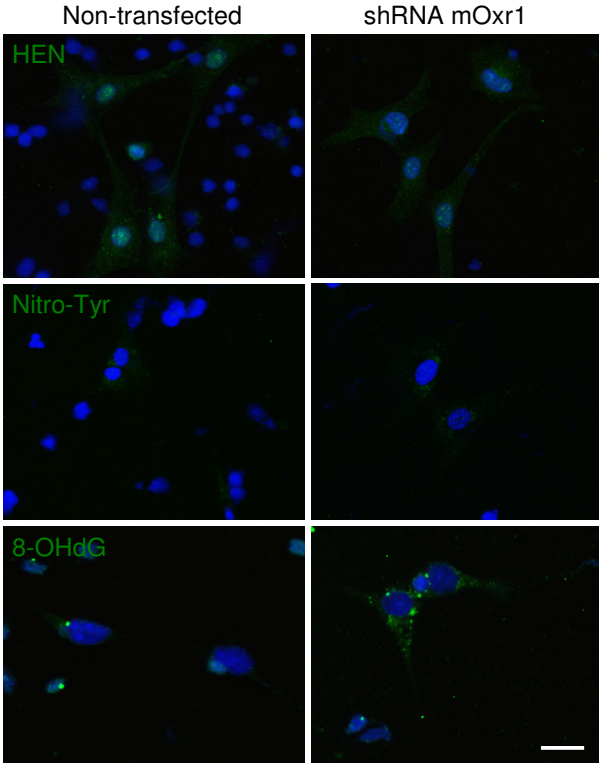


Figure 26. Loss of *Oxr1* induces DNA damage. Wild-type GCs treated with H_2O_2 and transfected with the *Oxr1* shRNA were stained for various markers of oxidative-induced damages to lipid (HEN), protein (Nitro-Tyr) and DNA (8-OHdG). Staining of 8-OHdG is increased in cells transfected with the *Oxr1* shRNA compared to the non-transfected cells. Pictures are representative of 3 independent experiments.

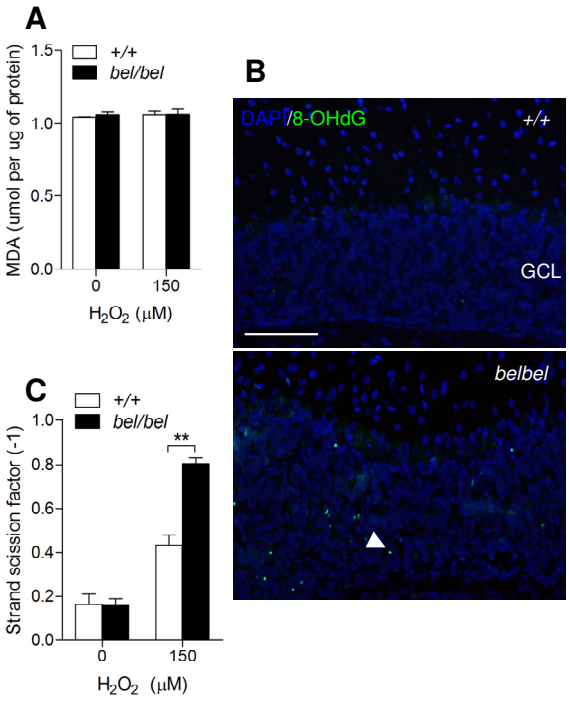


Figure 27. *Bella* GCs present an increase in DNA damage. (**A**) Lipid peroxidation as marker of oxidative damage to lipid was assessed in wild-type (*+/+*) and *bella* (*bel/bel*) GCs treated with H_2O_2. No significant difference is detected between (+/+) and (*bel/bel*) GCs. (**B**) P24 paraffin-sections were stained for DNA damage marker (8-OHdG). 8-OHdG-positive GCs are only detected in *bella* sections (arrowhead). (**C**) DNA damage was quantified using picogreen. A significant increase in DNA damage is seen in (*bel/bel*) GCs compared to (*+/+*) treated with H_2O_2. Asterisks indicate statistical significance (**$p < 0.01$; ANOVA)

To quantify the increase in DNA damage observed in *bella* GCs, DNA fragmentation, corresponding to the level of DNA damage, was assessed using the fluorescent marker picogreen. A significant increase in DNA damage in *bella* GCs compared to wild-type GCs was confirmed (**Figure 27C**). Taken together, this suggests that Oxr1 may have a role in preventing DNA damage in cells under OS conditions.

4.1.3. Deregulation of genes involved in the oxidative stress-response occurs in the *bella* mouse

To determine whether loss of *Oxr1* in *bella* mice affects the expression of key OS response genes, qRT-PCR was carried out from *bella* or wild-type whole cerebellar tissue. In this thesis, the expression of 17 genes involved in the OS-response was assessed in *bella* and wild-type brain and cerebellum, and the expression of two of these genes appeared to be significantly different in *bella* compared to wild-type tissues, the remaining genes were unchanged. The full list of genes tested can be found in appendix 4. A significant downregulation in *gpx* and *catalase* levels were detected in the ceberellum and brain respectively, but no significant difference in *sod1* and *sod2* levels (**Figure 28A and B**). Thus, the levels of catalase enzyme activity were quantified extracts from *bella* and wild-type brains and cerebella, but no significant difference was detected (**Figure 28C**). As the JNK pathway has very recently been shown to be induced by OS and to regulate *Oxr1* expression in *Anopheles gambiae*, it was investigated if JNK levels and JNK phosphorylation could be deregulated in *bella* brains and cerebella using western-blotting (Saitoh, Nishitoh et al. 1998; Adler, Yin et al. 1999; Finkel and Holbrook 2000; Martindale and Holbrook 2002; Jaramillo-Gutierrez, Molina-Cruz et al. 2010). JNK and phospho-JNK levels were unaffected in *bella* cerebella and brains compared to wild-type (**Figure 28D**).

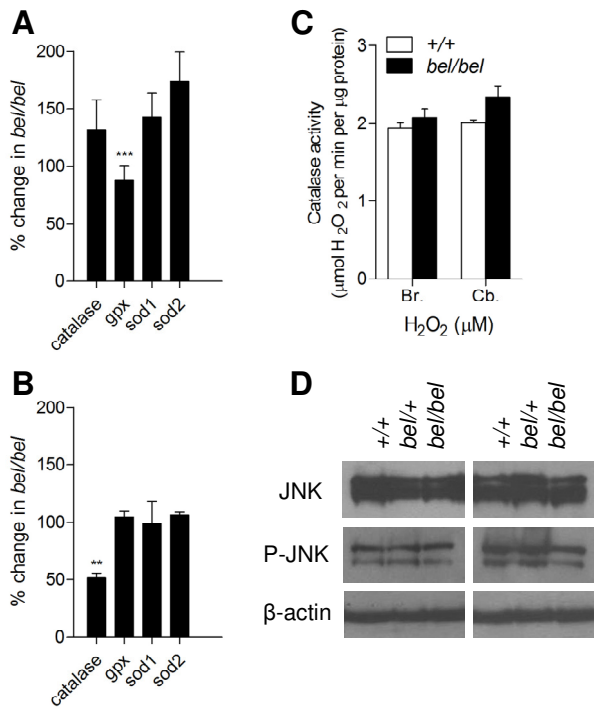


Figure 28. Genes involved in the OS-response are deregulated in the *bella* mouse. mRNA levels of *catalase, gpx, sod1* and *sod2* were determined by qRT-PCR from cerebellum (**A**) and brain (**B**) extracts. A significant difference is observed in the *catalase* and *gpx* levels in the *bella* brain and cerebellum respectively. (**C**) Catalase activity was quantified from wild-type (*+/+*) or *bella* (*bel/bel*) brain (Br.) and cerebellum (Cb.). No significant difference is detected. (**D**) Western blot showing JNK and phospho-JNK (P-JNK) from cerebellum extracts. No difference is seen between wild-type and *bella* JNK and P-JNK levels. Similar results were found in brain extracts. Asterisks indicate statistical significance (** $p<0.01$, *** $p< 0.001$; ANOVA)

4.2. Role of Oxr1 in the oxidative stress-response in mammalian systems

4.2.1. Restoring Oxr1 levels can rescue the *bella* phenotype both *in vitro* and *in vivo*

The combination of the tissue expression profile of *Oxr1* and the GC culture experiments strongly suggests that *Oxr1*, not *Abra*, is responsible for the *bella* phenotype. However, to confirm this hypothesis, *Oxr1* was replaced in *bella* GCs by lentiviral expression. Restoration of *Oxr1* levels was confirmed by qRT-PCR (**Figure 29A**). Restoration of *Oxr1* expression in *bella* GCs rescued the level of apoptotic cell death in H_2O_2-treated cells down to wild-type levels (**Figure 29B**). Similarly, to definitively prove that deletion of *Oxr1* caused the *bella* phenotype, a genetic rescue experiment with two independent *Oxr1* transgenic lines was performed by Dr Peter Oliver. Ubiquitous expression of the full-length *Oxr1* cDNA in the brain was confirmed by *in situ* hybridisation (performed by Dr Peter Oliver) in *bella* mutants carrying the transgene (*bel/bel*; Tg^{Oxr1}+/-) (**Figure 29C**). Animals

of this genotype displayed no ataxia or growth defects, and no cell death was detected in any region of the brain, including the cerebellar GCL, compared to littermates that did not contain the *Oxr1* transgene (*bel/bel*; Tg^{Oxr1} -/-) (**Figure 29C**). These data confirm that ND in *bella* is caused by loss of *Oxr1*.

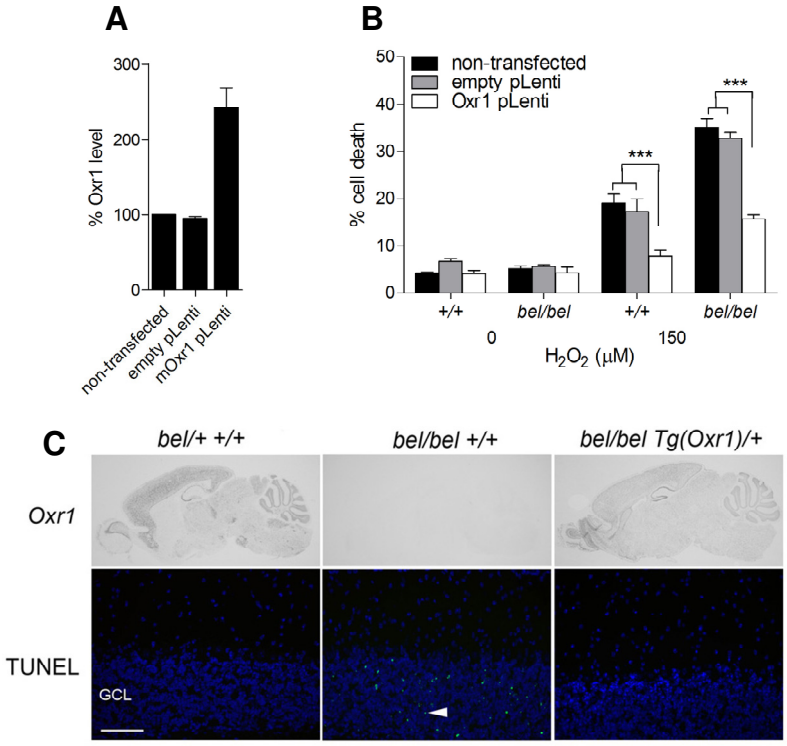


Figure 29. The *bella* phenotype can be rescued by an *Oxr1* transgene. (**A**) qRT-PCR of relative total *Oxr1* expression level after lentiviral over-expression from 3 independent experiments. (**B**) GCs were cultured as above and infected with *Oxr1*-FL constructs in a pLenti expression vector. After peroxide treatment, the proportion of apoptotic cells was assessed, showing that *Oxr1*-FL construct is effective at preventing cell death in both wild-type (+/+) and *bella* (*bel/bel*) GCs. Asterisks indicate statistical significance (***$p < 0.001$; ANOVA). (**C**) *In situ* hybridisations of *Oxr1* from littermates at P24 show the ubiquitous expression of the *Oxr1* transgene (from *bel/bel Tg(Oxr1)/+* sections) in the brain. Two independent lines of *bel/bel Tg(Oxr1)/+* 'rescue' mice (one shown in figure) show no ataxia and no apoptotic cell death in the cerebellum as shown by TUNEL staining (arrowhead) compared to control *bella* mice that do not express the transgene (*bel/bel +/+*), demonstrating that replacement of *Oxr1* is sufficient to rescue the *bella* phenotype. Scale bar 50μM.

4.2.2. Overexpression of Oxr1 protects cells against oxidative stress

It was then determined whether Oxr1 could protect neurons exposed to stress by over-expressing *Oxr1* in wild type GCs. From quantification of lentiviral expression of the *Oxr1*

construct, it was shown that Oxr1 was expressed at approximately twice its endogenous level (**Figure 29A**). Interestingly, lentiviral overexpression of *Oxr1* in wild-type GCs led to a significant reduction in apoptosis compared to cells expressing endogenous levels of the gene, the level of apoptosis being inversely proportional to Oxr1 level in the cell (**Figure 29B**). This demonstrates that Oxr1 can also protect neurons exposed to stress.

4.3. Oxr1 expression and its functional regulation

4.3.1. Oxr1 is expressed as different isoforms in various tissues

As previous data on the tissue distribution of *Oxr1* have only been at the RNA level, and to further characterize *Oxr1* expression in relation to the timing of cell death in *bella* mice, Oxr1 levels were determined by western blot using protein extracts from various tissues at a range of time points (P0, P3, P7, P14, P17, P21, P28 and P56). Oxr1 was expressed in the brain and cerebellum at high levels, and in skeletal muscles and heart to a lesser extent from P17 (**Figure 30A**). Oxr1 levels were generally lower during the first 2 weeks. Interestingly, Oxr1 isoforms were expressed in a tissue-specific manner. Three isoforms were present in the brain (84, 55 and 40 kDa), while only two were in the cerebellum (84 and 40kDa). In skeletal muscles and heart an intermediate isoform and long isoform (Oxr1-FL) were respectively present (**Figure 30B**).

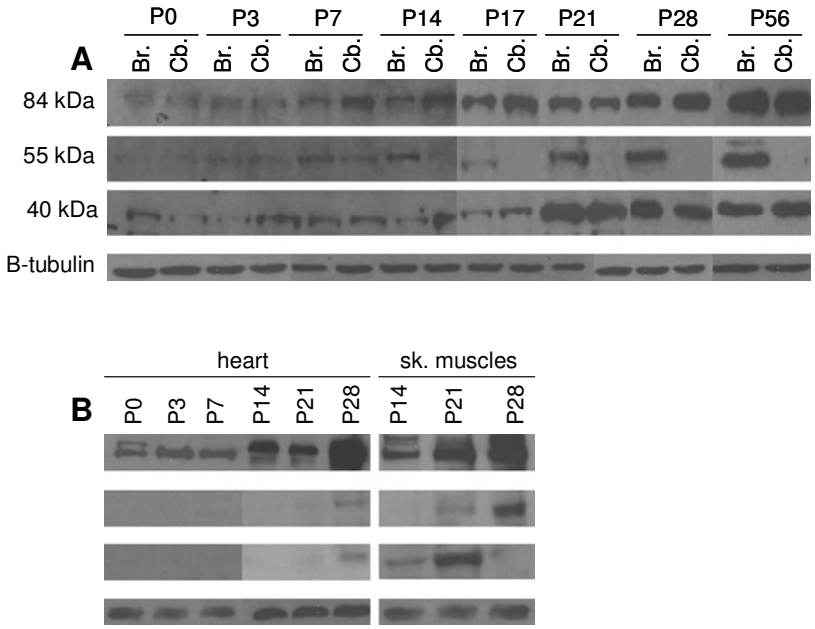


Figure 30. Oxr1 is highly expressed in the brain, cerebellum, heart and skeletal muscles as various isoforms. Proteins were extracted from wild-type brain and cerebellum (**A**) and heart and skeletal muscles (**B**) and probed for Oxr1 using Oxr1 antiserum.

Another shorter isoform (25kDa) was also barely detectable in brain and cerebellum. A similar 40 kDa intermediate isoform of Oxr1 was observed in HeLa cells extracts in a previous paper, although the splice variant or post-translation processing that generated this isoform is unknown (Volkert et al. 2000). However, it was confirmed by mass spectrometry that the two intermediate isoforms (40 and 55kDa) were indeed Oxr1 (data not shown). Thus, it was confirmed that using the current antibody, Oxr1 is expressed as four major isoforms (84, 55, 40 and 25 kDa). The 84 and 25kDa isoforms will be referred later as Oxr1-FL and Oxr1-S. It is important to note that the antibody used in this study was designed to recognise the conserved C-terminal region, including the TLDc domain, common to all isoforms (chapter 5, **Figure 22**),

4.3.2. Oxr1 is induced by oxidative stress and is localised to the mitochondria

Previous studies have described the presence of Oxr1 in the mitochondria of HeLa cells, but also in the nucleus and nucleolus in other mammalian cell lines using different antibody (Fischer, Zhang et al. 2001; Elliott and Volkert 2004). Thus to clarify the localisation of Oxr1, immunofluorescence was carried out in N2A cells and GCs. Using our antibody, Oxr1 was not detectable in GCs unless the cells were treated with H_2O_2, which clearly increased protein levels (**Figure 31A**). In treated cells, Oxr1 also co-localised with the mitochondrial marker Cox4, consistent with published studies (**Figure 31A**) (Elliott and Volkert 2004). Interestingly, during these experiments it was noted that the induction of Oxr1 continued up to 2 hours after treatment although the protein appeared to diffuse from the mitochondria. Thus to analyse this phenomenon, cytoplasmic and mitochondrial fractions were taken at 0, 1 and 2 hours post-treatment and quantified by western blotting (**Figure 31B and C**). These data confirmed the induction of Oxr1 expression and also demonstrated for the first time that the localisation of the protein shifts from predominantly in the mitochondria to the cytoplasm after an OS insult.

4.3.3. *Oxr1* transcription may be regulated by Nrf2

In this study it was shown that Oxr1 expression was induced under OS; this is consistent with early studies of the gene in HeLa cells (Elliott and Volkert 2004). Thus, as *Oxr1* appeared to be responsive to OS, it was determined whether this phenomenon occurred downstream of transcriptional factors activated by OS, such as the nuclear E2-related factor 2 (Nrf2) (Venugopal and Jaiswal 1996; Itoh, Wakabayashi et al. 1999; McMahon, Itoh et al. 2001).

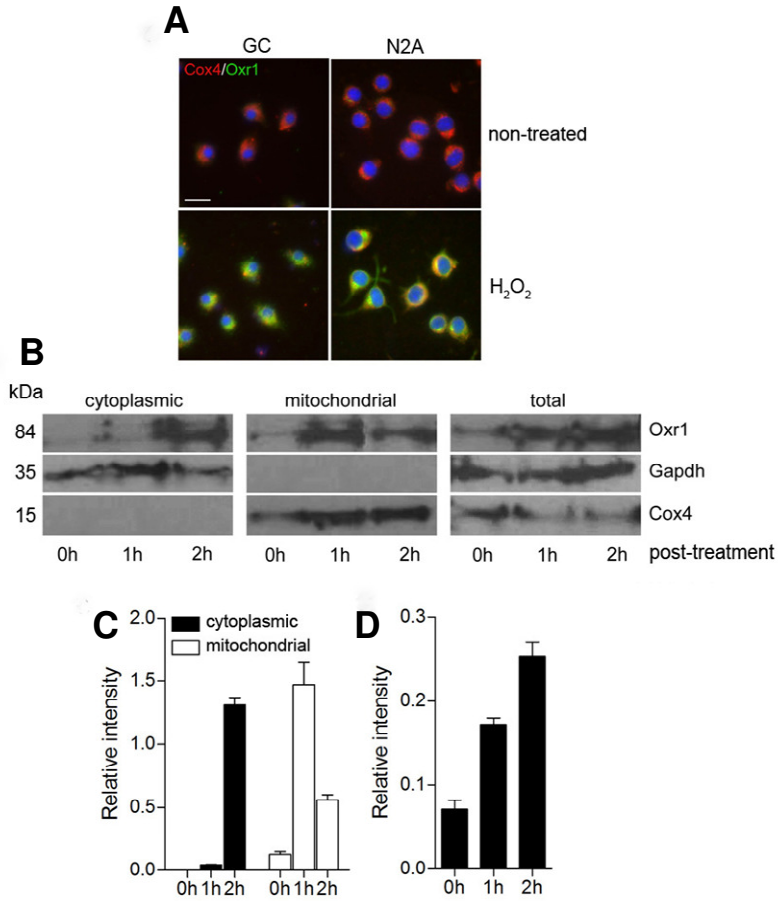


Figure 31. Oxr1 shuttles between the mitochondrial and cytoplasmic compartment. (**A**) Immunostainings of GCs and N2A cells demonstrate induction and co-localisation of Oxr1 with the cox4 mitochondrial marker 1h after peroxide treatment. These observations are confirmed by western blotting in N2A cells (**B**), also showing a shift in expression of full-length Oxr1 from the mitochondrial to the cytoplasmic fraction of neuronal cells after increasing recovery time. Induction of Oxr1 after peroxide treatment is also demonstrated in the signal from the total protein extract, and quantified in from 3 independent replicate experiments (**C, D**). β-actin was used as a control to quantify the bands intensity (data not shown). Apart from the full-length protein at 85kDa, shorter isoforms of Oxr1 are not detectable by western blot in N2A cells.

It has been demonstrated previously that Nrf2 levels in cells are modulated by retinoic acid (RA) or tert-butylhydroquinone (tBHQ) to either inhibit *Nrf2* transcription or stabilise Nrf2 respectively (Li, Johnson et al. 2005; Wang, Hayes et al. 2007). Levels of Nrf2 were modulated using RA and tBHQ and determined by western blotting (**Figure 32A and B**). Using this approach, it was determined whether *Oxr1* expression would vary depending

on Nrf2 levels. It was shown that an increase in Nrf2 led to the activation of *Oxr1* transcription while a decrease in Nrf2 led to a reduction of *Oxr1* transcription under non-OS conditions (**Figure 32C**). This suggests that *Oxr1* transcription could possibly be regulated by Nrf2 under OS conditions.

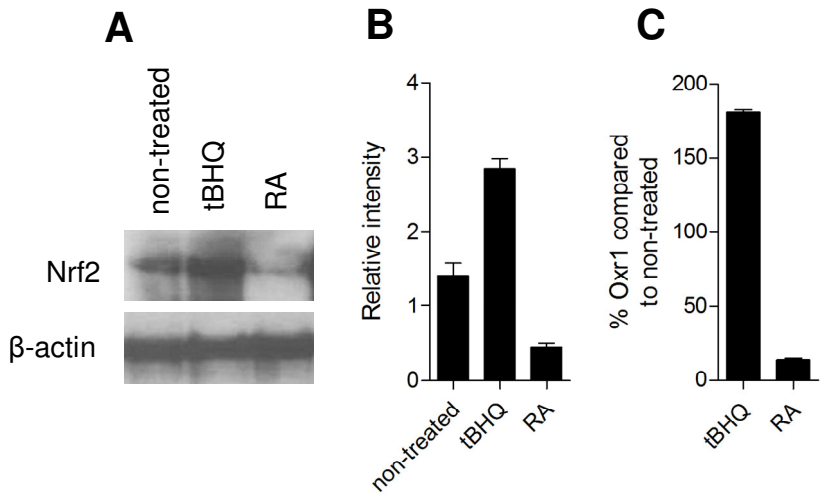


Figure 32. *Oxr1* could be regulated by Nrf2. N2A cells were treated with tBHQ or RA to respectively increase or decrease Nrf2 levels in cells as confirmed by western blotting (**A**) and gel quantification (**B**). (**C**) RNA was extracted from treated cells and *Oxr1* levels were determined by qRT-PCR. Levels of *Oxr1* vary in the same directions as Nrf2 levels.

4.4. Potential involvement of OXR1 in neurodegenerative disease

4.4.1. OXR1 is overexpressed in ALS

As discussed in chapter 1, OS is one of the common features described in NDDs. Thus, considering the involvement of Oxr1 in protecting neurons against OS and its high level of expression in the spinal cord, levels of OXR1 was analysed in ALS human biopsy samples (**Figure 8A**). Western blots of ALS spinal cord tissue showed an obvious up-regulation of various OXR1 isoforms, and to a lesser extend of the full-length protein, compared to age-matched controls (**Figure 33A**).

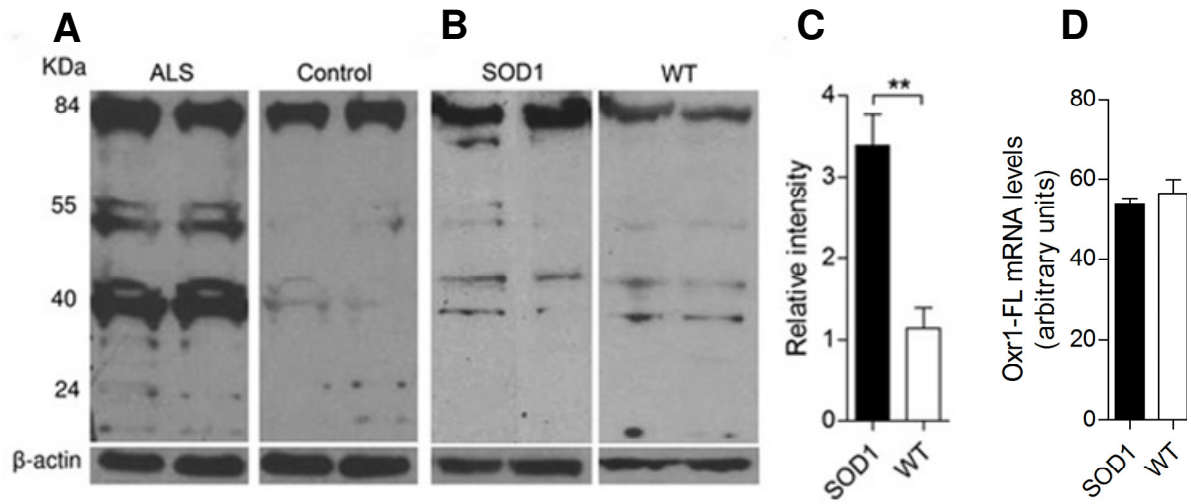


Figure 33. OXR1 is overexpressed in ALS and in an ALS-mouse model. (**A**) Western blot showing up-regulation of OXR1 in spinal cord biopsy samples from ALS patients versus age-matched controls. (**B**) Representative western blot demonstrating the expression of Oxr1 in spinal cord tissue from pre-symptomatic SOD1 G93A low-copy transgenic mice and (**C**) quantification of full-length Oxr1 (85kDa), $n = 6$ each genotype (**$P < 0.01$; ANOVA). (**D**) Oxr1 mRNA levels were determined by RT-qPCR from pre-symptomatic SOD1 G93A low-copy transgenic mice. No significant difference is detected between SOD1 and WT tissues.

4.4.2. Oxr1 is up-regulated in pre-symptomatic SOD1 G93A mice

As the previous data were obtained from patients at the end-stage of disease, it was also important to ascertain whether the up-regulation of OXR1 observed was not just a consequence of a general increase in OS usually observed in NDDs. Therefore, protein levels in spinal cord tissue from pre-symptomatic superoxide dismutase 1 (SOD1) low-copy transgenic mouse (TgN[SOD1*G93A]Gur1), a mouse model of ALS, were determined. These data showed up-regulation of Oxr1 in SOD1 mutants at 5 months of age compared to littermate controls (**Figure 33B and C**). This represents a time point prior to the first reported signs of neuropathology in this particular line, suggesting that OXR1 is a novel early marker of the OS-response in ND (Guipponi, Li et al. 2010). Moreover, no difference in Oxr1 mRNA levels was detected between SOD1 or wild-type spinal cords at any time point tested (**Figure D**).

4.5. Discussion

In this study, using both *in vitro* and *in vivo* models, Oxr1 was shown for the first time to be involved in the regulation of OS resistance in a mammalian system. These data showed that the sensitivity of neurons to exogenous stress can be exquisitely controlled by the level of *Oxr1* expression and that Oxr1 could be an early marker of OS prior to neuropathology. Other key mitochondrial proteins have also been linked to ataxia in mouse models. For example, in the Harlequin (*Hq*) mutant, a 80% reduction of the apoptosis-inducing factor (*Aif*) involved in oxidative phosphorylation causes ataxia and OS-related GC loss (Klein, Longo-Guess et al. 2002). The *Hq* phenotype is far less severe than that observed in the *bella* mouse, however; the first signs of apoptosis in the *Hq* cerebellum does not appear until 4 months of age, followed by necrotic PCs death and degeneration of other brain regions (El Ghouzzi, Csaba et al. 2007). The *Hq* model highlights the limits of the *bella* mouse as a general model of NDD. The *bella* mouse presents GCs degeneration at an early age and dies soon after, unlike the *Hq* mouse that shows a long process of degeneration occurring over a longer time period. Thus, one should be conscious that the *bella* mouse is not able to mimic the pathological features of NDD such as ALS or PD. In addition, the early death of *bella* precludes genetic crossing of this line to other mouse NDDs mutants to determine whether loss of *Oxr1* exacerbates their pathological phenotypes. However, the *bella* mouse still can be a useful model to unravel the function of unknown proteins, like Oxr1, and the link between OS and the onset of ND.

4.5.1. Granule cells are more susceptible to reactive oxygen species insults than other neuronal populations

In this study, the sensitivity of GCs and CCs to OS was compared showing that GCs were more vulnerable to ROS insults than CCs. Experiments and data from others suggest that different neuronal types have varying endogenous sensitivity to peroxide damage (White,

Zheng et al. 1998; Klein, Longo-Guess et al. 2002; Wang and Michaelis 2010). The apparent difference in sensitivity between cerebellar GCs and CCs to OS has been recently investigated (Wang and Michaelis 2010). It was demonstrated that more vulnerable neurons (e.g. cerebellar GCs and neurons from the hippocampal CA1 region) expressed higher levels of genes involved in processes such as cell stress defence, DNA damage repair, and cell cycle control compared to neurons that were more resistant to OS (e.g. neurons from the cerebral cortex or hippocampal CA3 region) (Wang, Lao et al. 2009). Moreover, these OS-sensitive neurons expressed fewer genes related to energy generation, suggesting that a short-fall in the energy required to carry out cellular repair might render GCs more sensitive to ROS (Wang, Lao et al. 2009). Thus, resistant neurons, like CCs, may have additional peroxide scavenging systems or other mechanisms to cope with peroxide production and therefore would be less sensitive to the loss of *Oxr1*. NDDs often present such selective neuronal vulnerability. For example, neurons in the cerebral cortex, hippocampus and amygdala are affected in AD while dopaminergic neurons of the substantia nigra specifically degenerated in PD despite widespread expression of the mutated gene(s) involved (Hyman, Van Hoesen et al. 1984; Rowland and Shneider 2001; Dauer and Przedborski 2003). Thus, the *bella* mouse may constitute a valuable model to help determine why certain neurons are targeted while others are spared (Wang and Michaelis 2010).

4.5.2. OXR1 may have a role in ALS pathology

OS has consistently been implicated in ALS, both in human and in mouse models, so it was decided that OXR1 levels will be determined in samples from ALS patients (Barber and Shaw 2010). Indeed, many markers of oxidative damage have been reported in post-mortem human brains as well as in SOD1 transgenic mice confirming the crucial role of OS in this disease (Robberecht, Van Den Bosh et al. 2000; Barber and Shaw 2010). After observing OXR1 up-regulation in post-mortem human tissues, it was then tested if this up-

regulation was not simply as a consequence of a general increase in OS levels which is often reported in ND biopsy samples (Vielhaber, Kunz et al. 2000; Lu, Pan et al. 2004; Ilieva, Ayala et al. 2007). Interestingly, up-regulation of Oxr1 was detected in low-copy SOD1 G93A mice well before any neuro-pathological signs have been reported (Turner and Talbot 2008). Several studies have been carried out on SOD1 transgenic mice to identify early markers of degeneration, however Oxr1 has never been implicated (Perrin, Boisset et al. 2005; Ferraiuolo, Heath et al. 2007). As no difference in *Oxr1* mRNA levels was detected from SOD1 and wild-type spinal cords, it was suggested that Oxr1 post-transcriptional regulation and stabilisation of Oxr1 protein may be occurring in SOD1 mice (**Figure 33D**).

4.5.3. The pathway in which Oxr1 plays a role is still unknown

As many enzymes involved in the OS response are regulated by Nrf2, it was tested if *Oxr1* could also be regulated by this key transcriptional factor activated by OS. Data from *in vitro* experiments suggested that Nrf2 might mediate *Oxr1* transcription (**Figure 32**). Most enzymes regulated by Nrf2 are regulated through a *cis*-acting antioxidant response elements (AREs) situated in their promoter region, which subsequently allow adaption of their transcription to the cellular redox status (Remaclea , Raesa et al. 1995; Venugopal and Jaiswal 1996; Itoh, Wakabayashi et al. 1999; Nguyen, Huang et al. 2000; Nose 2000; McMahon, Itoh et al. 2001; Turpaev 2002; Nguyen, Sherratt et al. 2003; Nguyen, Nioi et al. 2009). However, analysis of *Oxr1* sequence showed that *Oxr1* does not present any consensus ARE sequence within 30kb of the UTR in any of its splice variants (Wang, Tomso et al. 2007); unpublished observations). This argues against a regulation of *Oxr1* by Nrf2 and further supports the SOD1 data suggesting that Oxr1 is an early marker of OS.

The fate of a cell under OS will be determined by the balance between numerous major signalling pathways that will influence the ability of a cell to survive or die (**Figure 34**). Few of the pathways activated by oxidant injuries are clearly linked to enhanced survival or cell death, while others can produce either effect dependent on the circumstances (**Figure 34**). To unravel Oxr1 function, it will be crucial to define where and when Oxr1 acts through one of these known pathways. A recent study performed in the mosquito *A.gambiae* proposed that Oxr1 may regulate the levels of antioxidant proteins catalase and gpx (Jaramillo-Gutierrez, Molina-Cruz et al. 2010). *Gpx* and *catalase* mRNA levels were indeed downregulated in the cerebellum and brain of the *bella* mouse (**Figure 28**). As loss of *Oxr1* in the *bella* mouse led to a downregulation of *gpx* and *catalase* mRNA levels, it is plausible that Oxr1 could act upstream of these enzymes and regulate their transcription although the lack of nuclear localisation of Oxr1 argues against that hypothesis.

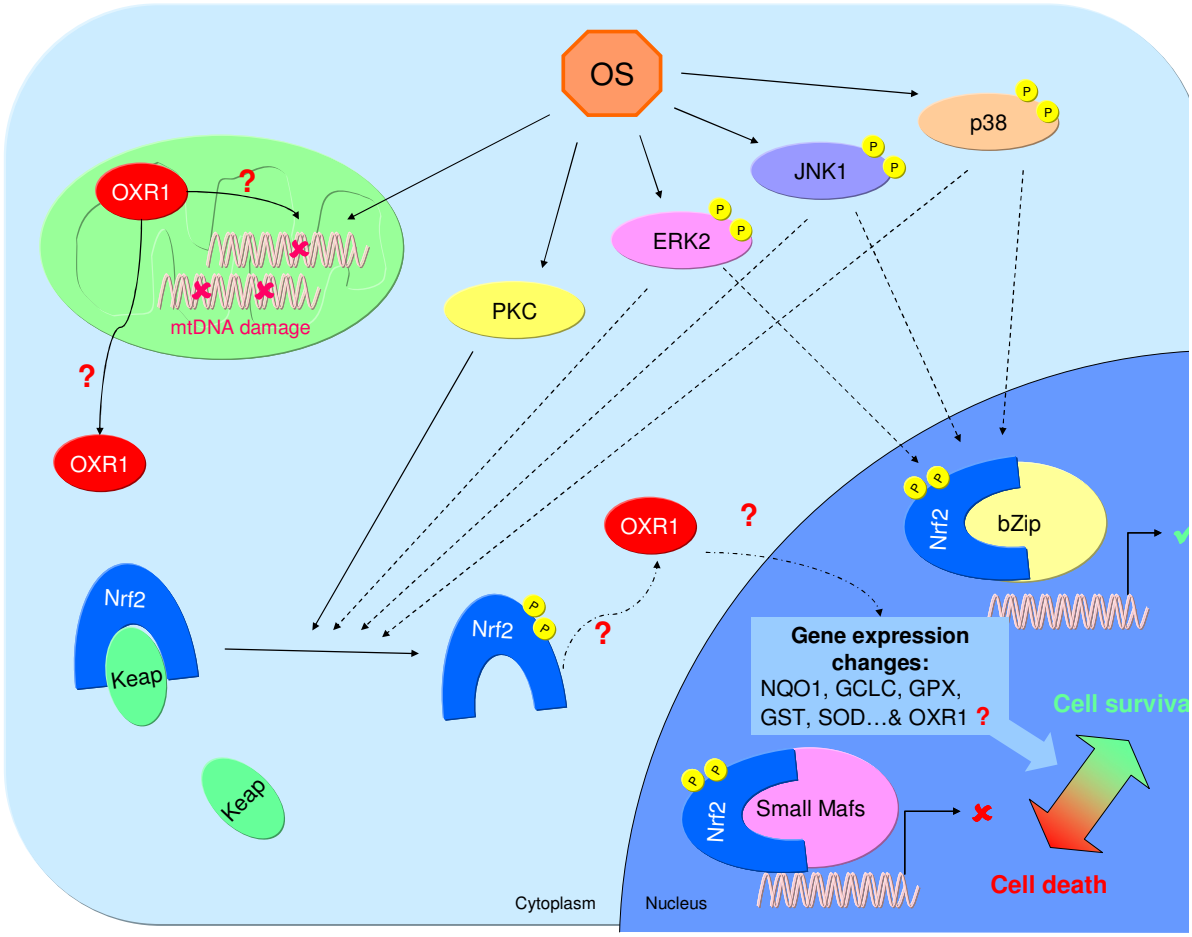


Figure 34. Summary: Oxr1 has a role in the OS-response. Increase in ROS leads to OS and can damage biological macromolecules like DNA. Oxr1 was shown to be involved in reducing DNA damage under OS. Moreover, Oxr1 shuttles between the mitochondria and the cytoplasm. OS can activate a range of proteins that lead to modulation of pathways; the balance between these pathways determining if a cell will die or survive. Few pathways are clearly linked to cell survival, like the protein kinase C (PKC) pathway, while others can produce effects dependent on the circumstances, like MAP kinases (ERK and JNK1 pathways). The defence systems to prevent cell damage include various molecules like NAD(P)H:quinone oxidoreductase (NQO1), glutathione S-transferase (GST), glutamate-cysteine ligase (GCLC), glutathione peroxidise (GPX), superoxide dismutases (SOD) and maybe OXR1. Transcription of these proteins is coordinately regulated through antioxidant response elements (AREs) activated or repressed by the transcription factor Nrf2 (NF-E2-related factor 2). Inactive Nrf2 is retained in the cytosol by association in a complex with the cytoskeletal protein Keap1. Cytosolic Nrf2 is phosphorylated and translocates into the nucleus in response to protein kinase C activation and Map kinase pathways. In the nucleus, Nrf2 activates genes through AREs by interacting with transcription factors in the bZIP family. Nrf2 activation of genes is opposed by small maf proteins maintaining a counterbalance to Nrf2 and balancing the oxidation level of the intracellular environment. Preliminary data show that *Oxr1* expression may be induced by Nrf2 under OS and that it could participate to the modulation of *gpx* and *catalase* expression.

4.5.4. Oxr1 has common features with key antioxidants linked to NDDs

In this study, the importance of Oxr1 induction by OS and its effect on cell survival was described; taken together, these data suggest that Oxr1 may be a critical feature of the defence mechanisms against OS. Furthermore, it displays features common to many of the most important antioxidant proteins. The defence systems to prevent cell damage include various enzymatic scavengers of ROS (e.g., superoxide dismutases, catalase, and gpx) as well as non-enzymatic molecules (e.g., glutathione, α-tocopherol, and ascorbate) (**Figure 34**) (Halliwell 1992; Halliwell 1999). Cellular and mouse studies of these key antioxidant proteins show that cells are sensitive to their relative expression levels; indeed, like Oxr1, SOD2 can be lethal when disrupted but neuroprotective when over-expressed *in vivo* (Kokoszka, Coskun et al. 2001; Massaad, Washington et al. 2009).

Moreover, Oxr1 presents a number of common features with DJ-1, a protein linked to autosomal recessive forms of PD (Bonifati, Rizzu et al. 2003; Dodson and Guo 2007; Jendrach, Gispert et al. 2009). Loss of DJ-1 leads to increased susceptibility of neurons to OS and death (Kim, Smith et al. 2005; Aleyasin, Rousseaux et al. 2007). Like Oxr1, endogenous DJ-1 can be found in the mitochondria although its localization is also cytosolic (Zhang, Shimoji et al. 2005; Junn, Jang et al. 2009). This study raises the question of whether there are links between Oxr1 and mitochondria function, as the link between mitochondria dysfunction and ND is well characterised (Lee and Wei 2005; Lin and Beal 2006; Dodson and Guo 2007). First, *bella* neurons would have to be analysed by electron microscopy to determine if swollen mitochondria can be detected. Indeed, aberrant mitochondrial morphology has been observed in DJ-1 deficient cell lines and cells from patients with DJ-1 mutations (Irrcher, Aleyasin et al. 2010). Loss of DJ-1 also affects mitochondrial dynamics (Irrcher, Aleyasin et al. 2010). Similarly, mitochondrial fusion rate, respiration and ATP production could be evaluated in *bella* cerebellum to determine mitochondrial function and dynamics (Hao, Giasson et al. 2009; Irrcher,

Aleyasin et al. 2010). In addition, as shown for Oxr1, DJ-1 is also overexpressed in AD as well as in PD brains and studies in SOD-1 mutants have shown that DJ-1 is over-expressed in spinal cord tissues, although only after the onset of the first neurodegenerative signs (Choi, Eom et al. 2004; Choi, Sullards et al. 2006; Baulac, Lu et al. 2009; Lev, Ickowicz et al. 2009). It can be supposed that, similar to DJ-1, OXR1 may also have additional functions not related to protection against OS, as it will next be investigated in chapter 5 (Xu, Zhong et al. 2005; Honbou et al. 2003 ; Kim, Peters et al. 2005; Olzmann, Bordelon et al. 2007).

5. The TLDc domain as a functional domain defining a conserved family of eukaryotic proteins

In chapter 4, it was shown that Oxr1 plays an important role in OS resistance in mammalian cells. It was also found that Oxr1 is expressed as various isoforms, all containing the conserved TLDc domain. The shortest of these, originally named Oxr1-C7C or Oxr1-S in this thesis, is constituted almost exclusively by this domain (Volkert, Elliott et al. 2000) (**Figure 8B**). The function of this TLDc domain has not been established, yet it was originally identified as a potentially catalytic motif (Doerks, Copley et al. 2002). However, expression of this TLDc domain alone in *Escherishia coli* is sufficient to suppress the strain sensitivity to OS, suggesting that the TLDc domain confers Oxr1 its OS-related function (Fischer, Zhang et al. 2001; Durand, Kolpak et al. 2007).

A previous study identified additional mammalian proteins that contained the TLDc domain. In addition to OXR1, this family contains nuclear receptor coactivator 7 (NCOA7, formerly called the 140 kDA estrogen receptor associated protein, ERAP140) and three proteins that have not been characterised, C20ORF118, KIAA1609 and TBC1D24 (Shkolnik, Ben-Dor et al. 2008). C20ORF118 exists only in a short form with a very unique N-terminal portion and TLDc; KIAA1609 and TBC1D24 are more distantly related. OXR1 and NCOA7 have very similar genomic structures, and it was concluded from this evolutionary study that NCOA7 is a relatively recent duplication of OXR1 (Shkolnik, Ben-Dor et al. 2008). Both OXR1 and NCOA7 contain LysM and Gram domains, though only NCOA7 has an estrogen-receptor binding domain (ERαbd) and a nuclear localisation sequence (NLS) (**Figure 8B**). NCOA7 was first identified as a novel interactor with the carboxyl-terminal ligand binding domain of the estrogen receptors (ER), ERα and ERβ in a ligand-induced fashion (Shao, Halachmi et al. 2002). NCOA7 was shown to associate with a variety, but still in a specific manner, of nuclear receptors under estradiol treatment,

although NCOA7 shares no sequence and little structural homology with other nuclear receptor cofactors (Shao, Halachmi et al. 2002; Shkolnik, Ben-Dor et al. 2008). Moreover, like OXR1, NCOA7 is capable of reducing the DNA damaging effects of ROS when expressed in bacteria, indicating that NCOA7 may also have an activity that can contribute to OS resistance (Durand, Kolpak et al. 2007).

Interestingly, Ncoa7 has a short isoform (Ncoa7B or Ncoa7-S) that is very similar in structure to the Oxr1 short isoform (Oxr1-S) (**Figure 8B**) (Shao, Halachmi et al. 2002; Durand, Kolpak et al. 2007; Shkolnik, Ben-Dor et al. 2008). Ncoa7B is expressed only in the reproductive system, whereas the full-length Ncoa7 protein is highly expressed in the CNS; however the function of both of these proteins is unknown. Thus, it was decided to focus on not only the function of Oxr1 but also to consider the function of Ncoa7 in parallel based on their obvious sequence similarity and potential relevance to the CNS and known roles in OS resistance (Elliott and Volkert 2004; Shkolnik, Ben-Dor et al. 2008).

Aims:

- **Investigate the role of the TLDc domain** by assessing cell death of GCs overexpressing the short TLDc domain-containing isoforms of Oxr1 under OS both *in vitro* and *in vivo.*

- **Determine if Ncoa7 has a similar role as Oxr1** by manipulating expression levels of Ncoa7 and screening for OS resistance.

- **Determine the basic features of Ncoa7 localisation and expression** and compare these data with data from chapter 4.

- **Study Oxr1 and Ncoa7 function** by identifying potential binding partners both under normal and OS conditions using immunoprecipitation and mass spectrometry.

- **Confirm and further analyse promising interacting proteins** in tissue extracts and investigate their interaction properties.

5.1. Study of general features of the TLDc domain and its involvement in protecting cells against oxidative stress

5.1.1. The conserved TLDc domain of Oxr1 is sufficient to confer protection against oxidative stress both *in vitro* and *in vivo*

To investigate whether Oxr1-S was functional in neurons, the peroxide sensitivity assays performed in chapter 4 were repeated in *bella* GCs using constructs coding for this isoform as well as full-length Oxr1 (Oxr1-FL). In these experiments, a bicistronic vector containing GFP was used to assay the proportion of transfected cells that were apoptotic (**Figure 35**). These data showed that Oxr1-S was able to confer protection against OS as efficiently as the full-length protein in both wild-type and *bella* GC culture.

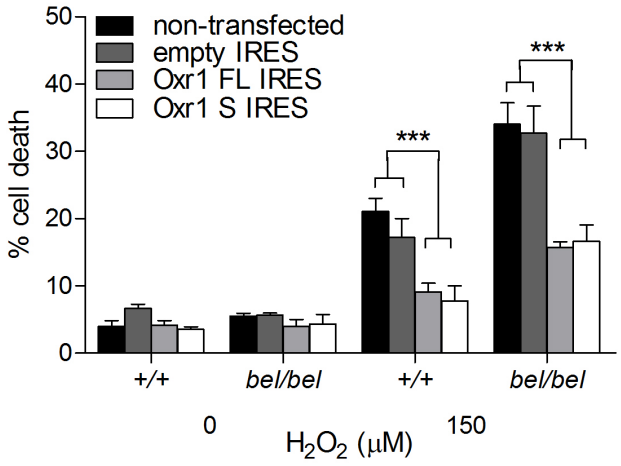


Figure 35. Oxr1 confers resistance to OS *in vitro*. GCs from P7 *bella* (*bel/bel*) mice or wild-type (*+/+*) mice cultured for 11 days and transfected for 3 days with Oxr1-FL or –S constructs in an IRES-GFP expression vector. After peroxide treatment, the proportion of cells successfully transfected (GFP positive) that were apoptotic were calculated, showing that both constructs were as effective at preventing cell death in both (*+/+*) and (*bel/bel*) GCs. Asterisks indicate statistical significance (***$p < 0.001$; ANOVA).

Moreover, to confirm these findings *in vivo*, a gene-trap mouse containing the vector insertion between exons 3 and 4 of *Oxr1*, which was therefore expected to only express the shorter isoform of the gene, was generated from ES cells by Dr Ben Davies' group. Mice homozygous for the insertion were successfully generated and the exact position of the trap vector was confirmed by Dr Peter Oliver (**Figure 36A**). These mice displayed no gait or pathological abnormalities in the CNS up to 12 months of age (data not shown) and western blotting confirmed that the gene-trap insertion had almost completely ablated the expression of *Oxr1-FL* as expected, the short isoform being expressed normally (**Figure 36B**). Interestingly, the proportion of Oxr1-S was much higher in these cerebellar extracts than in whole brain (compare **Figures 30A and 36B**), suggesting that Oxr1-S may play a more significant functional role in the cerebellum than in other regions of the CNS. These data demonstrate that TLDc domain-containing Oxr1 isoforms other than the full-length protein are also functional.

5.1.2. Ncoa7 can protect cells against oxidative stress through its TLDc domain

To determine if Ncoa7 had similar protective features as Oxr1 in mammalian cells, GCs overexpressing full length Ncoa7 (Ncoa7-FL) were treated with hydrogen peroxide (H_2O_2) as described previously. Similar to Oxr1, a significant reduction in cell death was observed in cells over-expressing Ncoa7-FL (**Figure 37A**). To further investigate the specificity of this effect, all Ncoa7 isoforms were knocked-down by shRNA to <10% of endogenous levels of wild-type GCs, resulting in almost twice the level of cell death compared to neurons transfected with control constructs (**Figure 37B**). Then, in order to investigate if this function was conveyed by the TLDc domain, a similar experiment was performed using cells transfected with Ncoa7 short isoform (*Ncoa7-S*). Cells transfected with this construct showed a strong resistance to OS, with values similar to experiments

using the full-length molecule (**Figure 37A**). These data therefore confirmed that Ncoa7 has a similar role as Oxr1 and that the C-terminal domain of both Oxr1 and Ncoa7 confers their function in a mammalian system. It should be noted that Ncoa7-S is normally expressed mainly in the reproductive tract and not expressed at high levels in neurons, but these data showed that it still has a function as neuroprotector when overexpressed in neurons.

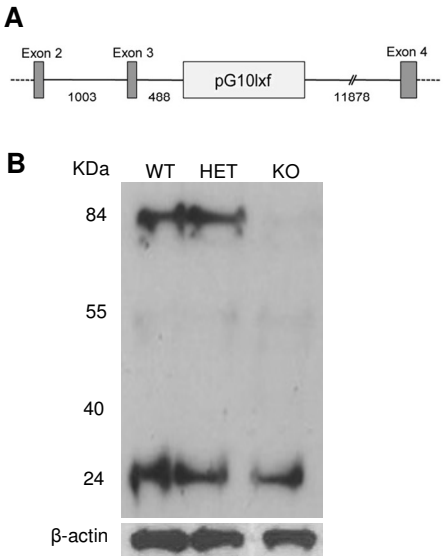


Figure 36. The shortest Oxr1 isoform containing the TLDc domain is sufficient to confer resistance to OS *in vivo*. (**A**) Position of the RRR195 gene-trap insertion (pG101xf vector), 488bp from the end of *Oxr1* exon 3, as determined by PCR (performed by Dr Peter Oliver). (**B**) Western blot of cerebellar tissue from littermates in the gene-trap cross showing that in homozygous gene-trap mice the Oxr1-FL isoform at approximately 85kDa is barely detectable, whereas Oxr1-S is unchanged.

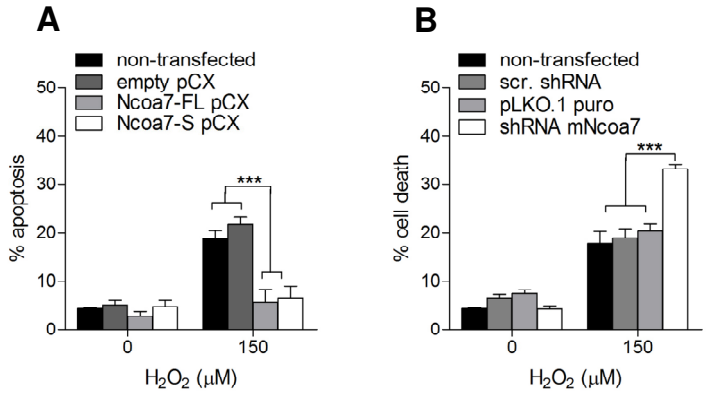


Figure 37. Ncoa7 regulates sensitivity of GC neurons to OS. (**A**) GCs were cultured as previously and subjected to peroxide treatment. Cells transfected with *Ncoa7-FL* or *-S* constructs show a significant decrease in apoptotic cell death compared to cells transfected with empty vector. (**B**) GCs were infected with *Ncoa7* shRNA knock-down construct before being treated with H_2O_2. A significant increase in apoptotic cell death was detected in contrast with mock transfected (pLKO.1puro) and scrambled shRNA transfected (scr. shRNA) cells. Similar results were found in N2A cells. Asterisks indicate statistical significance (*** $p< 0.001$; ANOVA).

5.1.3. Ncoa7 is induced by OS and is localised to the nucleus

A previous study has shown that *Ncoa7* was induced by estrogen stimulation only; however, in order to investigate the similarities between Ncoa7 and Oxr1, it was tested if *Ncoa7* could be induced by OS as observed for *Oxr1* (Shao, Halachmi et al. 2002). Non-transfected N2A cells were treated for various time periods, and *Ncoa7* and *Oxr1* mRNA levels were determined by qRT-PCR. Both *Oxr1* and *Ncoa7* were induced by OS, peaking after 45 minutes of treatment (**Figure 38**). *Oxr1-FL* was overexpressed 3-fold more than *Ncoa7-FL*, however *Ncoa7-FL* presented a higher basal level than *Oxr1-FL*. Interestingly, short isoforms are not induced at the same time as the full-length transcripts suggesting that short and full-length isoforms may be involved at different stages of the OS-response (**Figure 38**).

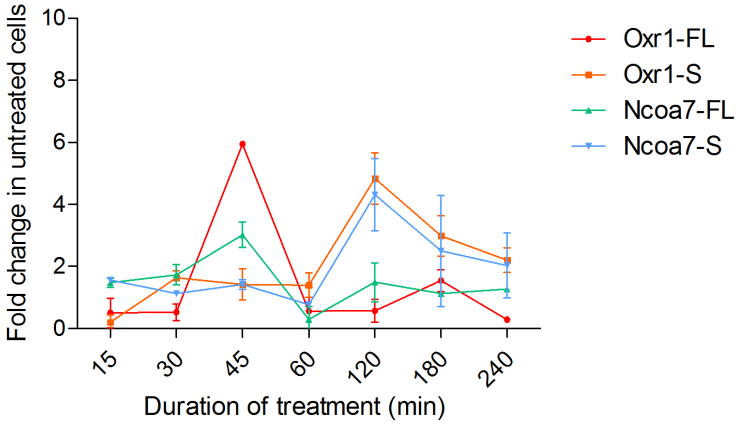


Figure 38. *Oxr1* and *Ncoa7* are induced by OS. Wild-type GCs cells were subjected to peroxide treatment for various durations. RNA was extracted and mRNA levels of *Oxr1-FL, -S* and *Ncoa7-FL, -S* were quantified by qRT-PCR. Full-length isoforms for both *Oxr1* and *Ncoa7* were induced after 45min treatment while short isoforms were induced later after 120min treatment. Similar results were found in N2A cells.

In addition, while Oxr1 was previously shown to be expressed in the mitochondria, Ncoa7 localisation was also determined in these cells. Non-transfected N2A cells treated with H_2O_2 were stained with Ncoa7 antiserum, showing that the protein is localised mainly to the nucleus as expected based on its known nuclear localisation signal (**Figure 39**).

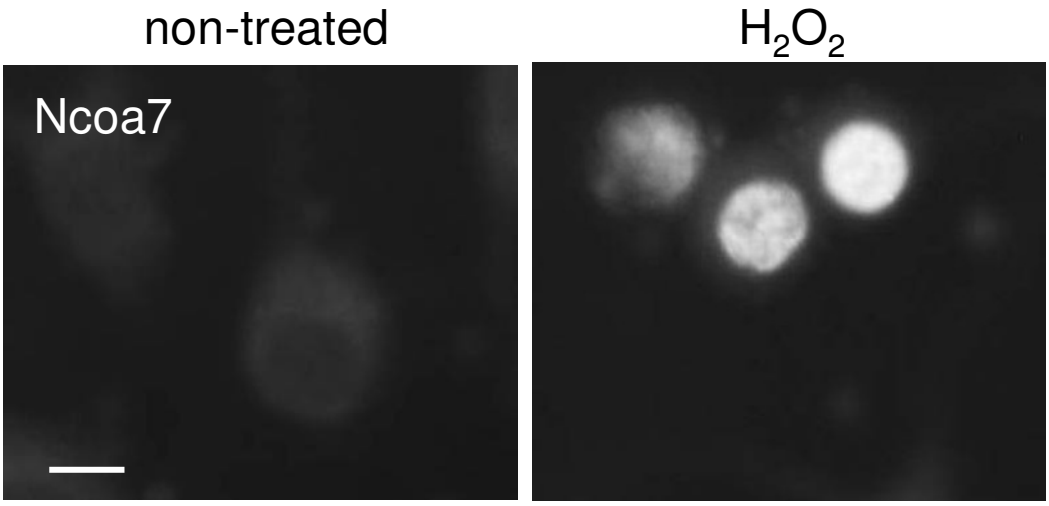


Figure 39. Nco7 is localised to the nucleus under OS. N2A cells were subjected to peroxide treatment. Cells were then fixed and stained with Ncoa7 antiserum. Scale bar: 10µm

5.1.4. A residue in Oxr1 TLDc domain is crucial for Oxr1 function

To further investigate the function of the TLDc domain in OS sensitivity, a point mutation was introduced into the *Oxr1-S* sequence. This mutation (E158A) changes a glutamate residue conserved in all Ncoa7 and Oxr1 orthologues and was chosen as it was potentially the class of amino acid that is found in the active site of enzymes (Doerks, Copley et al. 2002; Shkolnik, Ben-Dor et al. 2008); C. Ponting, personal communication) (**Figure 40A**). N2A cells were transfected with this mutant *Oxr1-S* construct (*Oxr1* EA-*S*) and the normal expression of this sequence was first confirmed by qRT-PCR (**Figure 40B**). N2A cells were then treated with H_2O_2 and cell death was assessed as previously described. Interestingly, cells transfected with *Oxr1* EA-*S* were not protected against OS as efficiently as cells transfected with *Oxr1-S* (**Figure 40C**). This confirms the crucial role of Oxr1 TLDc domain to confer its function.

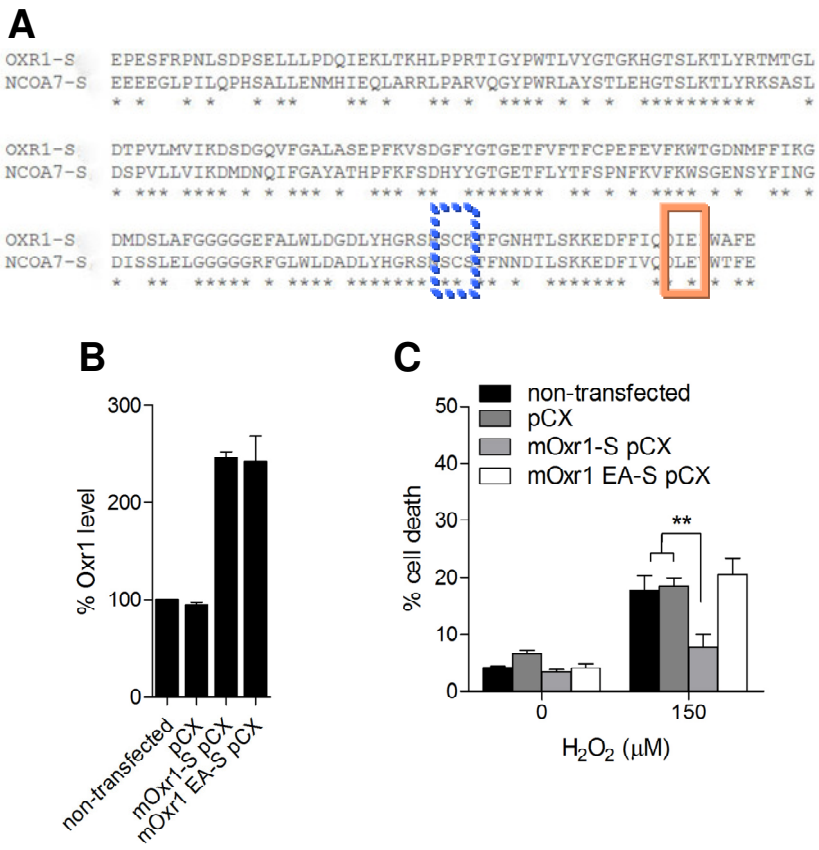


Figure 40. The TLDc domain confers Oxr1 its OS-related function. (**A**) Sequences alignment of Oxr1-S and Ncoa7-S. The residue mutated in mOxr1 EA-S is showed in orange box. (**B**) Expression levels were determined by qRT-PCR. No difference in expression level is detected for *Oxr1-S* or *Oxr1* EA-*S*. (**C**) GCs were cultured as previously and subjected to peroxide treatment. Cells transfected with the mutant construct presents a significant increase in apoptotic cell death compared to cells transfected with *Oxr1-S*. Similar results were found in N2A cells. Asterisks indicate statistical significance (** $p < 0.01$; ANOVA).

5.2. Study of Oxr1 regulation

5.2.1. Oxr1 regulation is not through phosphorylation or glycosylation

Next, it was tested whether activation of Oxr1 function could be through post-transcriptional modifications as these findings could be next used to modulate Oxr1 activity in future experiments. Two possible post-transcriptional modifications were tested: phosphorylation and glycosylation. Immunoprecipitated Oxr1-FL and Oxr1-S were treated with enzymes removing 5´ phosphates or N-linked glycosylation respectively. No band shift was detected when Oxr1-FL or Oxr1-S were treated with the enzymes or the buffer only, suggesting that Oxr1 is not phosphorylated or glycosylated so it is unlikely that these mechanisms regulate Oxr1 activity (**Figure 41**).

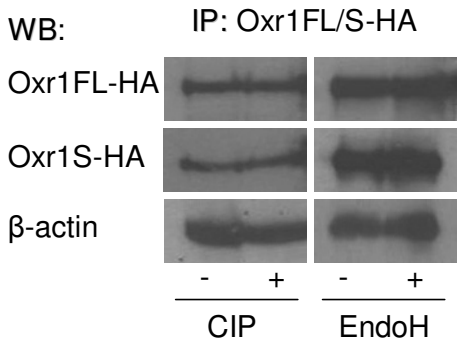


Figure 41. Oxr1 is not phosphorylated or glycosylated. *Oxr1-FL* and *-S* were transfected in N2A cells and proteins were immunoprecipitated and treated with CIP or EndoH enzymes. No difference is detected between immunoprecipitated proteins incubated with the enzyme (+) or with the buffer only (-). The efficiency of the reaction was checked using phosphorylated myelin basic protein and RNase B respectively as controls (data not shown).

5.2.2. Oxr1 can form multimers through a residue in its TLDc domain

Due to the similarities between Oxr1 and DJ-1 as discussed in chapter 4, the possibility that Oxr1 could form multimers, like DJ-1, was tested. Full-length Oxr1 (*Oxr1-FL-HA*) and short (*Oxr1-S-MYC*) isoforms were co-transfected in N2A cells and co-immunoprecipitated. The full-length and the short isoforms were always immunoprecipitated together suggesting that they may form multimers (**Figure 42A**). To determine if the TLDc domain could be involved in this dimerization, *Oxr1* EA*-FL-HA* was co-transfected with *Oxr1-S-MYC* and a co-immunoprecipitation was performed as previously. The interaction between Oxr1-FL and Oxr1-S was completely abolished by the mutation occurring in the TLDc domain (**Figure 42B**). These data show that Oxr1 can form multimers and that this dimerization is likely to occur via the TLDc domain.

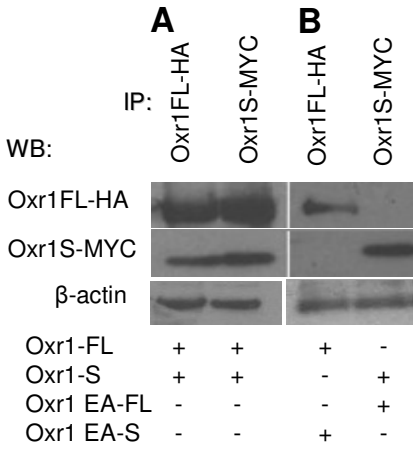


Figure 42. Oxr1 forms a dimer through its TLDc domain. (**A**) *Oxr1-FL-HA* and *Oxr1-S-MYC* were co-transfected in N2A cells. Proteins were immunoprecipitated using anti-HA or –MYC beads and western blots were probed with anti-MYC or -HA antibody respectively. Oxr1-FL and -S were always immunoprecipitated together. (**B**) A similar experiment was performed using constructs presenting a point mutation in their TLDc domain. The interaction between Oxr1 EA-FL and -S was lost.

5.3. Study of Oxr1 novel functions

5.3.1. Oxr1-FL has many binding partners under oxidative stress

As no clues as to the function of Oxr1 can be gleaned from protein alignment or structural predictions, it was decided to learn more about the role of Oxr1 by identifying binding partners. The *Oxr1-FL* construct was transfected into N2A cells that were either untreated or treated with H_2O_2 for various durations (from 15 minutes to 240 minutes) followed by co-immunoprecipitation. Peroxide treatment was used to model Oxr1 function as Oxr1 was previously shown to be induced by OS in N2A cells; this condition is therefore a critical feature of its antioxidant role as Oxr1 may only be required under stress.

Immunoprecipitated proteins were identified by mass spectrometry and the results were analysed using Ingenuity software. Few proteins were found in all stress conditions (**Appendix 4** for list of proteins). In general, it was found that most of the proteins were part of two main canonical pathways: the Nrf2-mediated stress response and the RNA signalling pathway (predominantly RNA post-transcriptional modifications) (**Figure 43A**).

5.3.2. Oxr1-S has specific binding partners

To determine which of the Oxr1-FL binding partners were relevant to the TLDc domain, and to identify any interactors unique to different isoforms, the *Oxr1-S* construct was used in the same experiment as above (**Figure 43B**). Binding partners common to the Oxr1-FL screen were also found to be part of Nrf2-mediated stress response and the RNA signalling pathways (**Figure 43C**). Moreover, proteins involved in protein folding, post-translational modifications and cell cycle were also identified. Taken together, it was concluded that Oxr1-FL and -S had similar function in OS-response as well as in RNA processing (specifically RNA splicing); and that Oxr1-S had specific functions related to protein processing and cell cycle. It should be noted that no targets of Oxr1-S were identified under the untreated conditions.

To confirm that these interactions in N2A cells could be recapitulated in tissue, a selection of binding partners were tested in brain and cerebellum extracts by co-immunoprecipitation. 8 targets out of 11 tested were confirmed, highlighting the specificity of the mass spectrometry experiment previously used and the robustness of the strategy used (**Figure 44**).

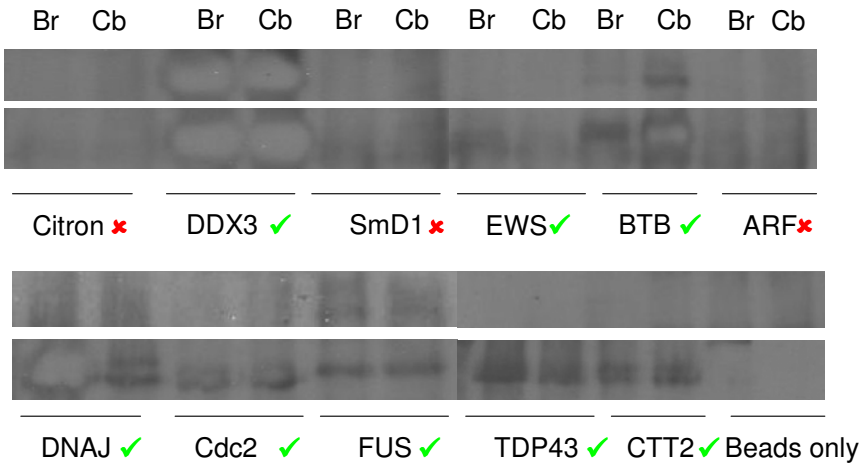


Figure 44. Targets identified by mass spectrometry analysis in N2A cells were confirmed in the brain (Br) and cerebellum (Cb). Oxr1 was co-immunoprecipitated from brain and cerebellum extracts using antibodies against the proteins indicated and that were identified previously by mass spectrometry. Targets that could be confirmed (or not) are marked by a green tick (or by a red cross). 8 out of 11 tested proteins were confirmed.

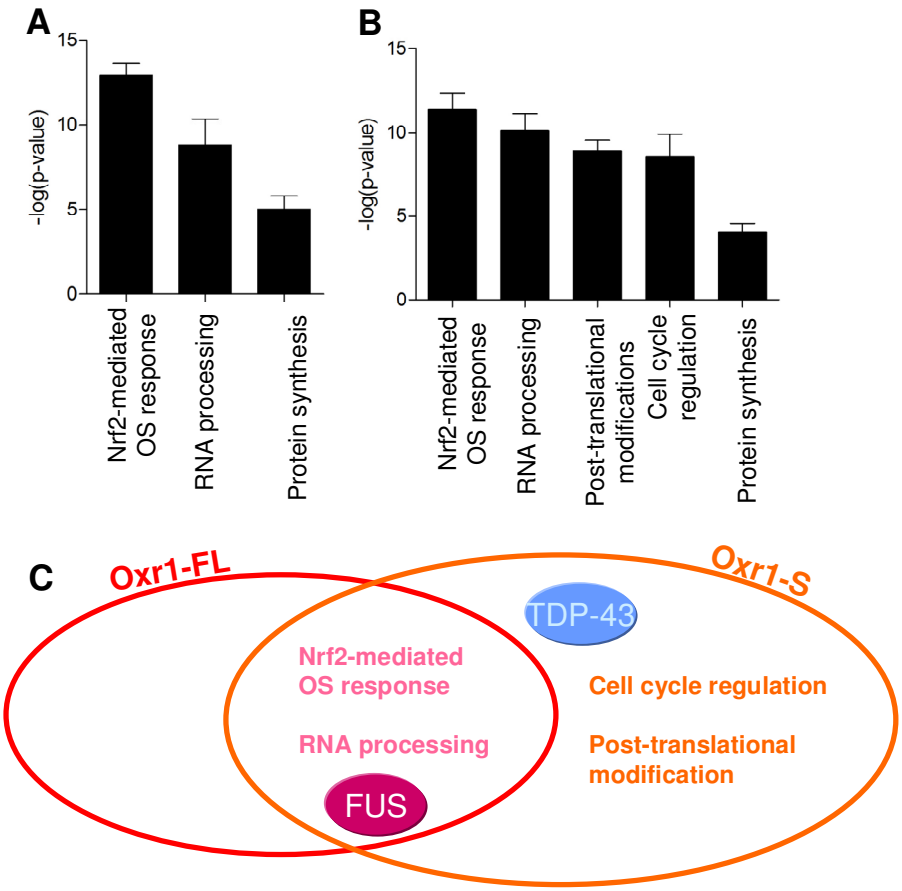


Figure 43. Oxr1 is involved in RNA processing and cell cycle regulation. (**A**) *Oxr1-FL* was transfected in N2A cells and proteins interacting with Oxr1-FL were co-immunoprecipitated. These proteins were then identified by mass spectrometry and analysed using Ingenuity software. Only the most significant functions detected by the software are summarized in the graph. Oxr1-FL is involved in Nrf2-mediated OS-response and in RNA processing, especially RNA splicing. (**B**) A similar approach was used for Oxr1-S. Oxr1-S interacts with proteins involved in the Nrf2-mediated OS-response, in RNA processing as well as in post-translational modifications (in particular protein folding) and cell cycle regulation. (**C**) A schematic view presents the common and specific functions of Oxr1-FL and -S.

5.3.3. Ncoa7-FL and Oxr1-FL have common binding partners

Similarly, as the function of Ncoa7 is still unclear, it was decided to identify its binding partners using the same method. It can be supposed that the common binding partners between Oxr1 and Ncoa7 are likely to bind to their common TLDc domain. As expected, a majority of Ncoa7 binding partners were involved in the estrogen receptor signalling

confirming Ncoa7 function as an estrogen receptor (**Figure 45A**). But more importantly, Ncoa7-FL had common binding partners with Oxr1-FL and -S, all involved in RNA post-transcriptional modifications (**Figure 45B**). These data suggested that the TLDc domain, as well as being involved in the OS-response, takes part in RNA processing, which is a function of the OXR-family members that has not previously been identified.

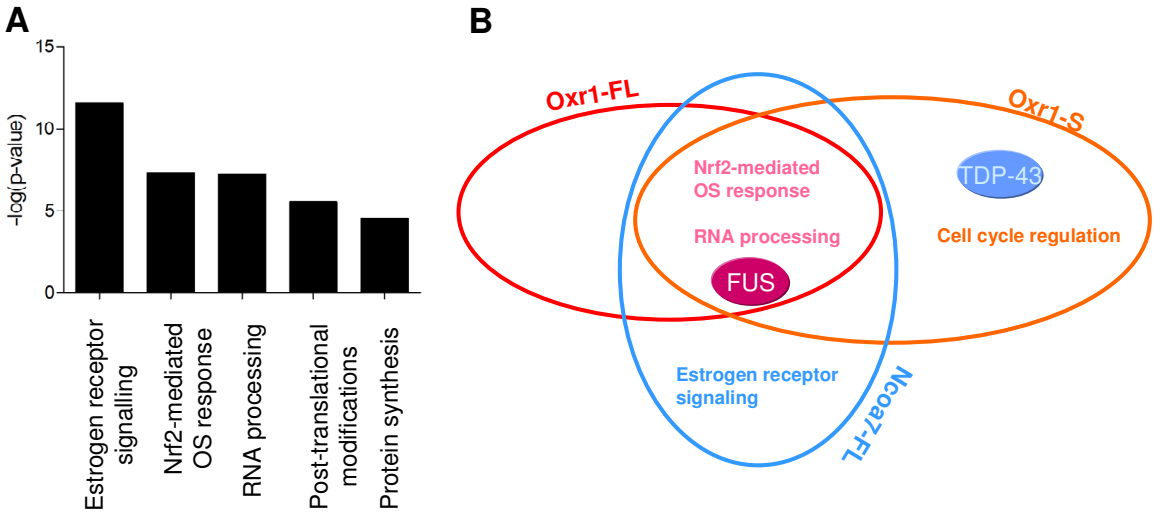


Figure 45. Ncoa7-FL is involved in OS-response and RNA processing. (**A**) *Ncoa7-FL* was transfected in N2A cells and proteins interacting with Ncoa7-FL were co-immunoprecipitated. These proteins were identified by mass spectrometry. The targets were analysed using Ingenuity software. Only the most significant functions detected by the software are summarized in the graph. Ncoa7-FL interacts with proteins involved in the estrogen receptor signalling, Nrf2-mediated OS-response and in RNA processing. (**B**) A schematic view presents the common and specific functions of Oxr1-FL, -S and Ncoa7-FL.

5.4. Study of Oxr1 and FUS/TDP-43 interaction

5.4.1. Oxr1 binds to FUS and TDP-43 under oxidative stress

Fus and Tdp-43 were two of Oxr1 binding targets previously identified by mass spectrometry. Mutations in FUS and TDP-43 are known to be linked to ALS, therefore it was decided to further characterise these interactions as a potential link between Oxr1, ALS and OS (Kwiatkowski, Orr et al. 1993; Doi, Okamura et al. 2008; Lagier-Tourenne and Cleveland 2009; Vance, Rogelj et al. 2009). First, it was confirmed by co-

immunoprecipitation from untreated cells co-expressing *Oxr1* and *FUS* or *TDP-43* that FUS can interact with Oxr1-FL and Oxr1-S while TDP-43 can interact with Oxr1-S only (**Figure 46A**). Similar results were found using cells treated with H_2O_2.

This interaction was then tested in FUS or TDP-43-transfected cells with no treatement or treated with H_2O_2. Overexpressed FUS and TDP-43 were successfully co-immunoprecipitated with endogenous Oxr1 only when cells were under OS, no interaction being detected in non-treated conditions (**Figure 46B**). Taken together, these data show that Oxr1-S interacts with FUS and TDP-43 under stress conditions, while Oxr1-FL interacts only with FUS, also under OS.

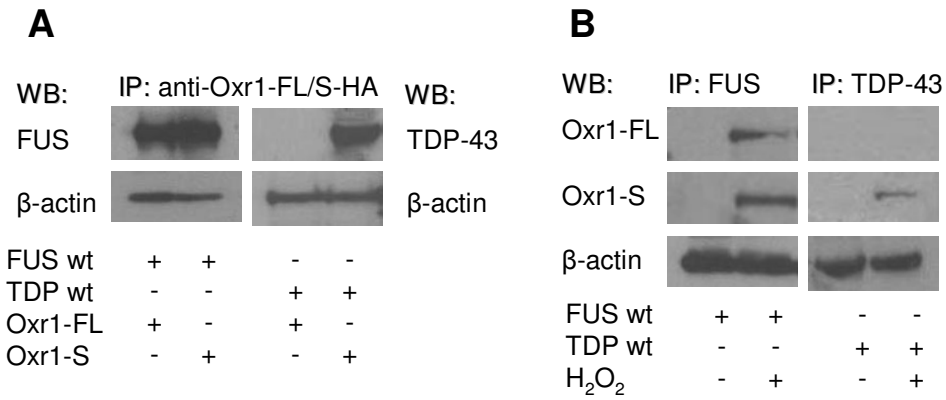


Figure 46. Oxr1 interacts with FUS and TDP-43 under OS. (**A**) N2A cells were co-transfected with *Oxr1-FL*, *-S -HA* and *FUS-MYC* or *TDP-43-FLAG*. Proteins were co-immunoprecipitated with an anti-HA antibody. FUS was always co-precipitated with Oxr1-FL and -S, while TDP-43 was co-immunoprecipitated with Oxr1-S only. (**B**) *FUS-MYC* and *TDP-43-FLAG* were transfected in N2A cells. Cells were subjected to peroxide treatment and proteins were co-immunoprecipitated. Endogenous Oxr1 is immunoprecipitated with FUS or TDP-43 only under OS conditions.

5.4.2. Oxr1 binds to FUS and TDP-43 not through RNA or through a conserved glutamic acid residue in Oxr1 TLDc domain

As the functions of FUS and TDP-43 have been linked to RNA splicing, it was tested whether the interaction between Oxr1 and FUS and TDP relied on the presence of RNA.

Co-immunoprecipited proteins treated with RNase revealed that interaction between Oxr1 and its potential binding partners FUS and TDP-43 was not through RNA, as when all RNAs were degraded, the interaction between FUS/TDP-43 and Oxr1 was still intact (**Figure 47A**).

Next, as it was shown previously that Oxr1 could form multimers through its TLDc domain, it was investigated if this domain could also be responsible for interactions of Oxr1 with other proteins. Co-immunoprecipitation from cells overexpressing FUS or TDP-43 and Oxr1 EA mutants showed that the interaction between FUS and TDP-43 and Oxr1 was not affected by disruption of a potentially crucial residue in the TLDc domain (**Figure 47B**).

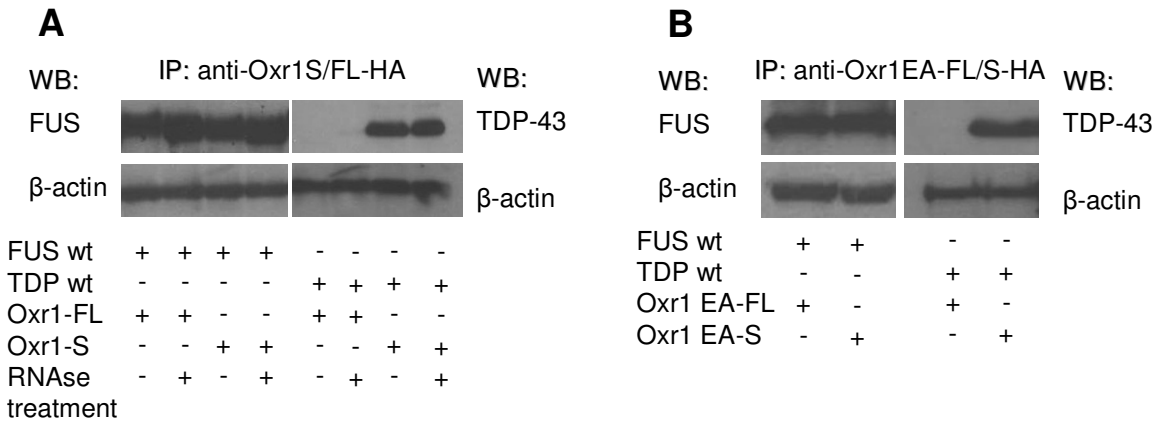


Figure 47. Oxr1 does not interact with FUS and TDP-43 through RNA or a conserved glutamic acid residue in Oxr1 TLDc domain. (**A**) N2A cells were co-transfected with *Oxr1-HA* and *FUS-MYC* or *TDP-43-FLAG* vectors. Proteins were co-immunoprecipitated and subjected to RNAse treatment. Protein interactions were similar when immunoprecipitated proteins were treated with RNAse (+) or buffer only (-). (**B**) A similar experiment was conducted using *Oxr1* EA-*FL-HA* and *-S* mutants. The mutation in the TLDc domain does not influence the interaction with FUS or TDP-43.

5.4.3. Oxr1, FUS and TDP-43 form a complex

Two recent studies in cell culture showed that FUS and TDP-43 bind to one another as part of a larger complex (Kim, Shanware et al. 2010; Ling, Albuquerque et al. 2010). The function of this complex is still unclear, although it seems to be necessary to co-regulate

histone deacetylase 6 (*HDAC6*) mRNA (Kim, Shanware et al. 2010). To determine whether Oxr1 was also present in this complex, protein extracts from cells transfected with the three constructs *FUS*, *TDP-43* and *Oxr1-S* were used for co-immunoprecipitation. Interestingly, the three proteins were always precipitated together, suggesting that Oxr1-S, FUS and TDP-43 may be part of a larger protein complex (**Figure 48**).

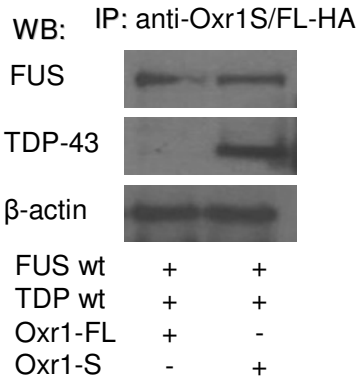


Figure 48. Oxr1-S, FUS and TDP-43 form a complex. N2A cells were co-transfected with *Oxr1-S-HA*, *FUS-MYC* and *TDP-43-FLAG*. Proteins were co-immunoprecipitated using an antibody against HA. Western blots were probed with anti-FUS or TDP-43. FUS and TDP-43 are co-immunoprecipitated with Oxr1-S.

5.4.4. Mutations linked with ALS alter FUS and TDP-43 binding to Oxr1 and their localisation under oxidative stress

Next it was investigated if known pathogenic mutations in FUS (P525L and R521C) and TDP-43 (A371G, D168G, Q331H, H337V) linked to ALS could alter their binding to Oxr1-S (Sreedharan, Blair et al. 2008; Kwiatkowski Jr., Bosco et al. 2009; Vance, Rogelj et al. 2009). The various mutants were first overexpressed in N2A cells on their own, and it was confirmed by qRT-PCR that the mutation did not affect their mRNA levels compared to wild-type constructs (**Figure 49A and B**). Then, these constructs were co-expressed with Oxr1-S, and both FUS and TDP-43. Significantly, these data showed that the interaction between Oxr1-S and the various mutants was altered (**Figure 49C and D**); the interaction was assessed by quantifying band intensity on western blots using Image J.

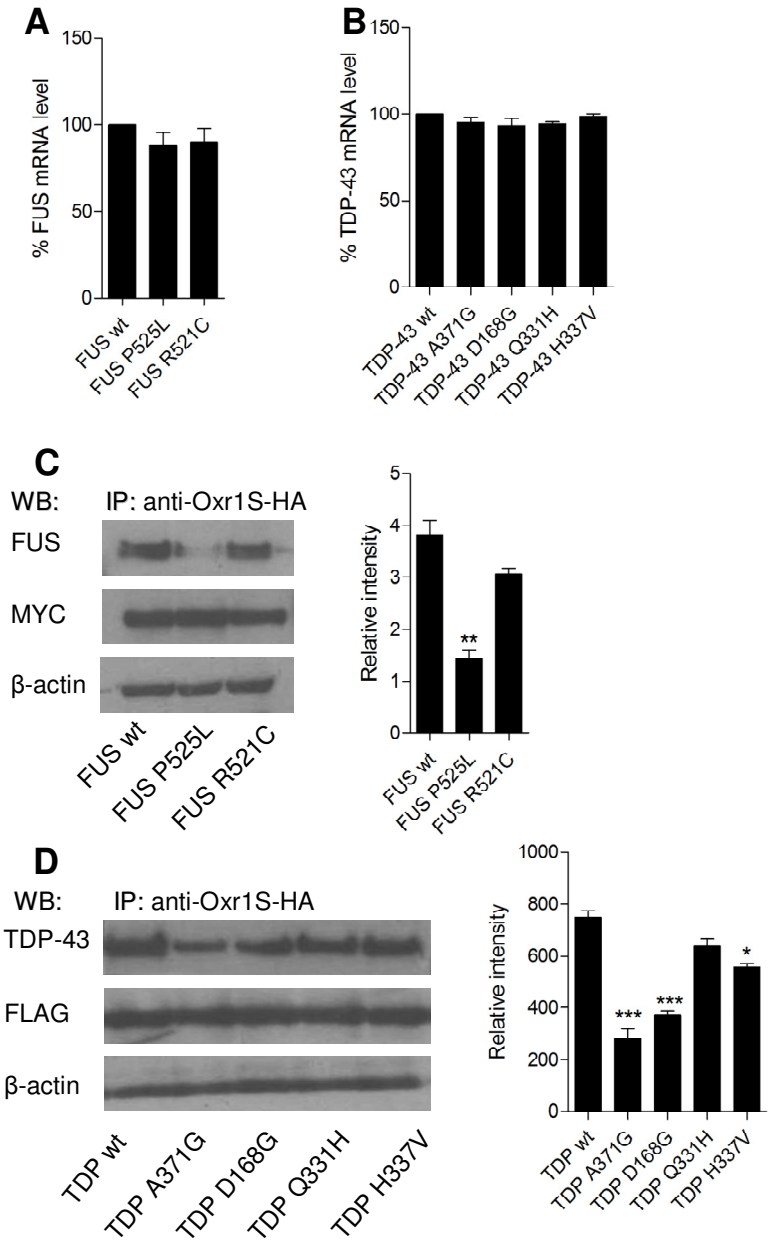


Figure 49. Mutations in FUS or TDP-43 alter their interaction with Oxr1. (**A**) and (**B**) Expression levels of FUS and TDP-43 mutants were determined by qRT-PCR. Mutants present a similar level of expression as wild-type constructs. (**C**) N2A cells were co-transfected with *Oxr1-FL-HA* and *FUS-MYC* wt or mutants. Proteins were co-immunoprecipitated using an anti-HA antibody. Representative western blot showing that FUS P525L interaction with Oxr1-FL is depleted, while the interaction of FUS R521C is not altered compared to the interaction of the wild-type construct. Similar results were found with Oxr1-S. (**D**) A similar experiment was performed with *Oxr1-S* and *TDP-43* mutant constructs. The interaction of TDP-43 A371G and D168G with Oxr1-S is altered while the other mutants have an interaction similar to the wild-type construct. (B) and (C) Western blot quantifications were performed using at least 3 independent replicate experiments (*** $p< 0.001$; ** $p< 0.01$; ANOVA).

In particular, FUS P525L and TDP-43 A371G constructs showed a significant decrease in the interaction with Oxr1-S by decreased by almost 2-fold compared to wild-type FUS or TDP-43.

Finally, as it was showed that FUS and TDP-43 mutants were mislocalised into cytoplasmic aggregates of unknown function, it was tested if co-expression with Oxr1-S could restore their localisation to the nucleus (Andersson, Stahlberg et al. 2008; Winton, Igaz et al. 2008; Vance, Rogelj et al. 2009). Firstly, single expression of wild-type FUS and TDP-43 was carried out in HeLa cells, as previous studies have investigated localisation in this cell type. In addition N2A cells were tested in parallel. These data showed nuclear localisation of the TDP-43 and FUS to the nucleus as expected (**Figure 50A**). Transfection of the various mutant constructs showed that cytoplasmic aggregates formed, varying from a mixed population of cells presenting normal nuclear localisation with few aggregates to most of the cells presenting aggregates (**Figure 50A**). When the mutants were co-expressed with *Oxr1-S*, a partial relocalisation of both the FUS and TDP-43 mutants to the nucleus as well as a decrease in number of cells presenting aggregates were observed (**Figure 50B and C**). It should be noted that FUS/TDP-43-containing aggregates also co-localised with Oxr1-S (**Figure 50A**, arrows). Interestingly, the degree of restoration of the normal nuclear localisation was directly related to the affinity of the mutant for Oxr1-S and to the amount of Oxr1-S expressed in a given cell. Indeed, cells expressing high levels of Oxr1 were more likely to be aggregate-free than cells without Oxr1. In addition, FUS (R521C) and TDP-43 (Q331H and H337V) mutants that were shown previously to bind Oxr1 displayed fewer aggregates compared to other mutants that were unable to bind Oxr1 (**Figure 49 and 50**). This suggests that a potential interaction between Oxr1 and FUS/TDP-43 is required for the normal localisation of mutant FUS and TDP-43.

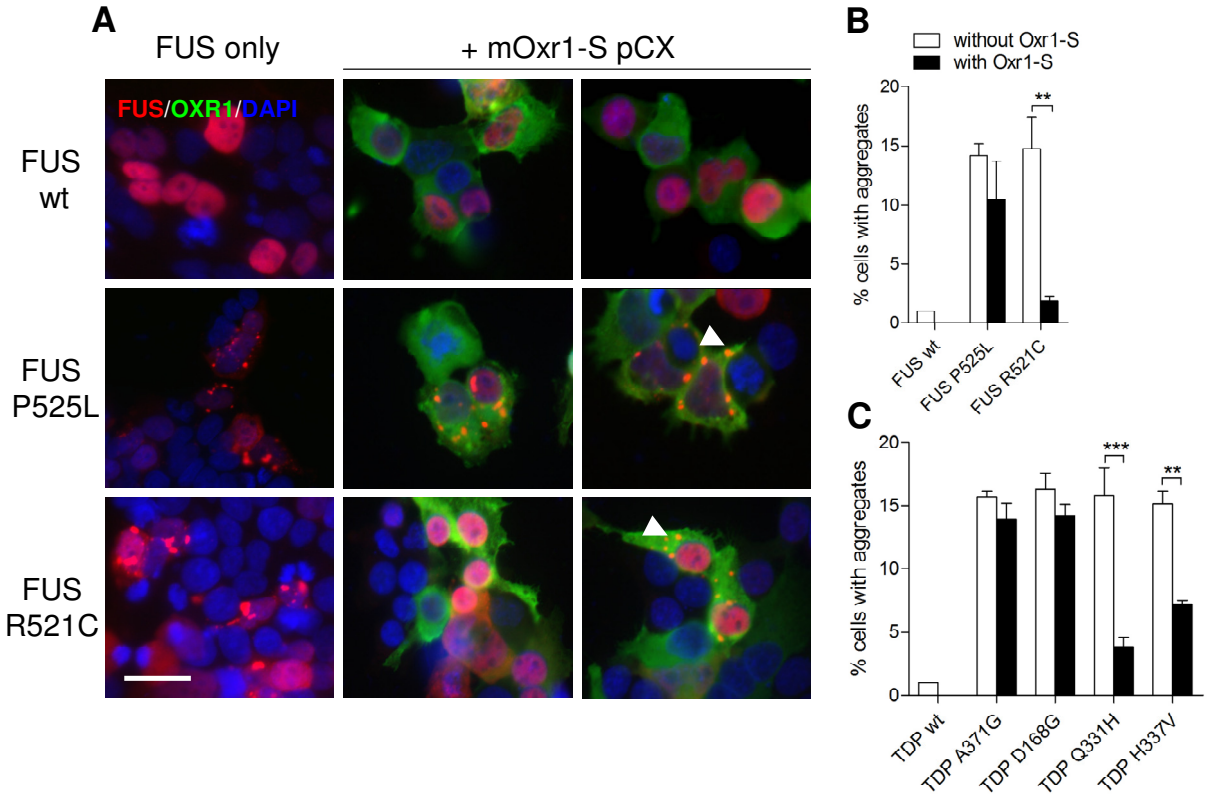


Figure 50. Oxr1 can restore localisation of FUS and TDP-43 mutants. (**A**) HeLa cells were transfected with wild-type FUS (*FUS wt*) or mutants constructs alone or with *Oxr1-FL*. Cells were subjected to peroxide treatment and stained for MYC (FUS) and HA (Oxr1). FUS wt localises to the nucleus while mutants also form aggregates in the cytoplasm. Oxr1 restores partially the localisation of FUS R521C mutant as fewer cells present aggregates and most of FUS is localised to the nucleus. Oxr1 does not restore P525L mutant as almost all cells present aggregates and only a small proportion of FUS is localised to the nucleus. Note that FUS and Oxr1 co-localise in cytoplasmic aggregates (arrowhead). Similar results were found in N2A cells. (**B**) Cells presenting aggregates were counted. Oxr1-S could reduce the number of cell presenting aggregates when co-expressed with FUS R521C but not FUS P525L. (**C**) A similar approach was used and cells presenting aggregates when transfected with TDP-43 wild-type (*TDP wt*) or mutants with or without *Oxr1-S* were counted. Oxr1-S reduces the number of cells with aggregates only when co-expressed with TDP-43 Q331H and H337V; however, no difference is detected in the number of cells presenting cytoplasmic aggregates when mutants A371G and D168G were co-expressed with or without Oxr1-S. (** $p<0.01$, *** $p<0.001$; ANOVA)

5.5. Discussion

In this chapter, it was demonstrated that the principal conserved domain in both Oxr1 and Ncoa7 (TLDc) is sufficient to confer protection against OS in neuronal cells. Indeed, this domain is highly conserved in all species; in lower organisms such as flies and yeast, only a single copy of a TLDc-domain containing protein is found, and these short proteins are very similar in structure to the Oxr1-S and Ncoa7-S transcripts in mouse. It was, however, important to determine that mammalian sequences missing the additional LysM and GRAM domains found in higher organisms were still functional *in vivo*. Moreover, an immunoprecipitation approach combined with mass spectrometry showed that both Oxr1 and Ncoa7 were likely to be involved in pathways other than their known antioxidant function, such as RNA processing and cell cycle regulation. The fact that Ncoa7 and Oxr1 have common functions despite being localised to different cellular compartments raises the possibility that Ncoa7 encodes the nuclear counterpart of the mitochondrial Oxr1 protein. However, this study did not shed light on the function of the other domains present in Oxr1, like the LysM and GRAM domains. Nevertheless, it was found that the different Oxr1 isoforms may have specific roles in addition to their common OS-protective function. Finally, a potential interaction between Oxr1 and two proteins linked to ALS, FUS and TDP-43 was investigated and it appeared that known pathogenic mutations in FUS and TDP-43 led to a mislocalisation of these proteins as well as disruption of their interaction with Oxr1. Interestingly, Fus was shown to bind to Ncoa7-FL as well.

The approach used to find binding partners of the OXR family members generated a significant number of interacting proteins. Although this was the first attempt to identify Oxr1 binding proteins, some of the data indicated that this was a valid approach. For example, from the Ncoa7 screen, members of the estrogen receptor pathway were isolated (Shao, Halachmi et al. 2002). In addition, interactors involved in the Nrf2-stress

response were found for Oxr1, consistent with the known role of Oxr1 in OS resistance (Volkert, Elliott et al. 2000; Elliott and Volkert 2004). Moreover, a significant proportion of potential interactions could also be confirmed in brain and cerebellum, supporting the use of N2A cells for the primary screen. Ideally, it would have been more biologically relevant to perform a co-immunoprecipitation from tissue extracts to identify interactions that occur *in vivo*; unfortunately, the antiserum available could not be used to immunoprecipitate Oxr1 with enough specificity. One should still be cautious with the data presented here as the strategy used may have generated false positive results. Indeed, the overexpressed protein (Oxr1 or Ncoa7) was localised to both the cytoplasmic and mitochondrial compartments even under no stress conditions, which may have led to interactions that would not be encountered under physiological conditions. For example, many studies to determine FUS and TDP-43 interactors have been carried out previously. However, Oxr1 has never been identified as a potential binding partner for these proteins (Kim, Shanware et al. 2010; Ling, Albuquerque et al. 2010). This discrepancy may be because 1) previous studies on FUS and TDP-43 were performed with no oxidative treatment and the interaction described here only occurs under OS (**Figure 46B**), or 2) *in vivo*, Oxr1 is highly expressed in the cell only under OS. It should be noted that when both FUS/TDP-43 and Oxr1 were co-expressed in cells, they could interact, even without treatment, confirming that the absolute levels of Oxr1 are critical for this interaction to take place (**Figure 46A**). As the function of FUS and TDP-43 is still under intense scrutiny at present due to their direct involvement with ALS, any new findings on these two proteins may also help to unravel Oxr1 function. Significantly, comparison of our data with recent studies that have screened for FUS and TDP-43 binding partners shows that many common binding partners have been isolated (Ling, Albuquerque et al. 2010) (**Figure 51**). Some of these binding partners and other potential leads generated from the Oxr1/Ncoa7 interaction study are discussed below:

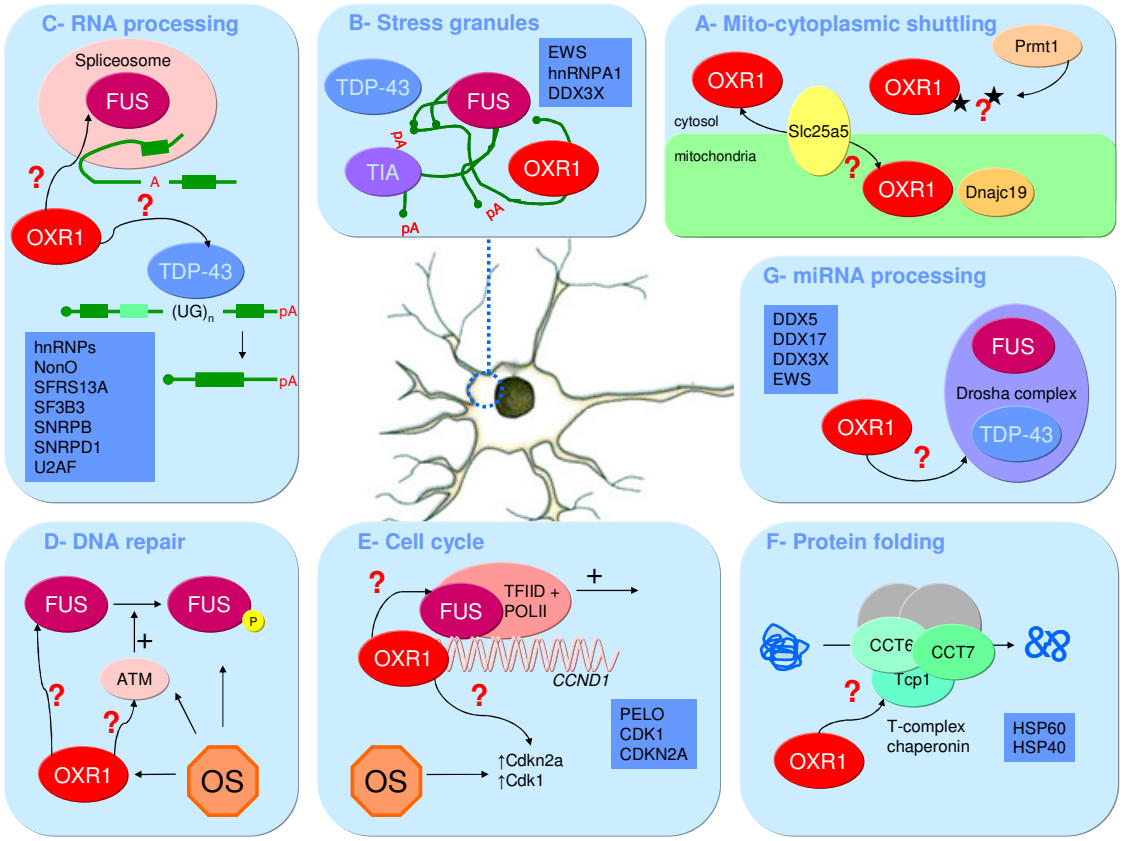


Figure 51. Summary: Oxr1 is a multifunctional protein that can bind to FUS and TDP-43. (**A**) Oxr1 may shuttle between the mitochondria and cytoplasm under OS. (**B**) Oxr1 is incorporated in SGs where it forms complexes with mRNAs and other RNA binding proteins, like FUS and TDP-43. (**C**) Oxr1 may be part of the spliceosome and together with FUS and TDP-43 may regulate RNA processing. (**D**) Oxr1 expression reduces level of DNA damage under OS. Oxr1 interacts with FUS which is activated by ATM under OS and involved in the DNA repair process. (**E**) Oxr1-S may directly or indirectly modify the function of key modulators of cell cycle. It also binds to FUS which subsequently alters gene transcription of cell cycle regulators. (**F**) Oxr1-S could play a role in protein folding by directly binding to the T-complex chaperonin or to various heat-shock proteins. (**G**) Oxr1 interacts with proteins that were found in the Drosha complex, suggesting that it may be involved in miRNA processing. Proteins highlighted in blue were found as binding partners for Oxr1 and are discussed below.

5.1.1. Oxr1 and DNA damage

First, it was demonstrated in chapter 4 that Oxr1 was involved in protecting cells against OS and specifically OS-related DNA damage. This function could be explained by Oxr1 binding to FUS. Indeed, FUS is a key transcriptional regulatory sensor of DNA damage signals. FUS is recruited to the *cyclin D1* promoter after cellular stress and is phosphorylated by the ataxia-telangiectasia mutated (ATM) upon induction of double-

strand breaks (Gardiner, Toth et al. 2008; Wang, Arai et al. 2008). FUS is required for the maintenance of genomic integrity and may have a role in DNA double strand break repair promoting the annealing of homologous DNA and the formation of DNA D-loops, an essential step in DNA repair by homologous recombination (Baechtold, Kuroda et al. 1999; Bertrand, Akhmedov et al. 1999).

5.1.2. Oxr1 and cell cycle

Moreover, in response to DNA damage, FUS is recruited by sense and antisense non coding RNA transcribed in the 5' regulatory region of the cyclin D1 (*CCND1*) gene. An RNA-dependent allosteric modification of FUS results in repression of *CCND1* transcription (Wang, Arai et al. 2008). As cyclin D1 acts as a cell cycle regulatory switch, by regulating cyclin D1 expression FUS indirectly regulates the cell cycle (Stacey 2003). FUS has also been linked to cell proliferation (Bertrand, Akhmedov et al. 1999). Although, it is still unknown if Oxr1 could regulate directly the transcription of genes involved in cell cycle, it was however demonstrated that Oxr1-S could bind to proteins involved in cell cycle regulation, like Pelo, Cdk1 and Cdkn2a/p16 (Adham, Sallam et al. 2003; Wohlbold and Fisher 2009). Interestingly, Cdk1 has been shown to be induced by OS and been part of the pathway leading to DNA damage repair (Krantic, Mechawar et al. 2005; Wohlbold and Fisher 2009). Cdkn2a/p16 upregulation has been described in AD brains (McShea, Harris et al. 1997; Zhu, Rottkamp et al. 2000). Moreover, Cdkn2a/p16 has been recently shown to be upregulated under OS, and that its loss led to an increase in DNA damage under OS, but how Cdkn2a/p16 acts to reduce OS in the cell is still unknown (Jenkins, Liu et al. 2010). The critical role of the cell cycle in ND has been demonstrated in the Harlequin mouse (*Hq*) (Klein, Longo-Guess et al. 2002). In this mouse model, a downregulation of the apoptosis-inducing factor (*Aif*) gene led to cell cycle re-entry of cerebellar GCs before they underwent apoptosis. Thus, it has to be investigated in the

bella mouse, if loss of *Oxr1* could induce cell cycle disruption as it would shed light on Oxr1 involvement in cell cycle regulation.

5.1.3. Oxr1 and protein folding

Another function, specific to Oxr1-S, is the regulation of protein folding. Indeed, Oxr1-S binds to Cct6, Cct7, Tcp1, Hspd1/Hsp 60 and Dnaj/Hsp40 that are all proteins known to be involved in protein folding (Ulrich Hartl and Martin 1995; Frydman 2001). Specifically, Cct6, Cct7 and Tcp1 are part of the T-complex chaperonin (Frydman 2001; Cong, Bakera et al. 2010). Noticeably, CCT7 has been shown to be upregulated in dopaminergic neurons, neurons affected in PD, when under peroxide treatment, highlighting the role of chaperones and protein folding in the mechanism of ND (Anantharam, Lehrmann et al. 2007). Hsp40 was found in intranuclear ataxin-3 aggregates in SCA3, and overexpression of the Dnaj/Hsp40 chaperones in cell culture could suppress aggregation of the mutant ataxin-3 suggesting that protein folding misregulation can lead to ND and ataxia as discussed in chapter 1 (Chai, Koppenhafer et al. 1999; Kobayashi, Kume et al. 2000).

5.1.4. Oxr1 and RNA processing

Evidence for a role of Oxr1 in mRNA processing and an indirect regulation of mRNA splicing comes from the identification of its association with many hnRNP proteins, indicating that Oxr1 may be part of hnRNP complexes, which associate with nascent transcripts and influence their fates (Dreyfuss, Matunis et al. 1993). Many of these hnRNP-related proteins are known to bind to TDP-43, such as hnRNP A1, C, D, H1, K, Q (Ling, Albuquerque et al. 2010). Interestingly, the interaction between TDP-43 and hnRNPA, B and C was required *in vitro* for splicing site selection (Buratti, Dork et al. 2001). FUS also binds to hnRNPA1 and C (Zinszner, Albalat et al. 1994). Beside hnRNPs, several additional Oxr1 binding proteins were shown to be involved in RNA

splicing regulation: NonO/ p54^{nrb}, Sfrs13a, Sf3b3, Snrpb, andSnrpd1/Smd1 (Caceres, Stamm et al. 1994; Fury, Zhang et al. 1997; Sleeman, Ajuh et al. 2001; Caceres and Kornblihtt 2002; Shav-Tal and Zipori 2002; Golas, Sander et al. 2003; Ling and Estus 2010; Salton, Lerenthal et al. 2010). Another study showed that EWS, an Oxr1 potential binding partner, interacts with U2AF. This suggests that EWS and Oxr1 may form a complex involved in splicing regulation (Knoop and Baker 2000). Similarly, NonO/ p54^{nrb} a transcription/splicing factor has been shown to be part of large transcription-splicing complexes, that contain FUS, and bind the 3' and 5' splice sites of pre-mRNA (Kameoka, Duque et al. 2004; Law, Cann et al. 2006). It would therefore be interesting to investigate if splicing of RNA targets found for TDP-43 and FUS could be modified by modulation of Oxr1 levels. Indeed, TDP-43 regulates the alternative splicing of the cystic fibrosis transmembrane regulator (CFTR), apolipoprotein A-II and survival motor neuron (SMN) transcripts (Mercado, Ayala et al.; Buratti, Brindisi et al. 2005; Bose, Wang et al. 2008). FUS has been reported to alter the splicing of co-transfected reporter plasmids and to influence the splicing of H-ras (Lerga, Hallier et al. 2001; Rapp, Yang et al. 2002; Camats, Guil et al. 2008; Tan and Manley 2010).

5.1.5. Oxr1 and microRNA

A small number of proteins found in this study were previously shown to be components of Drosha microRNA processing complexe, including Ddx5, Ddx17, and Ddx3x (Gregory, Yan et al. 2004; Freibaum, Chitta et al. 2009). These proteins are also binding partners of TDP-43 (Ling, Albuquerque et al. 2010). Moreover, EWS, structurally very similar to FUS, another Oxr1 binding partner was also identified as a component of a larger Drosha complex (Gregory, Yan et al. 2004). Thus, Oxr1 may be involved in microRNA biogenesis due to its association with micro-processing complexes. Interestingly, a recent study showed that microRNA malfunction could lead to spinal motor neuron disease

demonstrating the crucial role of microRNA in neuronal survival (Haramati, Chapnik et al. 2010).

5.1.6. Oxr1 and its shuttling between mitochondria and cytoplasm

This study and others have confirmed that TDP-43 and FUS were both present in the nucleus or the cytoplasm depending on the conditions (Zinszner, Sok et al. 1997; Andersson, Stahlberg et al. 2008; Ayala, Misteli et al. 2008). For its part, Oxr1 shuttles between the mitochondria and the cytoplasm and it is supposed from this study that, like TDP-43 and FUS, it may localise to stress granules (SGs) in the cytoplasm when under OS conditions (Andersson, Stahlberg et al. 2008; Colombrita, Zennaro et al. 2009). Indeed, many other potential Oxr1 binding partners also localise to stress granules, like Ddx3x, hnRNPA1 and Ews (Guil, Long et al. 2006; Andersson, Stahlberg et al. 2008; Goulet, Boisvenue et al. 2008).

Surprisingly, very few proteins specific to the mitochondria were found as binding targets of Oxr1. Dnajc19, an inner mitochondrial membrane co-chaperone and Slc25a5, a mitochondrial carrier, bind to Oxr1 and are involved in protein trafficking in and out of the mitochondria, and they may be responsible for Oxr1 shuttling from mitochondria to cytoplasm. Interestingly, a mutation in the Dnajc19 gene has been linked to a Barth syndrome–like condition presenting ataxia (Mokranjac, Sichting et al. 2003; Davey, Parboosingh et al. 2006). Another protein that could affect Oxr1 localisation is Prmt1 which binds to Oxr1-S and that has been shown to mediate arginine residues methylation (Nicholson, Chen et al. 2009). Noticeably, Oxr1 short isoform presents many arginine residues in its TLDc domain. The importance of arginine methylation of proteins for their proper localisation has been demonstrated for FUS and a related protein TAF-15 as the methylation by PRMT1 is essential for TAF-15 shuttling between compartments (Jobert, Argentini et al. 2009). Interestingly, mutations in FUS are usually occurring in the FUS

protein arginine residues; this has been suggested to prevent its subsequent methylation by PRMT1 and would explain why FUS mutants are retained to the cytoplasm in ALS (Rappsilber, Friesen et al. 2003; Nicholson, Chen et al. 2009). Thus, Oxr1 shuttling between the different cellular compartments may be mediated by the methylation of its arginine residues. Oxr1 localisation to the mitochondria may be crucial for its OS-related function as shown for DJ-1, so understanding the mechanism leading to Oxr1 mitochondrial localisation is essential (Junn, Jang et al. 2009). To investigate this feature specifically, it may be useful to perform a cell fractionation and study binding partners specific to the mitochondria or use overexpressing constructs that could force Oxr1 to remain in the mitochondria.

Moreover, Oxr1 binds to kinesin, desmin and dynein. Kinesin has been linked to transport of peroxisomes, neurofilaments, and Golgi-derived vesicles into neuritis (Stamer, Vogel et al. 2002). Interestingly, dynein and kinesin regulate SGs formation (Loschi, Leishman et al. 2009). They also are involved in organelles trafficking, like mitochondria (Hirokawa 1998). Misregulation of their activity has been linked to many NDDs (Piccioni, Pinton et al. 2002; Gunawardena and Goldstein 2005). For example, a mouse mutant with gait abnormalities, the sprawling (*Swl*) mouse presents a mutation in the *dynein heavy chain 1* gene. It also presents late-onset motor neuron loss, with a severe, early-onset proprioceptive sensory neuropathy highlighting the potential involvement of dynein in ND (Chen, Levedakou et al. 2007; Banks and Fisher 2008). Therefore, Oxr1 may also have a role in intra-cellular transport, and the ND in the *bella* mouse could thus be due to a combination of pathway misregulation as it was demonstrated here that Oxr1 has many functions.

Finally, it was confirmed that Ncoa7 had a role in the estrogen signalling pathway. However, it was shown here that Ncoa7 expression could be induced by OS independent of stimulation by estrogen suggesting that Ncoa7 may have other functions, separate from

the estrogen pathway. Indeed, it was demonstrated here that Ncoa7 can protect mammalian cells against OS through its TLDc domain. Moreover, preliminary experiments suggested that it may also have a role in RNA signalling but further studies are required to dissect its other functions, in neurons especially, as it had so far mainly be studied only in the reproductive tract (Shkolnik, Ben-Dor et al. 2008).

5.1.7. Oxr1, a multifunctional protein

From the large number of interacting proteins identified, potentially new functions for Oxr1 and Ncoa7 have emerged, including RNA processing. Many lines of evidence have demonstrated the importance of this process in ND, for example splicing alterations and mRNA-editing errors are observed in ALS (Lin, Bristol et al. 1998; Kawahara, Ito et al. 2004; Rabin, Kim et al. 2010). Interestingly, it was shown that Oxr1 could form a complex with FUS and TDP-43, both linked with ALS and both having roles in RNA splicing (see section 5.1.4). Mutations in these proteins have been suggested to cause the splicing alterations observed in ALS (Lagier-Tourenne, Polymenidou et al. 2010). Moreover, it was shown that mutants FUS and TDP-43 mislocalised to the cytoplasm, forming aggregates and that these mutants had an altered binding with Oxr1. It also appeared from this study that Oxr1 could partially restore normal localisation of FUS and TDP-43 mutants. Thus, it would be interesting to test if Oxr1 could also restore or at least ameliorate their splicing function and if it could improve the ALS phenotype.

To conclude, this study has demonstrated that Oxr1 is potentially a multifunctional protein with roles in key pathways known to be disrupted in NDDs like ALS. This supports the continued analysis of Oxr1 and related proteins to understand their functions in both the OS-response and in other processes leading to ND.

6. Discussion:

The aim of this project was to understand the molecular mechanisms underlying movement disorders and to identify new genes involved in ND. Using mice from the Harwell ENU mutagenesis screen, two mutants displaying ataxia were analysed and both have provided important new insights into cell death and survival in the brain. The study of the *robotic* mouse demonstrated how a mutation in a transcription factor can deregulate pathways downstream of Igf-1 which lead to PCs death. Analysis of the *bella* mouse identified a novel gene linking OS and ND and further *in vitro* studies have begun to reveal the function of the conserved TLDc domain of Oxr1 and the related protein Ncoa7. Thus, this work has highlighted the value of a phenotype-driven approach to investigate novel neurodegenerative pathways.

Since the identification of the *robotic* mutant, analysis of this line has not only facilitated study of ALF family proteins in transcription, but also has highlighted specific mechanisms of cell death in the cerebellum and potential therapeutic targets for human ataxias. This work will undoubtedly assist future studies aimed at identifying the gene targets deregulated in ALF-associated ND, mental retardation and leukemia. This study also raises the possibility that few components of the transcriptional regulatory protein network containing ALF proteins may be involved in other disorders of the central nervous system.

After characterising the phenotype of the *bella* mutant, this study then went on to identify the TLDc domain as the region of Oxr1 and Ncoa7 proteins that is able to confer neuroprotection against OS. This is the first time that any functional information on this protein family has been obtained in mammalian systems. Further studies are required to understand the exact function of the TLDc domain as well as the proteins themselves. Sequences alignment reveals a number of residues that are highly conserved and that could be subjected to mutagenesis to help dissect the role of these residues in this

domain (**Figure 40A** in chapter 5). The *bella* mouse itself was limited as an *in vivo* model system due to its early lethality; however, an ENU point mutant in the TLDc domain may have a more subtle phenotype. Therefore, based on *in vitro* data, screening the ENU archive for this domain in Oxr1 and Ncoa7 would be worthwhile. Assaying any new mutant(s) *in vitro* would then be carried out to determine whether rederivation of the corresponding ENU mouse line would be likely to provide valuable functional information. Furthermore, considering that a defective OXR1 protein may lead to an enhancement of OS in NDD, screening patient samples for mutations in this region could be carried out.

In parallel to a mutagenesis approach, a direct biochemical strategy could be used to identify the function of Oxr1. For example, like DJ-1, Oxr1 could act as a free-radical scavenger and eliminate hydrogen peroxide by oxidizing itself (Taira, Saito et al. 2004). Experiments such as hydrogen peroxide clearance assays would quantify this potential activity. Such post-translational regulation may be critical to the activation of Oxr1 in response to OS, facilitating a change in its isoelectric point (pI) or conformation (dimerisation or cleavage) depending on the oxidative conditions in the cell, as described for DJ-1 and PINK-1 (Mitsumoto and Nakagawa 2001; Honbou, Suzuki et al. 2003; Wilson, Collins et al. 2003; Baulac, LaVoie et al. 2004; Taira, Saito et al. 2004; Ooe, Maita et al. 2006; Liu, Vives-Bauza et al. 2009). Oxidation of specific cysteine residues could be responsible for the relocalisation of Oxr1 from the mitochondria to the cytoplasm under OS (Junn, Jang et al. 2009). It is therefore interesting that a highly conserved cysteine is found in the TLDc domain of both Oxr1 and Ncoa7 (Volkert, Elliott et al. 2000; Sanchez, Riddle et al. 2008; Lee, Dietz et al. 2010) (**Figure 40A**, blue box).

An alternative strategy would be to determine the 3-D structure of the TLDc domain as it may have a similar structure a known protein. Indeed, studying the structure of a protein may often help elucidating its function. For example, studying PINK1 structure identified a kinase domain that later appeared to be necessary for PINK1 to associate with the

mitochondrial complexes and to perform its function (Zhou, Huang et al. 2008; Liu, Vives-Bauza et al. 2009). However this strategy cannot be used when no characterised domain can be identified. This was the case of DJ-1 and its structure had first to be resolved by crystallography. The solution of its crystal structure then provided the basis for predictions regarding of the mode of action of this redox-reactive protein (Honbou, Suzuki et al. 2003; Huai, Sun et al. 2003; Tao and Tong 2003; Wilson, Collins et al. 2003; Wilson, Amour et al. 2004). Structural studies demonstrated that DJ-1 resembled a heat shock protein 31 of bacteria and yeast and that DJ-1 possessed an oxidised/active form when under OS suggesting that DJ-1 may function as a redox-activated chaperone (Wilson, Collins et al. 2003; Wilson, Amour et al. 2004). Moreover, these studies demonstrated that DJ-1 may be active only in its dimerised form (Tao and Tong 2003; Wilson, Collins et al. 2003). Thus, defining the TLDc crystal structure appears to be a crucial step to understand the function of this highly conserved domain.

Furthermore, Oxr1 stability under OS conditions could be investigated by determining its degree of degradation by the ubiquitin-proteasome pathway in correlation with fluctuations of oxidative conditions in the cell, as observed for Nrf2 (Itoh, Wakabayashi et al. 2003; McMahon, Itoh et al. 2003; He and Ma 2009). Indeed, many potential binding partners of Oxr1 were involved in the process of ubiquitination/de-ubiquitination of proteins and the regulation of protein turnover; few of these proteins being Uba52, Usp-ps, and Btbd6 BTB/POZ (Bury, Moers et al. 2008; Burrows, Kelvin et al. 2009; Sobieszczuk, Poliakov et al. 2010).

Moreover, in chapter 5 it was demonstrated that Oxr1-FL and -S had common but also specific functions. Thus, it would be interesting to investigate if Oxr1 isoforms may also have a specific localisation related to these specific functions. Indeed, proteins involved in molecule trafficking between the mitochondria and the cytoplasm were only associated with Oxr1-S, suggesting that only Oxr1-S may be shuttling in-and-out of the mitochondria.

Such a difference in localisation for various protein isoforms has been described for PINK1; Indeed, only the truncated form of PINK1 shuttles to the cytoplasm, the full-length protein always remaining in the mitochondria (Lin and Kang 2008). To answer this question, antibodies specific for Oxr1-FL and Oxr1-S would have to be generated.

Moreover, as stated previously, the *bella* mouse is a limited *in vivo* model to study Oxr1 function and role in NDD as the mice die before reaching maturity. Importantly, the fact that Oxr1 is expressed in all major regions of the CNS as shown by *in situ* hybridisation suggests that the gene plays a neuroprotective role outside of the cerebellum (**Figure 52**). Thus, to investigate the role of Oxr1 in other cell types and to study if loss of *Oxr1* can cause ND in other regions of the CNS, a conditional knockout line disrupting all known isoforms is being generated. Animals lacking *Oxr1* in specific regions of the CNS relevant to major NDDs, such as in motor neurons and the striatum can then be produced by crossing to the respective cre-recombinase reporter line (Kos 2004). Mice will be subsequently examined for signs of cell death and neurodevelopmental problems. If the phenotype is mild and the mice survive into adulthood, they may be bred with other NDD mouse models to determine whether an increased susceptibility to ROS-related cell death exacerbates their particular disease phenotypes.

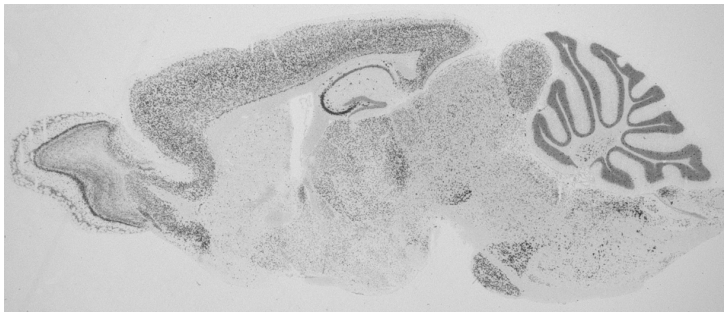


Figure 52. *Oxr1* is expressed in the brain in the adult mouse. *In situ* hybridisation from wild-type mouse (P56) showing that *Oxr1* is expressed in various regions in the brain (performed by Dr Peter Oliver).

In addition to demonstrating that loss of *Oxr1* was detrimental to cell survival, it was also shown that an increase in Oxr1 levels were sufficient to prevent ND. From these findings, it can be hypothesised that Oxr1 could be used as an antioxidant therapeutic target. It has to be noted that externally applied antioxidant therapies have been tried for the treatment

of MDDs, like AD and FRDA, but they have been only mildly effective (Hart, Lodi et al. 2005; Pandolfo 2007). This was perhaps because the antioxidant administration was not sufficiently robust or because of their nonspecific nature or incorrect timing of administration. Thus, the specificity of the antioxidant applied, the timing of treatment and the mode of delivery need to be optimised to be efficient enough for the treatment of NDDs. Nevertheless, due to the frequent association between OS and NDD, it is worthwile to pursue the investigation of potential target candidates for antioxidant drug development to treat NDDs. In the mouse, overexpression of SOD2 in a model of AD decreased hippocampal superoxide, prevented AD-related learning and memory deficits, and reduced Aβ plaques (Ju, Chen et al. 2005; Quinn, Joseph et al. 2007; Massaad, Washington et al. 2009). Therefore, further studies on Oxr1 neuroprotective effect *in vivo* are worth pursuing. The first step would therefore be to test whether an increase of Oxr1 levels in neurons would reduce ND in NDD mouse models. Thus, it will be necessary to generate a mouse expressing high levels of Oxr1 in neuronal cells specifically using an overexpressing vector with a strong neuronal promoter, like a Prp prion promoter (Borchelt, Davis et al. 1996). Then this mouse would have to be crossed with other mouse models of NDDs and neuropathology would be quantified at various time points. The transgenic lines used for genetic rescue of the *bella* phenotype expressed Oxr1 in the CNS, although the expression levels were lower than the endogenous gene, thus these lines would not be suitable for this purpose. However, as Oxr1 was very highly expressed in heart and muscle in two of the four founder *Tg(Oxr1)* transgenic lines (data not shown), it would be interesting to use this line to study the role of OS in non-NDD models. For example, the dystrophin-deficient mutant (*mdx*), a model for Duchenne Muscular Dystrophy (DMD), has been shown to display high levels of OS in both heart and skeletal muscles (Williams and Allen 2007). Therefore, crossing the Oxr1 transgenic line with *mdx* mice might ameliorate or slow-down progression of the muscle degeneration normally observed (Khouzami, Bourin et al.; Menazza, Blaauw et al.; Ragusa, Chow et al. 1997; Williams and Allen 2007; Vercherat, Chung et al. 2009).

An alternative approach is to use a viral delivery strategy to increase Oxr1 levels; this method was used to overexpress the antioxidant enzyme *gpx* in nigral dopaminergic neurons in a drug-induced PD model which led to a small but yet significant neuroprotective effect of gpx in these cells (Ridet, Bensadoun et al. 2006). A similar approach using lentiviral or adenoviral vectors expressing *Oxr1*, or the TLDc domain only, could be tried in mouse models of NDD already presenting signs of ND. It has to be noted that although this approach gave at first very promising results, a number of technical issues have still to be overcome to consider this approach as a viable therapeutic strategy (McBride, Ramaswamy et al. 2006; Ridet, Bensadoun et al. 2006). For example, as highlighted by many groups, viral injections in affected regions allow the transduction of only a very small proportion of cells. Moreover, further studies are required to assess the safety of these viral vectors and to understand virus-host interactions (McBride, Ramaswamy et al. 2006; Ridet, Bensadoun et al. 2006; Young, Searle et al. 2006; Dodge, Haidet et al. 2008).

In conclusion, the work in this thesis has highlighted the value of a phenotype-driven approach to investigate novel neurodegenerative pathways and demonstrates how mouse mutants can successfully be used to understand the function of new molecules and pathways involved in ND and to test, in the long run, potential therapies for NDDs.

References

Abbott, L. C., M. Bump, et al. (2000). "Investigation of the role of the cerebellum in the myoclonic-like movement disorder exhibited by tottering mice." Mov. Disord. **1**: 53-9.

Abe, T., K. Abe, et al. (1997). "Ocular Changes in Patients With Spinocerebellar Degeneration and Repeated Trinucleotide Expansion of Spinocerebellar Ataxia Type 1 Gene." Arch Ophthalmol **115**(2): 231-236.

Abeliovitch, A., Y. Schmitz, et al. (2000). "Mice Lacking α-Synuclein Display Functional Deficits in the Nigrostriatal Dopamine System." Cell **25**(1): 293-252.

Acevedo-Arozena, A., S. Wells, et al. (2008). "ENU Mutagenesis, a Way Forward to Understand Gene Function." Annual Review of Genomics and Human Genetics **9**(1): 49-69.

Adler, V., Z. Yin, et al. (1999). "Regulation of JNK signaling by GSTp." EMBO J **18**(5): 1321-1334.

Albrecht, M. (2005). "LRRK2 mutations and Parkinsonism." The Lancet **365**(9466): 1230-1230.

Aleyasin, H., M. W. C. Rousseaux, et al. (2007). "The Parkinson's disease gene DJ-1 is also a key regulator of stroke-induced damage." Proceedings of the National Academy of Sciences **104**(47): 18748-18753.

Allen, G. (2005). "The cerebellum in autism." Clinical neurophychiatry **2**(6): 321-337

Alvina, K. and K. Khodakhah (2010). "The Therapeutic Mode of Action of 4-Aminopyridine in Cerebellar Ataxia." J. Neurosci. **30**(21): 7258-7268.

Amir, R. E., I. B. Van den Veyver, et al. (1999). "Rett syndrome is caused by mutations in X-linked MECP2, encoding methyl-CpG-binding protein 2." Nature **23**: 185-188.

Andersen, J. (2004). "Oxidative stress: cause or consequence?" Nature Reviews Neuroscience **5**: S18-S25.

Andersson, M., A. Stahlberg, et al. (2008). "The multifunctional FUS, EWS and TAF15 proto-oncoproteins show cell type-specific expression patterns and involvement in cell spreading and stress response." BMC Cell Biology **9**(1): 37.

Arai, A., J. A. Spencer, et al. (2002). "STARS, a striated muscle activator of Rho signaling and serum response factor-dependent transcription." J. Biol. Chem. **277**(27): 24453-9.

Armstrong, J. S. (2006). "Mitochondrial membrane permeabilization: the sine qua non for cell death." BioEssays **28**(3): 253-260.

Bains, M., M. L. Florez-McClure, et al. (2009). "IGF-I prevent the accumulation of autophagic vesicles and cell death in Purkinje neurons by increasing the rate of autophagosome-to-lysosome fusion and degradation." The American Society for Biochemistry and Molecular Biology.

Baker, J., L. Jeh-Ping, et al. (1993). "Role of insulin-like growth factors in embryonic and postnatal growth." Cell **75**(1): 73-82.

Baldaçara, L., J. G. F. Borgio, et al. (2008). "Cerebellum and psychiatric disorders." Revista Brasileira de Psiquiatria **30**: 281-289.

Ballatori, N., S. M. Krance, et al. "Plasma membrane glutathione transporters and their roles in cell physiology and pathophysiology." Molecular Aspects of Medicine **30**(1-2): 13-28.

Banerjee, R., A. A. Starkov, et al. (2010). "Mitochondrial dysfunction in the limelight of Parkinson's disease pathogenesis." Biochim Biophys Acta. **1792**(7): 651-663.

Banoei, M., M. Houshmand, et al. (2007). "Huntington's Disease and Mitochondrial DNA Deletions: Event or Regular Mechanism for Mutant Huntingtin Protein and CAG Repeats Expansion?!" Cellular and Molecular Neurobiology **27**(7): 867-875.

Barber, S. C. and P. J. Shaw (2010). "Oxidative stress in ALS: Key role in motor neuron injury and therapeutic target." Free Radical Biology and Medicine **48**(5): 629-641.

Barclay, J., N. Balaguero, et al. (2001). "Ducky Mouse Phenotype of Epilepsy and Ataxia Is Associated with Mutations in the Cacna2d2 Gene and Decreased Calcium Channel Current in Cerebellar Purkinje Cells." J. Neurosci. **21**(16): 6095-6104.

Basergaa, R., A. Hongoa, et al. (1997). "The IGF-I receptor in cell growth, transformation and apoptosis " Biochimica et Biophysica Acta (BBA) - Reviews on Cancer **1332**(3): F105-F126.

Bauer, P. O. and N. Nukina (2009). "The pathogenic mechanisms of polyglutamine diseases and current therapeutic strategies." Journal of Neurochemistry **110**(6): 1737-1765.

Baulac, S., H. Lu, et al. (2009). "Increased DJ-1 expression under oxidative stress and in Alzheimer's disease brains." Molecular Neurodegeneration **4**(1): 12.

Bauman, M. and T. L. Kemper (1985). "Histoanatomic observations of the brain in early infantile autism." Neurology **35**(6): 866-.

Bäurle, J., K. Kranda, et al. (2006). "On the variety of cell death pathways in the <i>Lurcher</i> mutant mouse." Acta Neuropathologica **112**(6): 691-702.

Bawa, B. and L. Abbott (2008). "Analysis of Calcium Ion homeostasis and mitochondrial function in cerebellar granule cells of adult Cav 2.1 Calcium Ion channel mutant mice." Neurotoxicity Research **13**(1): 1-18.

Beal, M. F. "Parkinson's disease: a model dilemma." Nature **466**(7310): S8-S10.

Beal, M. F. (2006). "Parkinson's disease: a model dilemma." Nature **466**(7310): S8-S10.

Becker, E. and D. R. Richardson (2001). "Frataxin: its role in iron metabolism and the pathogenesis of Friedreich's ataxia." The International Journal of Biochemistry & Cell Biology **33**(1): 1-10.

Benzer, S. (1971). "From the Gene to Behavior." JAMA **218**(7): 1015-1022.

Bhattacharya, K., D. Saadia, et al. (2002). "Brain Magnetic Resonance Imaging in Multiple-System Atrophy and Parkinson Disease: A Diagnostic Algorithm." Arch Neurol **59**(5): 835-842.

Bitoun, E., P. L. Oliver, et al. (2007). "The mixed-lineage leukemia fusion partner AF4 stimulates RNA polymerase II transcriptional elongation and mediates coordinated chromatin remodeling." Hum. Mol. Genet. **16**(1): 92-106.

Blatt, J. (2000). "IGF1 AND LEUKEMIA." Pediatric Hematology-Oncology **17**(3): 199-201.

Blesch, A. (2006). "Neurotrophic Factors in Neurodegeneration." Brain Pathology **16**(4): 295-303.

Bonapace, G., D. Concolino, et al. (2003). "A novel mutation in a patient with insulin-like growth factor 1 (IGF1) deficiency." Journal of Medical Genetics **40**(12): 913-917.

Bondy, C. A., H. Werner, et al. (1990). "Cellular Pattern of Insulin-Like Growth Factor-I (IGF-I) and Type I IGF Receptor Gene Expression in Early Organogenesis: Comparison with IGF-II Gene Expression." Mol Endocrinol **4**(9): 1386-1398.

Bonifati, V., P. Rizzu, et al. (2003). "Mutations in the DJ-1 Gene Associated with Autosomal Recessive Early-Onset Parkinsonism." Science **299**(5604): 256-259.

Bonini, N. M. and M. E. Fortini (2006). "Human neurodegenerative disease modeling using Drosophila." Annu. Rev. Neurosci. **26**: 627-56.

Borchelt, D. R., J. Davis, et al. (1996). "A vector for expressing foreign genes in the brains and hearts of transgenic mice." Genetic Analysis: Biomolecular Engineering **13**(6): 159-163.

Bossers, K., G. Meerhoff, et al. (2008). "Analysis of Gene Expression in Parkinson's Disease: Possible Involvement of Neurotrophic Support and Axon Guidance in Dopaminergic Cell Death." Brain Pathology **19**(1): 91-107.

Bové, J., D. Prou, et al. (2005). "Toxin-Induced Models of Parkinson's Disease." NeuroRx **2**(3): 484-494.

Brazil, D. P., Y. Zhong-Zhou, et al. (2004). "Advances in protein kinase B signalling: AKTion on multiple fronts." Trends in Biochemical Sciences **29**(5): 233-242.

Brown, S. D. M. and R. Balling (2001). "Systematic approaches to mouse mutagenesis." Current Opinion in Genetics & Development **11**(3): 268-273.

Brusse, E., J. Maat-Kievit, et al. (2007). "Diagnosis and management of early- and late-onset cerebellar ataxia." Clinical Genetics **71**(1): 12-24.

Bubber, P., V. Haroutunian, et al. (2005). "Mitochondrial abnormalities in Alzheimer brain: Mechanistic implications." Annals of Neurology **57**(5): 695-703.

Bürk, K., S. Bäsch, et al. (2001). "Executive Dysfunction in Spinocerebellar Ataxia Type 1." European Neurology **46**(1): 43-48.

Bürk, K., C. Globas, et al. (2003). "Cognitive deficits in spinocerebellar ataxia type 1, 2, and 3." Journal of Neurology **250**(2): 207-211.

Büttner, N., S. A. Johnsen, et al. (2010). "Af9/Mllt3 interferes with Tbr1 expression through epigenetic modification of histone H3K79 during development of the cerebral cortex." Proceedings of the National Academy of Sciences **107**(15): 7042-7047.

Caceres, J. F. and A. R. Kornblihtt (2002). "Alternative splicing: multiple control mechanisms and involvement in human disease." **18**: 186-193.

Cagnol, S. and J. C. Chambard (2010). "ERK and cell death: Mechanisms of ERK-induced cell death – apoptosis, autophagy and senescence." FEBS Journal **277**(1): 2-21.

Calmels, N. g., S. p. Schmucker, et al. (2009). "The First Cellular Models Based on Frataxin Missense Mutations That Reproduce Spontaneously the Defects Associated with Friedreich Ataxia." PLoS ONE **4**(7): e6379.

Campuzano, V., L. Montermini, et al. (1997). "Frataxin is Reduced in Friedreich Ataxia Patients and is Associated with Mitochondrial Membranes." Human Molecular Genetics **6**(11): 1771-1780.

Chahrour, M., S. Y. Jung, et al. (2008). "MeCP2, a Key Contributor to Neurological Disease, Activates and Represses Transcription." Science **320**(5880): 1224-1229.

Chakrabarti, L., J. Eng, et al. (2009). "Autophagy activation and enhanced mitophagy characterize the Purkinje cells of pcd mice prior to neuronal death." Mol Brain. **2**: 24.

Chakrabarti, L., J. Neal, et al. (2006). "The Purkinje cell degeneration 5J mutation is a single amino acid insertion that destabilizes Nna1 protein." Mammalian Genome **17**(2): 103-110.

Chakrabarti, L., R. Zahra, et al. (2010). "Mitochondrial Dysfunction in NnaD Mutant Flies and Purkinje Cell Degeneration Mice Reveals a Role for Nna Proteins in Neuronal Bioenergetics " Neuron **66**(6).

Chakrabarti, L., R. Zahra, et al. (2010). "Mitochondrial Dysfunction in NnaD Mutant Flies and Purkinje Cell Degeneration Mice Reveals a Role for Nna Proteins in Neuronal Bioenergetics " Neuron **66**(6): 835-847.

Chamberlain, S., J. Shaw, et al. (1988). "Mapping of mutation causing Friedreich's ataxia to human chromosome 9." Nature **334**(6179): 248-250.

Chandra, S., F. Fornai, et al. (2004). "Double-knockout mice for alpha- and beta-synucleins: Effect on synaptic functions." Proceedings of the National Academy of Sciences of the United States of America **101**(41): 14966-14971.

Chang, F., L. S. Steelman, et al. (2003). Regulation of cell cycle progression and apoptosis by the Ras/Raf/MEK/ERK pathway (Review).

Chao, M. (2003). "Neurotrophins and their receptors: a convergence point for many signalling pathways." Nat Neurosci **4**.

Chen, G., L. S. Popa, et al. (2009). "Low-frequency oscillations in the cerebellar cortex of the tottering mouse." Journal of neurophysiology **101**(1): 234-45.

Chen, H. and D. C. Chan (2009). "Mitochondrial dynamics–fusion, fission, movement, and mitophagy–in neurodegenerative diseases." Human Molecular Genetics **18**(2): R169-R176.

Chen, X., T.-S. Tang, et al. (2008). "Deranged Calcium Signaling and Neurodegeneration in Spinocerebellar Ataxia Type 3." J. Neurosci. **28**(48): 12713-12724.

Chinen, Y., T. Taki, et al. (2007). "Identification of the novel AML1 fusion partner gene, LAF4, a fusion partner of MLL, in childhood T-cell acute lymphoblastic leukemia

with t(2;21)(q11;q22) by bubble PCR method for cDNA." Oncogene **27**(15): 2249-2256.
Choi, J., M. C. Sullards, et al. (2006). "Oxidative Damage of DJ-1 Is Linked to Sporadic Parkinson and Alzheimer Diseases." J. Biol. Chem. **281**(16): 10816-24.
Choi, W.-S., D.-S. Eom, et al. (2004). "Phosphorylation of p38 MAPK Induced by Oxidative Stress Is Linked to Activation of Both Caspase-8- and -9-mediated Apoptotic Pathways in Dopaminergic Neurons." Journal of Biological Chemistry **279**(19): 20451-20460.
Chu, Q., R. Moreland, et al. (2008). "Systemic Insulin-like Growth Factor-1 Reverses Hypoalgesia and Improves Mobility in a Mouse Model of Diabetic Peripheral Neuropathy." Mol Ther **16**(8): 1400-1408.
Cooper, J. M. and A. H. V. Schapira (2003). "Friedreich's Ataxia: Disease mechanisms, antioxidant and Coenzyme Q_10 therapy." BioFactors **18**(1): 163-171.
Cooper, J. M. and A. H. V. Schapira (2007). "Friedreich's ataxia: Coenzyme Q10 and vitamin E therapy." Mitochondrion **7**(Supplement 1): S127-S135.
Cossée, M., M. Schmitt, et al. (1997). "Evolution of the Friedreichâ€™s ataxia trinucleotide repeat expansion: Founder effect andâ€‰premutations." Proceedings of the National Academy of Sciences of the United States of America **94**(14): 7452-7457.
Cotman, C. (2005). "The Role of Neurotrophins in Brain Aging: A Perspective in Honor of Regino Perez-Polo." Neurochemical Research **30**(6): 877-881.
Courchesne, E., J. Piven, et al. (1999). "An MRI study of autism: The cerebellum revisited." Neurology **52**(5): 1106-.
Croci, L., V. Barili, et al. "Local insulin-like growth factor I expression is essential for Purkinje neuron survival at birth." Cell Death Differ.
Cummings, C. J., Y. Sun, et al. (2001). "Over-expression of inducible HSP70 chaperone suppresses neuropathology and improves motor function in SCA1 mice." Human Molecular Genetics **10**(14): 1511-1518.
Dauer, W. and S. Przedborski (2003). "Parkinson's disease: mechanisms and models." Neuron **39**(6): 889-909.
Dawson, T. M., H. S. Ko, et al. (2010). "Genetic animal models of Parkinson's disease." Neuron **66**(5): 646-61.
De Vos, K. J., A. J. Grierson, et al. (2008). "Role of Axonal Transport in Neurodegenerative Diseases." Annual Review of Neuroscience **31**(1): 151-173.
Delatycki, M. B., R. Williamson, et al. (2000). "Friedreich ataxia: an overview." Journal of Medical Genetics **37**(1): 1-8.
Denny, P., R. Bate, et al. (2001). "What use is the human genome for understanding the mouse?" Genome Biol. **2**(11).
Devi, L., B. M. Prabhu, et al. (2006). "Accumulation of Amyloid Precursor Protein in the Mitochondrial Import Channels of Human Alzheimer's Disease Brain Is Associated with Mitochondrial Dysfunction." J. Neurosci. **26**(35): 9057-9068.
DiMartino, J. F., P. M. Ayton, et al. (2002). "The AF10 leucine zipper is required for leukemic transformation of myeloid progenitors by MLL-AF10." Blood **99**(10): 3780-3785.
Distelmaier, F., W. J. H. Koopman, et al. (2009). "Mitochondrial complex I deficiency: from organelle dysfunction to clinical disease." Brain **132**(4): 833-842.
Dodge, J. C., A. M. Haidet, et al. (2008). "Delivery of AAV-IGF-1 to the CNS Extends Survival in ALS Mice Through Modification of Aberrant Glial Cell Activity." Molecular Therapy **16**(6): 056-1064.
Dodson, M. W. and M. Guo (2007). "Pink1, Parkin, DJ-1 and mitochondrial dysfunction in Parkinson's disease." Current Opinion in Neurobiology **17**(3): 331-337.
Dressler, D. and R. Benecke (2005). "Diagnosis and management of acute movement disorders." J. Neurol. **11**: 1299-306.
Du, W., J. F. Bautista, et al. "Calcium-sensitive potassium channelopathy in human epilepsy and paroxysmal movement disorder." Nature Genetics **37**(7): 733-738.

Dudek, H., S. R. Datta, et al. (1997). "Regulation of Neuronal Survival by the Serine-Threonine Protein Kinase Akt." Science **275**(5300): 661-665.

Durand, M., A. Kolpak, et al. (2007). "The OXR domain defines a conserved family of eukaryotic oxidation resistance proteins." BMC Cell Biology **8**(1): 13.

Ebadi, M., S. K. Sharma, et al. (2004). "Coenzyme Q10 inhibits mitochondrial complex-1 down-regulation and nuclear factor-kappa B activation." Journal of Cellular and Molecular Medicine **8**(2): 213-222.

Ebert, A. D., A. J. Beres, et al. (2008). "Human neural progenitor cells over-expressing IGF-1 protect dopamine neurons and restore function in a rat model of Parkinson's disease." Experimental Neurology **209**(1): 213-223.

Ebong, S., A. B. Chepelinsky, et al. (2004). "Characterization of the roles of STAT1 and STAT3 signal transduction pathways in mammalian lens development." Molecular Vision: 122-31.

El Ghouzzi, V., Z. Csaba, et al. (2007). "Apoptosis-Inducing Factor Deficiency Induces Early Mitochondrial Degeneration in Brain Followed by Progressive Multifocal Neuropathology." Journal of Neuropathology & Experimental Neurology **66**(9): 838-847 10.1097/NEN.0b013e318148b822.

Elliott, N. A. and M. R. Volkert (2004). "Stress induction and mitochondrial localization of OXR1 proteins in yeast and humans." Molec Cell Biol **24**: 3180 - 3187.

Elmore, S. (2007). "Apoptosis: A Review of Programmed Cell Death." Toxicol Pathol. **35**(4): 495-516.

Embiruçu, E. K., M. L. Martyn, et al. (2009). "Autosomal recessive ataxias: 20 types, and counting." Arquivos de Neuro-Psiquiatria **67**: 1143-1156.

Estable, M. C. M. C., M. H. M. H. Naghavi, et al. (2002). "MCEF, the newest member of the AF4 family of transcription factors involved in leukemia, is a positive transcription elongation factor-b-associated protein." Journal of biomedical science **9**(3): 234-45.

Farah, M. H. (2007). "RNAi Silencing in Mouse Models of Neurodegenerative Diseases." Current Drug Delivery **4**: 161-167.

Fatemi, S. H., T. J. Reutiman, et al. (2008). "The role of cerebellar genes in pathology of autism and schizophrenia." Cerebellum **7**(3): 278-84.

Fernandez-Funez, P., M. L. Nino-Rosales, et al. (2000). "Identification of genes that modify ataxin-1-induced neurodegeneration." Nature **408**(6808): 101-106.

Fernandez-Gonzalez, A., A. R. L. Spada, et al. (2002). "Purkinje cell degeneration (pcd) Phenotypes Caused by Mutations in the Axotomy-Induced Gene, Nna1." Science **295**(5561): 1904-1906.

Fernandez, A. M., E. M. Carro, et al. (2005). "Insulin-like growth factor I treatment for cerebellar ataxia: Addressing a common pathway in the pathological cascade?" Brain Research Reviews **50**(1): 134-141.

Fernandez, A. M., A. G. de la Vega, et al. (1998). "Insulin-like growth factor I restores motor coordination in a rat model of cerebellar ataxia." Proceedings of the National Academy of Sciences of the United States of America **95**(3): 1253-1258.

Ferraiuolo, L., P. R. Heath, et al. (2007). "Microarray Analysis of the Cellular Pathways Involved in the Adaptation to and Progression of Motor Neuron Injury in the SOD1 G93A Mouse Model of Familial ALS." J. Neurosci. **27**(34): 9201-9219.

Ferrante, K. L., J. Shefner, et al. (2005). "Tolerance of high-dose (3,000 mg/day) coenzyme Q10 in ALS." Neurology **65**(11): 1834-1836.

Filla, A., G. De Michele, et al. (2000). "Accuracy of clinical diagnostic criteria for Friedreich's ataxia." Movement Disorders **15**(6): 1255-1258.

Finder, V. H. and R. Glockshuber (2007). "Amyloid-β Aggregation." Neurodegener Dis **4**: 13-27.

Finkel, T. and N. J. Holbrook (2000). "Oxidants, oxidative stress and the biology of ageing." Nature **408**(6809): 239 - 247.

Fischer, H., X. U. Zhang, et al. (2001). "C7, a novel nucleolar protein, is the mouse homologue of the Drosophila late puff product L82 and an isoform of human OXR1." Biochem Biophys Res Commun **281**(3): 795 - 803.
Fischer, L. R. and J. D. Glass (2007). "Axonal Degeneration in Motor Neuron Disease." Neurodegenerative Diseases **4**(6): 431-442.
Fletcher, C. F., M. C. Lutz, et al. (1996). "Absence Epilepsy in Tottering Mutant Mice Is Associated with Calcium Channel Defects " Cell **87**(4): 607-617.
Ford, G. D., B. D. Ford, et al. (2008). "Analysis of transcriptional profiles and functional clustering of global cerebellar gene expression in PCD3J mice." Biochemical and Biophysical Research Communications **377**(2): 556-561.
Forman, M. S., V. M. Lee, et al. (2005). "Nosology of Parkinsons Disease: Looking for the Way Out of a Quackmire." Neuron **47**(4): 479-482.
Franco, R. (2009). "G-protein-coupled receptor heteromers or how neurons can display differently flavoured patterns in response to the same neurotransmitter." British Journal of Pharmacology **158**(1): 23-31.
Frank-Cannon, T., L. Alto, et al. (2009). "Does neuroinflammation fan the flame in neurodegenerative diseases?" Molecular Neurodegeneration **4**(1): 47.
Frank, S. (2006). "Dysregulation of mitochondrial fusion and fission: an emerging concept in neurodegeneration." Acta Neuropathologica **111**(2): 93-100.
Frydman, J. (2001). "Folding of newly translated proteins in vivo: the role of molecular chaperones." Annual Review of Biochemistry **70**(1): 603-647.
Fujigasaki, H., J.-J. Martin, et al. (2001). "CAG repeat expansion in the TATA box-binding protein gene causes autosomal dominant cerebellar ataxia." Brain **124**(10): 1939-1947.
Fukudome, Y., T. Tabata, et al. (2003). "Insulin-like growth factor-I as a promoting factor for cerebellar Purkinje cell development." European Journal of Neuroscience **17**(10): 2006-2016.
Gakh, O., S. Park, et al. (2006). "Mitochondrial iron detoxification is a primary function of frataxin that limits oxidative damage and preserves cell longevity." Human Molecular Genetics **15**(3): 467-479.
Galimberti, D., C. Fenoglio, et al. (2008). "Inflammation in Neurodegenerative Disorders: Friend or Foe?" Current Aging Science **1**: 30-41.
Gao, J.-P., S. Sun, et al. (2008). "Triptolide protects against 1-methyl-4-phenyl pyridinium-induced dopaminergic neurotoxicity in rats: Implication for immunosuppressive therapy in Parkinson's disease." Neuroscience Bulletin **24**(3): 133-142.
Gatchel, J. R., K. Watase, et al. (2008). "The insulin-like growth factor pathway is altered in spinocerebellar ataxia type 1 and type 7." Proceedings of the National Academy of Sciences **105**(4): 1291-1296.
Gauthier, L. R., B. C. Charrin, et al. (2004). "Huntingtin Controls Neurotrophic Support and Survival of Neurons by Enhancing BDNF Vesicular Transport along Microtubules." Cell **118**: 127-138.
Gecz, J. J. (2000). "The FMR2 gene, FRAXE and non-specific X-linked mental retardation: clinical and molecular aspects." Annals of human genetics **64**(Pt 2): 95-106.
Geschwind, D. H. (1999). "Focusing Attention on Cognitive Impairment in Spinocerebellar Ataxia." Arch Neurol **56**(1): 20-22.
Ghosh, S. and M. B. Feany (2004). "Comparison of pathways controlling toxicity in the eye and brain in Drosophila models of human neurodegenerative diseases." Human Molecular Genetics **13**(18): 2011-2018.
Gilad, S., L. Chessa, et al. (1998). "Genotype-phenotype relationships in ataxia-telangiectasia and variants." Am. J. Hum. Genet. **62**(3): 551-561.
Gilman, S., G. K. Wenning, et al. (2008). "Second consensus statement on the diagnosis of multiple system atrophy." Neurology **71**(9): 670-676.
Golstein, P. and G. Kroemer (2007). "Cell death by necrosis: towards a molecular definition." Trends in Biochemical Sciences **32**(1): 37-43.

Gonzales-Alegre, P. (2007). "Therapeutic RNA interference for neurodegenerative diseases: From promise to progress." Pharmacology & Therapeutics **114**: 34-55.

González-Cabo, P., C. Espinós, et al. (2009). Friedreich Ataxia: An Update on Animal Models, Frataxin Function and Therapies. Inherited Neuromuscular Diseases, Springer Netherlands. **652:** 247-261.

Gonzalez-Polo, R.-A., P. Boya, et al. (2005). "The apoptosis/autophagy paradox: autophagic vacuolization before apoptotic death." J Cell Sci **118**(14): 3091-3102.

Gorman, A. M. (2008). "Neuronal cell death in neurodegenerative diseases: recurring themes around protein handling." Journal of Cellular and Molecular Medicine **12**(6a): 2263-2280.

Gouw, L. G., C. D. Kaplan, et al. (1995). "Retinal degeneration characterizes a spinocerebellar ataxia mapping to chromosome 3p." Nat Genet **10**(1): 89-93.

Graybiel, A. M., K. Ohta, et al. (1990). "Patterns of cell and fiber vulnerability in the mesostriatal system of the mutant mouse weaver. I. Gradients and compartments." J. Neurosci. **10**(3): 720-733.

Gu, Y. and D. L. Nelson (2003). "FMR2 function: insight from a mouse knockout model." Cytogenetic and Genome Research **100**(1-4).

Guipponi, M., Q. X. Li, et al. (2010). "SAGE analysis of genes differentially expressed in presymptomatic TgSOD1G93A transgenic mice identified cellular processes involved in early stage of ALS pathology." J Mol Neurosci. **41**(1): 172-82.

Gundlfinger, A., Kapfhammer, J. P. et al. (2003). "Different regulation of Purkinje cell dendritic development in cerebellar slice cultures by protein kinase Calpha and -beta" Journal of Neurobiology **57**(1): 95-109.

Gurney, M. E., H. Pu, et al. (1994). "Motor neuron degeneration in mice that express a human Cu,Zn superoxide dismutase mutation." Science **264**(5166): 1772-1775.

Guy, J., B. Hendrich, et al. (2001). "A mouse Mecp2-null mutation causes neurological symptoms that mimic Rett syndrome." Nature **27**: 322-326.

Hafezparast, M., A. Ahmad-Annuar, et al. (2002). "Mouse models for neurological disease." Lancet Neurol. **1**(4): 215-24.

Halliwell, B. (1992). "Reactive Oxygen Species and the Central Nervous System." Journal of Neurochemistry **59**(5): 1609-1623.

Halliwell, B. (1999). "Antioxidant defence mechanisms: from the beginning to the end (of the beginning)." Free Radic. Res. **31**(4): 261-272.

Halliwell, B. (2006). "Oxidative stress and neurodegeneration: where are we now?" Journal of Neurochemistry **97**(6): 1634-1658.

Halliwell, B. and J. M. C. Cutteridge (1985). "Oxygen radicals and the nervous system." Trends in Neurosciences **8**(1): 22-26.

Hamamichi, S., R. N. Rivas, et al. (2008). "Hypothesis-based RNAi screening identifies neuroprotective genes in a Parkinson's disease model." Proceedings of the National Academy of Sciences **105**(2): 728-733.

Hamre, K., R. Tharp, et al. (1999). "Differential strain susceptibility following 1-methyl-4-phenyl-1,2,3,6-tetrahydropyridine (MPTP) administration acts in an autosomal dominant fashion: quantitative analysis in seven strains of Mus musculus." Brain Research **828**(1-2): 91-103.

Hao, L.-Y., B. I. Giasson, et al. (2009). "DJ-1 is critical for mitochondrial function and rescues PINK1 loss of function." Proceedings of the National Academy of Sciences **107**(21): 9747-9752.

Haring, M. M., S. S. Offermann, et al. (2007). "Chromatin immunoprecipitation: optimization, quantitative analysis and data normalization." Plant methods **3**: 11.

Harper, A. "Mouse models of neurological disorders--A comparison of heritable and acquired traits." Biochimica et Biophysica Acta (BBA) - Molecular Basis of Disease **1802**(10): 785-795.

Harris, A., J. I. Morgan, et al. (2000). "Regenerating Motor Neurons Express Nna1, a Novel ATP/GTP-Binding Protein Related to Zinc Carboxypeptidases." Molecular and Cellular Neuroscience **16**(5): 578-596.

Hart, P. E., R. Lodi, et al. (2005). "Antioxidant Treatment of Patients With Friedreich Ataxia: Four-Year Follow-up." Arch Neurol **62**(4): 621-626.

Hathorn, T., A. Snyder-Keller, et al. (2010). "Nicotinamide improves motor deficits and upregulates PGC-1[alpha] and BDNF gene expression in a mouse model of Huntington's disease." Neurobiology of Disease **In Press, Corrected Proof**.

Hayes, S. A. and F. J. Dice (1996). "Roles of Molecular Chaperones in Protein Degradation." The Journal of Cell Biology **132**(3): 255-258.

Heckroth, J. A. and L. C. Abbott (1994). "Purkinje cell loss from alternating sagittal zones in the cerebellum of leaner mutant mice." Brain Research **658**(1-2): 93-104.

Heintz, N. and H. Y. Zoghbi (2000). "Insights from Mouse Models into the Molecular Basis of Neurodegeneration." Annual Review of Physiology **62**(1): 779-802.

Heller, A. H., M. A. Dichter, et al. (1983). "Anticonvulsant Sensitivity of Absence Seizures in the Tottering Mutant Mouse." Epilepsia **24**(1): 25-34.

Herrup, K. and S. L. Wilczynski (1982). "Cerebellar cell degeneration in the leaner mutant mouse." Neuroscience **7**(9): 2185-96.

Hess, E. J. and M. C. Wilson (1991). "Tottering and leaner mutations perturb transient developmental expression of tyrosine hydroxylase in embryologically distinct Purkinje cells." Neuron **6**(1): 123-32.

Hillman, M. M. A. and J. J. Gecz (2001). "Fragile XE-associated familial mental retardation protein 2 (FMR2) acts as a potent transcription activator." Journal of human genetics **46**(5): 251-9.

Hirsch, E. C. (2003). "Animal models of Parkinson's disease in rodents induced by toxins: an overview." J. Neural. Transm. **65**: 89-100.

Hirsch, E. C. and S. Hunot (2009). "Neuroinflammation in Parkinson's disease: a target for neuroprotection?" The Lancet Neurology **8**(4): 382-397.

Hiwatari, M., T. Taki, et al. "Fusion of an AF4-related gene, LAF4, to MLL in childhood acute lymphoblastic leukemia with t(2;11)(q11;q23)." Oncogene **22**(18): 2851-2855.

Huen, N., S. Wong, et al. (2007). "Transcriptional malfunctioning of heat shock protein gene expression in spinocerebellar ataxias." The Cerebellum **6**(2): 111-117.

Hunot, S. and E. C. Hirsch (2003). "Neuroinflammatory processes in Parkinson's disease." Annals of Neurology **53**(S3): S49-S60.

Hyman, B. T., G. W. Van Hoesen, et al. (1984). "Alzheimer's disease: cell-specific pathology isolates the hippocampal formation." Science **225**(4667): 1168-1170.

Ichibangase, T., H. Saimaru, et al. (2008). "Proteomics of Caenorhabditis elegans over-expressing human α-synuclein analyzed by fluorogenic derivatization–liquid chromatography/tandem mass spectrometry: identification of actin and several ribosomal proteins as negative markers at early Parkinson's disease stages." Biomedical Chromatography **22**(3): 232-234.

Ilieva, E. V., V. r. Ayala, et al. (2007). "Oxidative and endoplasmic reticulum stress interplay in sporadic amyotrophic lateral sclerosis." Brain **130**(12): 3111-3123.

Imbrici, P., S. L. Jaffe, et al. (2004). "Dysfunction of the brain calcium channel CaV2.1 in absence epilepsy and episodic ataxia." Brain **127**(12): 2682-2692.

Inouye, M. and U. Murakami (1980). "Temporal and spatial patterns of Purkinje cell formation in the mouse cerebellum." The Journal of Comparative Neurology **194**(3): 499-503.

Irrcher, I., H. Aleyasin, et al. (2010). "Loss of the Parkinson's disease-linked gene DJ-1 perturbs mitochondrial dynamics." Human Molecular Genetics **19**(19): 3734-3746.

Isaacs, A. M., K. E. Davies, et al. (2000). "Identification of two new Pmp22 mouse mutants using large-scale mutagenesis and a novel rapid mapping strategy." Human Molecular Genetics **9**(12): 1865-1871.

Isaacs, A. M., P. L. Oliver, et al. (2003). "A Mutation in Af4 Is Predicted to Cause Cerebellar Ataxia and Cataracts in the Robotic Mouse." J. Neurosci. **23**(5): 1631-1637.

Isnard, P., N. Core, et al. (2000). "Altered lymphoid development in mice deficient for the mAF4 proto-oncogene." Blood **96**(2): 705-710.
Ito, M. (1998). "The Cerebellum: From Structure to Control." Trends in Cognitive Sciences **2**(9): 371.
Itoh, K., N. Wakabayashi, et al. (1999). "Keap1 represses nuclear activation of antioxidant responsive elements by Nrf2 through binding to the amino-terminal Neh2 domain." Genes & Development **13**(1): 76-86.
Jacquemont, S., R. J. Hagerman, et al. (2007). "Fragile-X syndrome and fragile X-associated tremor/ataxia syndrome: two faces of FMR1." The Lancet Neurology **6**(1): 45-55.
Jacquemont, S., A. Orrico, et al. (2005). "Spastic paraparesis, cerebellar ataxia, and intention tremor: a severe variant of FXTAS?" Journal of Medical Genetics **42**(2): e14-e14.
Jaramillo-Gutierrez, G., A. Molina-Cruz, et al. (2010). "The <italic>Anopheles gambiae</italic> Oxidation Resistance 1 (OXR1) Gene Regulates Expression of Enzymes That Detoxify Reactive Oxygen Species." PLoS ONE **5**(6): e11168.
Jellinger, K. A. (2010). "Basic mechanisms of neurodegeneration: a critical update." J. Cell. Mol. Med. **14**(3): 457-487.
Jen, J. C., T. D. Graves, et al. (2007). "Primary episodic ataxias: diagnosis, pathogenesis and treatment." Brain **130**(10): 2484-2493.
Jen, J. C., Q. Yue, et al. (1998). "Spinocerebellar ataxia type 6 with positional vertigo and acetazolamide responsive episodic ataxia." Journal of Neurology, Neurosurgery & Psychiatry **65**(4): 565-568.
Jendrach, M., S. Gispert, et al. (2009). "The mitochondrial kinase PINK1, stress response and Parkinson's disease." J Bioenerg Biomembr **41**: 481-486.
Johnson, G. L. and R. Lapadat (2002). "Mitogen-Activated Protein Kinase Pathways Mediated by ERK, JNK, and p38 Protein Kinases." Science **298**(5600): 1911-1912.
Jouvenceau, A., L. H. Eunson, et al. (2001). "Human epilepsy associated with dysfunction of the brain P/Q-type calcium channel." The Lancet **358**(9284): 801-807.
Junn, E., W. H. Jang, et al. (2009). "Mitochondrial localization of DJ-1 leads to enhanced neuroprotection." Journal of Neuroscience Research **87**(1): 123-129.
Kalla, R., S. Glasauer, et al. (2007). "4-Aminopyridine restores vertical and horizontal neural integrator function in downbeat nystagmus." Brain **130**(9): 2441-2451.
Kandel, E., J. Schwartz, et al. (2000). Principles of Neural Science, McGraw Hill Companies Inc.
Kazemi-Esfarjani, K. and S. Benzer (2002). "Suppression of polyglutamine toxicity by a Drosophila homolog of myeloid leukemia factor." Hum. Mol. Genet. **11**(21): 2657-2672.
Khatib, Z., A. Levi, et al. (2004). "Acute lymphocytic leukemia in a child with Beckwith-Wiedemann syndrome." J Pediatr Hematol Oncol: 45-7.
Kim, R. H., M. Peters, et al. (2005). "DJ-1, a novel regulator of the tumor suppressor PTEN." Cell **7**(3): 263-273.
Kim, R. H., P. D. Smith, et al. (2005). "Hypersensitivity of DJ-1-deficient mice to 1-methyl-4-phenyl-1,2,3,6-tetrahydropyrindine (MPTP) and oxidative stress." Proceedings of the National Academy of Sciences of the United States of America **102**(14): 5215-5220.
Kitada, T., A. Pisani, et al. (2007). "Impaired dopamine release and synaptic plasticity in the striatum of PINK1-deficient mice." Proceedings of the National Academy of Sciences **104**(27): 11441-11446.
Klein, J. A., C. M. Longo-Guess, et al. (2002). "The harlequin mouse mutation downregulates apoptosis-inducing factor." Nature **419**(6905): 367-374.
Kofuji, P., M. Hofer, et al. (1996). "Functional Analysis of the weaver Mutant GIRK2
K1 Channel and Rescue of weaver Granule Cells." Neuron **16**: 941-952.
Kokjohn, T. A. and A. Roher (2009). "Amyloid precursor protein transgenic mouse models and Alzheimer's disease: Understanding the paradigms, limitations, and

contributions." Alzheimer's & dementia : the journal of the Alzheimer's Association **5**(4): 340-347.

Kokoszka, J. E., P. Coskun, et al. (2001). "Increased mitochondrial oxidative stress in the Sod2 (+/âˆ') mouse results in the age-related decline of mitochondrial function culminating in increased apoptosis." Proceedings of the National Academy of Sciences of the United States of America **98**(5): 2278-2283.

Kraemer, B., G. D. Schellenberg*, et al. (2007). Using Caenorhabditis elegans Models of Neurodegenerative Disease to Identify Neuroprotective Strategies. International Review of Neurobiology, Academic Press. **Volume 77:** 219-246.

Kroemer, G., B. Dallaporta, et al. (1998). "The mitochondrial death/life regulator in apoptosis and necrosis." Annual Review of Physiology **60**(1): 619-642.

Krumewski, T. F., P. E. Neumann, et al. (1989). "Insertional mutation in a transgenic mouse allelic with Purkinje cell degeneration." Proc Natl Acad Sci U S A **86**(10): 3709-3712.

Kubo, E., D. P. Singh, et al. (2005). "Gene expression profiling of diabetic and galactosaemic cataractous rat lens by microarray analysis." Diabetologia **48**: 790-798.

Kulik, G., A. Klippel, et al. (1997). "Antiapoptotic signalling by the insulin-like growth factor I receptor, phosphatidylinositol 3-kinase, and Akt." Mol. Cell. Biol. **17**(3): 1595-1606.

Kwiatkowski, T. J., H. T. Orr, et al. (1993). "The gene for autosomal dominant spinocerebellar ataxia (SCA1) maps centromeric to D6S89 and shows no recombination, in nine large kindreds, with a dinucleotide repeat at the AM10 locus." Am J Hum Genet **53**(4): 391-400.

Landreth, K. S., R. Narayanan, et al. (1992). "Insulin-like growth factor-I regulates pro-B cell differentiation." Blood **80**(5): 1207-1212.

Lawlor, M. A. and D. R. Alessi (2001). "PKB/Akt: a key mediator of cell proliferation, survival and insulin responses?" J Cell Sci **114**(16): 2903-2910.

Lee, H. C. and Y. H. Wei (2005). "Mitochondrial biogenesis and mitochondrial DNA maintenance of mammalian cells under oxidative stress." The International Journal of Biochemistry & Cell Biology **37**: 822-834.

Lee, W. H., S. Javedan, et al. (1992). "Coordinate Expression of Insulin-like Growth Factor System Components by Neurons and Neuroglia during Retinal and Cerebellar Development" Journal of Neuroscience **12**(12): 4737-4744.

Lev, N., D. Ickowicz, et al. (2009). "DJ-1 Changes in G93A-SOD1 Transgenic Mice: Implications for Oxidative Stress in ALS." Journal of Molecular Neuroscience **38**(2): 94-102.

Leys, D., H. Petit, et al. (1989). "Refsum's disease revealed by cardiac disorders." Lancet **1**(8638): 621.

Li, J., X. Gu, et al. (2010). "Nna1 Mediates Purkinje Cell Dendritic Development via Lysyl Oxidase Propeptide and NF-κB Signaling." Neuron **68**(1): 45-60.

Li, J., D. Johnson, et al. (2005). "Stabilization of Nrf2 by tBHQ Confers Protection against Oxidative Stress-Induced Cell Death in Human Neural Stem Cells." Toxicological Sciences **83**(2): 313-328.

Lin, M. T. and M. F. Beal (2006). "Mitochondrial dysfunction and oxidative stress in neurodegenerative diseases." Nature **443**(7113): 787-795.

Liss, B., A. Neu, et al. (1999). "The weaver Mouse gain-of-function Phenotype of Dopaminergic Midbrain Neurons Is Determined by Coactivation of wvGirk2 and K-ATP Channels." J. Neurosci. **19**(20): 8839-8848.

Liu, J.-P. A.-B., Julie AU - Perkins, Archlbald S. AU - Robertson, Elizabeth J. AU - Efstratiadis, Argiris (1993). "Mice carrying null mutations of the genes encoding insulin-like growth factor I (Igf-1) and type 1 IGF receptor (Igf1r)." Cell **75**(1): 59-72.

Lu, T., Y. Pan, et al. (2004). "Gene regulation and DNA damage in the ageing human brain." Nature **429**(6994): 883-891.

Luengo-Fernandez, R., J. Leal, et al. (2010). Dementia 2010 - The prevalence, economic cost and research funding of dementia
compared with other major diseases H. E. R. Centre, University of Oxford for the Alzheimer's Research Trust.

Ma, C. and L. M. Staudt (1996). "LAF-4 encodes a lymphoid nuclear protein with transactivation potential that is homologous to AF-4, the gene fused to MLL in t(4;11) leukemias." Blood **87**(2): 734-745.

Mancuso, M., D. Orsucci, et al. (2010). "Current and emerging treatment options in the management of Friedreich ataxia." Neuropsychiatric Disease and Treatment **6**: 491-499.

Mancuso, M., D. Orsucci, et al. (2008). "Mitochondria, Mitochondrial DNA and Alzheimers Disease. What Comes First?" Current Alzheimer Research **5**: 457-468.

Manto, M. (2008). "The Cerebellum, Cerebellar Disorders, and Cerebellar Research—Two Centuries of Discoveries." The Cerebellum **7**(4): 505-516.

Manto, M. and D. Marmolino (2009). "Cerebellar Disorders—At the Crossroad of Molecular Pathways and Diagnosis." The Cerebellum **8**(4): 417-422.

Manto, M. and M. Pandolfo (2001). The Cerebellum and Its Disorders. New York, Cambridge University Press.

Marmolino, D. and F. Acqaviva (2009). "Friedreich's Ataxia: from the (GAA)n repeat mediated silencing to new promising molecules for therapy." Cerebellum **8**(3): 245-59.

Marmolino, D. and M. Manto (2009). "Past, Present and Future Therapeutics for Cerebellar Ataxias." Current Neuropharmacology **8**: 41-61.

Marti, J., M. C. Santa-Cruz, et al. (2009). "GIRK2 and neuronal pattern of generation and settling in homozygous weaver mice." Journal of Receptor, Ligand, and Channel Research **2**: 29-44.

Martin, J., L. Krols, et al. (1994). "On an autosomal dominant form of retinal-cerebellar degeneration: an autopsy study of five patients in one family." Acta Neuropathologica **88**(4): 277-286.

Martindale, J. and N. J. Holbrook (2002). "Cellular Response to Oxidative Stress: Signaling for Suicide and Survival." Journal of Cellular Physiology **192**: 1-15.

Massaad, C. A., T. M. Washington, et al. (2009). "Overexpression of SOD-2 reduces hippocampal superoxide and prevents memory deficits in a mouse model of Alzheimer's disease." Proc Natl Acad Sci U S A **106**(32): 13576-81.

McAllister, A. K. and J. Van de Water (2009). "Breaking Boundaries in Neural-Immune Interactions." Cell **64**(1): 9-12.

McBride, J. L., S. Ramaswamy, et al. (2006). "Viral delivery of glial cell line-derived neurotrophic factor improves behavior and protects striatal neurons in a mouse model of Huntington's disease." Proc Natl Acad Sci U S A **103**(24): 9345-9350.

McMahon, M., K. Itoh, et al. (2001). "The Cap 'n' Collar Basic Leucine Zipper Transcription Factor Nrf2 (NF-E2 p45-related Factor 2) Controls Both Constitutive and Inducible Expression of Intestinal Detoxification and Glutathione Biosynthetic Enzymes." Cancer Research **61**(8): 3299-3307.

Mendez, I., R. Sanchez-Pernaute, et al. (2005). "Cell type analysis of functional fetal dopamine cell suspension transplants in the striatum and substantia nigra of patients with Parkinson's disease." Brain **128**(7): 1498-1510.

Miki, T., T. A. Zwingman, et al. (2008). "Two novel alleles of tottering with distinct Ca(v)2.1 calcium channel neuropathologies." Neuroscience **155**(1): 31-44.

Mollet, J., I. Giurgea, et al. (2007). "Prenyldiphosphate synthase, subunit 1 (PDSS1) and OH-benzoate polyprenyltransferase (COQ2) mutations in ubiquinone deficiency and oxidative phosphorylation disorders." The Journal of Clinical Investigation **117**(3): 765-772.

Moloney, A., D. B. Sattelle, et al. (2010). "Alzheimer's disease: insights from Drosophila melanogaster models." Trends in Biochemical Sciences **35**(4): 228-235.

Monkul, E. S., J. P. Hatch, et al. (2008). "MRI study of the cerebellum in young bipolar patients." Progress in Neuro-Psychopharmacology and Biological Psychiatry **32**(3): 613-619.

Monroe, S. C., S. Y. Jo, et al. (2010). "MLL-AF9 and MLL-ENL alter the dynamic association of transcriptional regulators with genes critical for leukemia." Experimental Hematology **In Press, Accepted Manuscript**.

Montero, R., M. Pineda, et al. (2007). "Clinical, biochemical and molecular aspects of cerebellar ataxia and Coenzyme Q10 deficiency." Cerebellum **6**(2): 118-22.

Moore, D. J., A. B. West, et al. (2005). "Molecular Pathophysiology of Parkinson's Disease." Annu. Rev. Neurosci. **28**: 57-87.

Morfini, G. A., M. Burns, et al. (2009). "Axonal Transport Defects in Neurodegenerative Diseases." The Journal of Neuroscience **29**(41): 12776-12786.

Morley, J. F., H. R. Brignull, et al. (2002). "The threshold for polyglutamine-expansion protein aggregation and cellular toxicity is dynamic and influenced by aging in Caenorhabditiselegans." Proceedings of the National Academy of Sciences of the United States of America **99**(16): 10417-10422.

Morley, J. F. and R. I. Morimoto (2004). "Regulation of Longevity in Caenorhabditis elegans by Heat Shock Factor and Molecular Chaperones." Mol. Biol. Cell **15**(2): 657-664.

Mullen, R. J., E. M. Eicher, et al. (1976). "Purkinje cell degeneration, a new neurological mutation in the mouse." Proc Natl Acad Sci U S A **73**(1): 208-212.

Myers, M. G., T. C. Grammer, et al. (1994). "Insulin receptor substrate-1 mediates phosphatidylinositol 3'-kinase and p70S6k signaling during insulin, insulin-like growth factor-1, and interleukin-4 stimulation." Journal of Biological Chemistry **269**(46): 28783-28789.

Nahm, S.-S., T. C. Frank, et al. (2003). "Insulin-like growth factor-I improves cerebellar dysfunction but does not prevent cerebellar neurodegeneration in the calcium channel mutant mouse, leaner." Neurobiology of Disease **14**(2): 157-165.

Navarro, B., M. E. Kennedy, et al. (1996). "Nonselective and Gbeta gamma -Insensitive weaver K+ Channels." Science **272**(5270): 1950-1953.

Nguyen, T., H. C. Huang, et al. (2000). "Transcriptional Regulation of the Antioxidant Response Element: activation by Nrf2 and repression by MafK " Journal of Biological Chemistry **275**(20): 15466-15473.

Nguyen, T., P. Nioi, et al. (2009). "The Nrf2-Antioxidant Response Element Signaling Pathway and Its Activation by Oxidative Stress." Journal of Biological Chemistry **284**(20): 13291-13295.

Nguyen, T., P. J. Sherratt, et al. (2003). "Increased Protein Stability as a Mechanism That Enhances Nrf2-mediated Transcriptional Activation of the Antioxidant Response Element: degradation of Nrf2 by the 26S proteasome " Journal of Biological Chemistry **278**(7): 4536-4541.

Ni, Z., B. E. Schwartz, et al. (2004). "Coordination of transcription, RNA processing, and surveillance by P-TEFb kinase on heat shock genes." Mol. Cell. **13**: 55-65.

Niedzielski, M. F. M. F., R. R. Hopewell, et al. (2007). "MCEF is localized to the nucleus by protein sequences encoded within three distinct exons, where it represses HIV-1 Tat-transactivation of LTR-directed transcription." International journal of biological sciences **3**(4): 225-36.

Nilson, I., M. Reichel, et al. (1997). "Exon/intron structure of the human *AF-4* gene, a member of the *AF-4/LAF-4/FMR-2* gene family coding for a nuclear protein with structural alterations in acute leukaemia." British Journal of Haematology **98**(1): 157-169.

Noebels, J. L. and R. L. Sidman (1979). "Inherited epilepsy: spike-wave and focal motor seizures in the mutant mouse tottering." Science **204**(4399): 1334-1336.

Nolan, P. M., J. Peters, et al. (2000). "A systematic, genome-wide, phenotype-driven mutagenesis programme for gene function studies in the mouse." Nat Genet **25**(4): 440-443.

Nose, K. (2000). "Role of reactive oxygen species in the regulation of physiological functions." Biol Pharm Bull. **23**(8): 897-903.
Nusslein-Volhard, C. and E. Wieschaus (1980). "Mutations affecting segment number and polarity in Drosophila." Nature **287**(5785): 795-801.
O'Kusky, J. R., P. Ye, et al. (2000). "Insulin-like growth factor-I promotes neurogenesis and synaptogenesis in the hippocampal dentate gyrus during postnatal development." J. Neurosci. **20**: 8435-8442.
Oberdick, J., S. L. Baader, et al. (1998). "From zebra stripes to postal zones: deciphering patterns of gene expression in the cerebellum." Trends in Neurosciences **21**(9): 383-390.
Okada, Y., Q. Feng, et al. (2005). "hDOT1L Links Histone Methylation to Leukemogenesis." Cell **121**: 167-178.
Oldfors, A., P. Sourander, et al. (1990). "Rett syndrome: cerebellar pathology." Pediatr Neurol **6**: 310-314.
Oliver, P. L., E. Bitoun, et al. (2004). "Mediation of Af4 protein function in the cerebellum by Siah proteins." Proceedings of the National Academy of Sciences **101**(41): 14901-14906.
Oliver, P. L. and K. E. Davies (2005). "Analysis of human neurological disorders using mutagenesis in the mouse." Clin. Sci. **108**(5): 385-397.
Oliver, P. L., D. A. Keays, et al. (2007). "Behavioural characterisation of the robotic mouse mutant." Behavioural Brain Research **181**(2): 239-247.
Olzmann, J. A., J. R. Bordelon, et al. (2007). "Selective enrichment of DJ-1 protein in primate striatal neuronal processes: Implications for Parkinson's disease. ." The Journal of Comparative Neurology **500**(3): 585-599.
Ophoff, R. A., G. M. Terwindt, et al. (1996). "Familial hemiplegic migraine and episodic ataxia type-2 are caused by mutations in the Ca2+ channel gene CACNL1A4." Cell **87**(3): 543-52.
Orr, H. T. (2004). "Neurodegenerative disease: Neuron protection agency." Nature **431**(7010): 747-748.
Orr, H. T., M.-y. Chung, et al. (1993). "Expansion of an unstable trinucleotide CAG repeat in spinocerebellar ataxia type 1." Nat Genet **4**(3): 221-226.
Otis, T. S. and J. C. Jen (2006). "Blessed are the pacemakers." Nat Neurosci **9**(3): 297-298.
Palau, F. and C. Espinós (2006). "Autosomal recessive cerebellar ataxias." Orphanet J Rare Dis **1**(47).
Palazzolo, I., C. Stack, et al. (2009). "Overexpression of IGF-1 in Muscle Attenuates Disease in a Mouse Model of Spinal and Bulbar Muscular Atrophy." Neuron **63**(3): 316-328.
Pandey, N., R. E. Schmidt, et al. (2006). "The alpha-synuclein mutation E46K promotes aggregation in cultured cells." Experimental Neurology **197**(2): 515-520.
Pandolfo, M. (2007). "Drug Insight: antioxidant therapy in inherited ataxias." Nature Clinical Practice **4**(2): 86-96.
Patil, N., D. R. Cox, et al. (1995). "A potassium channel mutation in weaver mice implicates membrane excitability in granule cell differentiation." Nat Genet **11**(2): 126-129.
Paulson, H. L. (2009). "The Spinocerebellar Ataxias." J Neuroophthalmol **29**(3): 227-237.
Peng, J., Z. Wu, et al. (2002). "Inhibition of Caspases Protects Cerebellar Granule Cells of the Weaver Mouse from Apoptosis and Improves Behavioral Phenotype." Journal of Biological Chemistry **277**(46): 44285-44291.
Perrin, F. E., G. Boisset, et al. (2005). "No widespread induction of cell death genes occurs in pure motoneurons in an amyotrophic lateral sclerosis mouse model." Human Molecular Genetics **14**(21): 3309-3320.
Peruzzi, F., M. Prisco, et al. (1999). "Multiple Signaling Pathways of the Insulin-Like Growth Factor 1 Receptor in Protection from Apoptosis." Mol. Cell. Biol. **19**(10): 7203-7215.

Piehl, F. and T. Olsson (2009). "Inflammation and susceptibility to neurodegeneration: The use of unbiased genetics to decipher critical regulatory pathways." Neuroscience **158**(3): 1143-1150.

Powell-Braxton, L., P. Hollingshead, et al. (1993). "IGF-I is required for normal embryonic growth in mice." Genes & Development **7**(12b): 2609-2617.

Pramparo, T., S. Grosso, et al. (2005). "Loss-of-function mutation of the <i>AF9/MLLT3</i> gene in a girl with neuromotor development delay, cerebellar ataxia, and epilepsy." Human Genetics **118**(1): 76-81.

Prasad, R., T. Yano, et al. (1995). "Domains with Transcriptional Regulatory Activity within the ALL1 and AF4 Proteins Involved in Acute Leukemia." Proceedings of the National Academy of Sciences **92**(26): 12160-12164.

Puccio, H., D. Simon, et al. (2001). "Mouse models for Friedreich ataxia exhibit cardiomyopathy, sensory nerve defect and Fe-S enzyme deficiency followed by intramitochondrial iron deposits." Nat Genet **27**(2): 181-186.

Puccio, H. l. n. and M. KÅ“nig (2000). "Recent advances in the molecular pathogenesis of Friedreich ataxia." Human Molecular Genetics **9**(6): 887-892.

Qian, L., P. Flood, et al. "Neuroinflammation is a key player in Parkinson's disease and a prime target for therapy." Journal of Neural Transmission **117**(8): 971-979.

Rakic, P. S., R. L. (1973). "Weaver mutant mouse cerebellum: defective neuronal migration secondary to abnormality of Bergmann glia." Proc Natl Acad Sci U S A **70**(1): 240-4.

Ravina, B. M., S. C. Fagan, et al. (2003). "Neuroprotective agents for clinical trials in Parkinson's disease: A systematic assessment." Neurology **60**(8): 1234-1240.

Reinstein, E. and A. Ciechanover (2006). "Narrative Review: Protein Degradation and Human Diseases: The Ubiquitin Connection." Annals of Internal Medicine **145**(9): 676-684.

Remaclea , J., M. Raesa, et al. (1995). "Low levels of reactive oxygen species as modulators of cell function " Mutation Research/DNAging **316**(3): 103-122.

Rezai, Z. and C. H. Yoon (1972). "Abnormal rate of granule cell migration in the cerebellum of "weaver" mutant mice." Developmental Biology **29**(1): 17-26.

Ribe, E. M., E. Serrano-Saiz, et al. (2008). "Mechanisms of neuronal death in disease: defining the models and the players." Biochem. J. **415**: 165-182.

Ridet, J.-L., J.-C. Bensadoun, et al. (2006). "Lentivirus-mediated expression of glutathione peroxidase: Neuroprotection in murine models of Parkinson's disease." Neurobiology of Disease **21**(1): 29-34.

Riess, O., L. Schöls, et al. (1997). "SCA6 is caused by moderate CAG expansion in the a1A-voltage-dependent calcium channel gene." Hum. Mol. Genet. **6**(8): 1289-1293.

Ritvo, E. R., B. J. Freeman, et al. (1986). "Lower Purkinje cell counts in the cerebella of four autistic subjects: initial findings of the UCLA-NSAC Autopsy Research Report." Am J Psychiatry **143**(7): 862-866.

Rival, T., R. M. Page, et al. (2009). "Fenton chemistry and oxidative stress mediate the toxicity of the β-amyloid peptide in a Drosophila model of Alzheimer's disease." European Journal of Neuroscience **29**(7): 1335-1347.

Robberecht, W., L. Van Den Bosh, et al. (2000). "Amyotrophic lateral sclerosis : pathogenesis." Acta Neurol Belg. **100**: 181-187.

Rogers, D. C., E. M. C. Fisher, et al. (1997). "Behavioral and functional analysis of mouse phenotype: SHIRPA, a proposed protocol for comprehensive phenotype assessment." Mammalian Genome **8**(10): 711-713.

Ross, C. A. and I. Shoulson (2009). "Huntington disease: pathogenesis, biomarkers, and approaches to experimental therapeutics." Parkinsonism & related disorders **15**: S135-S138.

Roth, K. A. and C. D'Sa (2001). "Apoptosis and brain development." Mental Retardation and Developmental Disabilities Research Reviews **7**(4): 261-266.

Rothstein, J. D. (2009). "Current hypotheses for the underlying biology of amyotrophic lateral sclerosis." Annals of Neurology **65**(S1): S3-S9.
Rowland, L. P. and N. A. Shneider (2001). "Amyotrophic Lateral Sclerosis." New England Journal of Medicine **344**(22): 1688-1700.
Roy, S., B. Zhang, et al. (2005). "Axonal transport defects: a common theme in neurodegenerative diseases." Acta Neuropathologica **109**(1): 5-13.
Ruberte, J., E. Ayuso, et al. (2004). "Increased ocular levels of IGF-1 in transgenic mice lead to diabetes-like eye disease." J Clin Invest **113**(8): 1149-1157.
Ruberte, J. s., E. Ayuso, et al. (2004). "Increased ocular levels of IGF-1 in transgenic mice lead to diabetes-like eye disease." The Journal of Clinical Investigation **113**(8): 1149-1157.
Russ, A., G. Stumm, et al. (2002). "Random mutagenesis in the mouse as a tool in drug discovery." Drug Discovery Today **7**: 1175-1183.
Saitoh, M., H. Nishitoh, et al. (1998). "Mammalian thioredoxin is a direct inhibitor of apoptosis signal-regulating kinase (ASK) 1." EMBO J **17**(9): 2596-2606.
Salminen, A., J. Ojala, et al. (2009). "Inflammation in Alzheimer's disease: Amyloid-[beta] oligomers trigger innate immunity defence via pattern recognition receptors." Progress in Neurobiology **87**(3): 181-194.
Sarna, J. R. and R. Hawkes (2003). "Patterned Purkinje cell death in the cerebellum." Progress in Neurobiology **70**(6): 473-507.
Savitt, J. M. D., V. L. and T. M. Dawson (2006). "Diagnosis and treatment of Parkinson disease: molecules to medicine." J. Clin. Invest. **116**(7): 1744-1754.
Sawada, K., A. Kalam Azad, et al. (2009). "Striking pattern of Purkinje cell loss in cerebellum of an ataxic mutant mouse, tottering." Acta Neurol Exp. **69**: 138-145.
Schilling, G., M. L. Coonfield, et al. (2001). "Coenzyme Q10 and remacemide hydrochloride ameliorate motor deficits in a Huntington's disease transgenic mouse model." Neurosci. Lett. **315**(3): 149-53.
Schindowski, K., K. Belarbi, et al. (2008). "Neurotrophic factors in Alzheimer's disease: role of axonal transport." Genes, Brain and Behavior **7**: 43-56.
Schmahmann, J. D. (2004). "Disorders of the Cerebellum: Ataxia, Dysmetria of Thought, and the Cerebellar Cognitive Affective Syndrome." J Neuropsychiatry Clin Neurosci **16**(3): 367-378.
Schmidt, M., M. Goebeler, et al. (2000). "Ras-independent Activation of the Raf/MEK/ERK Pathway upon Calcium-induced Differentiation of Keratinocytes." Journal of Biological Chemistry **275**(52): 41011-41017.
Schmucker, S. and H. Puccio (2010). "Understanding the molecular mechanisms of Friedreich's ataxia to develop therapeutic approaches." Hum. Mol. Genet. **19**(R1): R103-R110.
Schulz, J. B., N. A. Di Prospero, et al. (2009). "Clinical experience with high-dose idebenone in Friedreich ataxia." J. Neurol. **1**: 42-5.
Selimi, F., M. Doughty, et al. (2000). "Target-Related and Intrinsic Neuronal Death in Lurcher Mutant Mice Are Both Mediated by Caspase-3 Activation." J. Neurosci. **20**(3): 992-1000.
Seznec, H., D. Simon, et al. (2004). "Idebenone delays the onset of cardiac functional alteration without correction of Fe-S enzymes deficit in a mouse model for Friedreich ataxia." Human Molecular Genetics **13**(10): 1017-1024.
Shelton, J. G. S., L. S. White, E. R. McCubrey, J. A. (2004). "Synergy between PI3K/Akt and Raf/MEK/ERK Pathways in IGF-1R Mediated Cell Cycle Progression and Prevention of Apoptosis in Hematopoietic Cells." Cell Cycle **3**(3): 372-379.
Shibuya, N., T. Taki, et al. (2001). "t(10;11)-acute leukemias with MLL-AF10 and MLL-ABI1 chimeric transcripts: specific expression patterns of ABI1 gene in leukemia and solid tumor cell lines." Genes Chromosomes Cancer **32**(1): 1-10.
Skovronsky, D. M., V. M. Y. Lee, et al. (2006). "Neurodegenerative diseases: New Concepts of Pathogenesis and Their Therapeutic Implications." Annual Review of Pathology: Mechanisms of Disease **1**(1): 151-170.

Smirnov, D. A. and V. G. Cheung (2008). "ATM Gene Mutations Result in Both Recessive and Dominant Expression Phenotypes of Genes and MicroRNAs." Am J Hum Genet **83**(2): 243-253.

Smith, D. F., L. Whitesell, et al. (1998). "Molecular Chaperones: Biology and Prospects for Pharmacological Intervention." Pharmacological Reviews **50**(4): 493-514.

Sonntag, W. E., C. Lynch, et al. (2000). "The effects of growth hormone and IGF-1 deficiency on cerebrovascular and brain ageing." Journal of Anatomy **197**(4): 575-585.

Soong, B.-w. and H. L. Paulson (2007). "Spinocerebellar ataxias: an update." Current Opinion in Neurology **20**(4): 438-446 10.1097/WCO.0b013e3281fbd3dd.

Spacey, S. D., M. E. Hildebrand, et al. (2004). "Functional implications of a novel EA2 mutation in the P/Q-type calcium channel." Annals of Neurology **56**(2): 213-220.

Stathopulos, P. B., J. A. O. Rumfeldt, et al. (2003). "Cu Zn superoxide dismutase mutants associated with amyotrophic lateral sclerosis show enhanced formation of aggregates in vitro." PNAS **100**(12): 7021–7026.

Steger, D. J., M. I. Lefterova, et al. (2008). "DOT1L/KMT4 Recruitment and H3K79 Methylation Are Ubiquitously Coupled with Gene Transcription in Mammalian Cells." Mol. Cell. Biol. **28**(8): 2825-2839.

Stolp, H. B. and K. M. Dziegielewska (2009). "Review: Role of developmental inflammation and blood–brain barrier dysfunction in neurodevelopmental and neurodegenerative diseases." Neuropathology and Applied Neurobiology **35**(2): 132-146.

Strupp, M., R. Kalla, et al. (2004). "Treatment of episodic ataxia type 2 with the potassium channel blocker 4-aminopyridine." Neurology **62**(9): 1623-1625.

Swerdlow, R. H., J. K. Parks, et al. (1996). "Origin and functional consequences of the complex I defect in Parkinson's disease." Annals of Neurology **40**(4): 663-671.

Taki, T., H. Kano, et al. (1999). "AF5q31, a newly identified AF4-related gene, is fused to MLL in infant acute lymphoblastic leukemia with ins(5;11)(q31;q13q23)." Proceedings of the National Academy of Sciences of the United States of America **96**(25): 14535-14540.

Taki, T., H. Kano, et al. (1999). "AF5q31, a newly identified AF4-related gene, is fused to MLL in infant acute lymphoblastic leukemia with ins(5;11)(q31;q13q23)." Proceedings of the National Academy of Sciences **96**(25): 14535-14540.

Teive, H. I. A. G. (2009). "Spinocerebellar ataxias." Arquivos de Neuro-Psiquiatria **67**: 1133-1142.

Tenreiro, S. and T. F. Outeiro "Simple is good: yeast models of neurodegeneration." FEMS Yeast Research: no-no.

Thompson, L. M. and J. L. Marsh (2003). "Invertebrate models of neurologic disease: insights into pathogenesis and therapy." Current neurology and neuroscience reports **3**(5): 442-8.

Torres-Aleman, I., S. Pons, et al. (1992). "Survival of Purkinje Cells in Cerebellar Cultures is Increased by Insulin-like Growth Factor I." European Journal of Neuroscience **4**(9): 864-869.

Toru, S., T. Murakoshi, et al. (2000). "Spinocerebellar Ataxia Type 6 Mutation Alters P-type Calcium Channel Function." Journal of Biological Chemistry **275**(15): 10893-10898.

Triarhou, L. C. (2002). Dopaminergic neuron transplantation in the weaver mouse model of Parkinson's disease, Landes Biosciences.

Tropea, D., E. Giacometti, et al. (2009). "Partial reversal of Rett Syndrome-like symptoms in MeCP2 mutant mice." Proceedings of the National Academy of Sciences **106**(6): 2029-2034.

Tsuji, S. (2008). "Genetics of neurodegenerative diseases: insights from high-throughput resequencing." Human Molecular Genetics **19**(R1): R65-R70.

Tsuji, S. and H. Meier (1971). "Evidence for allelism of leaner and tottering in the mouse." Genetics Research **17**(01): 83-88.

Turner, B. J. and K. Talbot (2008). "Transgenics, toxicity and therapeutics in rodent models of mutant SOD1-mediated familial ALS." Progress in Neurobiology **85**(1): 94-134.

Turpaev, K. T. (2002). "Reactive oxygen species and regulation of gene expression." Biochemistry (Mosc). **67**(3).

Urano, A., M. Endoh, et al. (2005). "Infertility with Defective Spermiogenesis in Mice Lacking AF5q31, the Target of Chromosomal Translocation in Human Infant Leukemia." Mol. Cell. Biol. **25**(15): 6834-6845.

Urdinguio, R. G., L. Lopez-Serra, et al. (2008). "*Mecp2*-Null Mice Provide New Neuronal Targets for Rett Syndrome." PLoS ONE **3**(11): e3669.

van de Warrenburg, B. P., J. A. Steijns, et al. (2005). "Falls in degenerative cerebellar ataxias." Movement Disorders **20**(4): 497-500.

van Ham, T. J., K. L. Thijssen, et al. (2008). "<italic>C. elegans</italic> Model Identifies Genetic Modifiers of Î±-Synuclein Inclusion Formation During Aging." PLoS Genet **4**(3): e1000027.

van Nieuwpoort, I. C. and M. L. Drent (2008). "Cognition in the adult with childhood-onset GH deficiency." Eur J Endocrinol **159**(suppl_1): S53-57.

Vanlangenakker, N., T. Vanden Berghe, et al. (2008). "Molecular Mechanisms and Pathophysiology of Necrotic Cell Death." Current Molecular Medicine **8**: 207-220.

Venugopal, R. and A. K. Jaiswal (1996). "Nrf1 and Nrf2 positively and c-Fos and Fra1 negatively regulate the human antioxidant response element-mediated expression of NAD(P)H:quinone oxidoreductase$_1$ gene." Proceedings of the National Academy of Sciences of the United States of America **93**(25): 14960-14965.

Vercherat, C. c., T.-K. Chung, et al. (2009). "Stra13 regulates oxidative stress mediated skeletal muscle degeneration." Human Molecular Genetics **18**(22): 4304-4316.

Vickers, J. C., A. E. King, et al. (2009). "Axonopathy and cytoskeletal disruption in degenerative diseases of the central nervous system." Brain Research Bulletin **80**(4-5): 217-223.

Vielhaber, S., D. Kunz, et al. (2000). "Mitochondrial DNA abnormalities in skeletal muscle of patients with sporadic amyotrophic lateral sclerosis." Brain **123**(7): 1339-1348.

Vig, P. J. S., S. H. Subramony, et al. (2006). "Intranasal administration of IGF-I improves behavior and Purkinje cell pathology in SCA1 mice." Brain Research Bulletin **69**(5): 573-579.

Villalba, M., J. l. Bockaert, et al. (1997). "Concomitant induction of apoptosis and necrosis in cerebellar granule cells following serum and potassium withdrawal." NeuroReport **8**(4): 981-985.

Vogel, T. and P. Gruss (2009). "Expression of Leukaemia associated transcription factor Af9/Mllt3 in the cerebral cortex of the mouse." Gene Expression Patterns **9**(2): 83-93.

Volkert, M. R., N. A. Elliott, et al. (2000). "Functional genomics reveals a family of eukaryotic oxidation protection genes." Proc Natl Acad Sci USA **97**: 14530 - 14535.

Walker, J., L. , Z. Liping, et al. (2002). "Role for alpha6 integrin during lens development: Evidence for signaling through IGF-1R and ERK." Developmental Dynamics **223**(2): 273-284.

Wang, T., U. Lao, et al. (2009). "TOR-mediated autophagy regulates cell death in Drosophila neurodegenerative disease " JCB **186**(5): 703-711.

Wang, V. Y. and H. Y. Zoghbi (2001). "Genetic regulation of cerebellar development." Nat Rev Neurosci **2**(7): 484-491.

Wang, X. and E. K. Michaelis (2006). "Selective neuronal vulnerability to oxidative stress in the brain." Frontiers in Aging Neuroscience **2**: 12.

Wang, X. and E. K. Michaelis (2010). "Selective neuronal vulnerability to oxidative stress in the brain." Frontiers in Aging Neuroscience **2**.

Wang, X., D. J. Tomso, et al. (2007). "Identification of polymorphic antioxidant response elements in the human genome." Human Molecular Genetics **16**(10): 1188-1200.

Wang, X. J., J. D. Hayes, et al. (2007). "Identification of retinoic acid as an inhibitor of transcription factor Nrf2 through activation of retinoic acid receptor alpha." Proceedings of the National Academy of Sciences **104**(49): 19589-19594.

Watase, K., C. F. Barrett, et al. (2008). "Spinocerebellar ataxia type 6 knockin mice develop a progressive neuronal dysfunction with age-dependent accumulation of mutant CaV2.1 channels." Proceedings of the National Academy of Sciences **105**(33): 11987-11992.

Watase, K., J. R. Gatchel, et al. (2007). "Lithium Therapy Improves Neurological Function and Hippocampal Dendritic Arborization in a Spinocerebellar Ataxia Type 1 Mouse Model." PLoS Med **4**(5): e182.

Weisz, C. J., R. S. Raike, et al. (2005). "Potassium Channel Blockers Inhibit the Triggers of Attacks
in the Calcium Channel Mouse Mutant tottering." The Journal of Neuroscience **25**(16): 4141-4145.

Welniak, L. A., R. Sun, et al. (2002). "The role of growth hormone in T-cell development and reconstitution." J Leukoc Biol **71**(3): 381-387.

White, A. R., H. Zheng, et al. (1998). "Survival of Cultured Neurons from Amyloid Precursor Protein Knock-Out Mice against Alzheimer's Amyloid-beta Toxicity and Oxidative Stress." J. Neurosci. **18**(16): 6207-6217.

Wilkins, A., S. Chandra, et al. (2001). "A Role for Oligodendrocyte-Derived IGF-1 in Trophic Support of Cortical Neurons." GLIA **36**: 48-57.

Wills, A. J., N. J. Manning, et al. (2001). "Refsum's disease." QJM **94**(8): 403-406.

Winslow, A. R. and D. C. Rubinsztein (2008). "Autophagy in Neurodegeneration and Development." BBA - Molecular Basis of Disease.

Wu, C. L., C. S. Hwang, et al. (2010). "Neuroprotective mechanisms of brain-derived neurotrophic factor against 3-nitropropionic acid toxicity: therapeutic implications for Huntington's disease." Annals of the New York Academy of Sciences **1201**(1): 8-12.

Wyllie, A. H. (1997). "Apoptosis: an overview." The British Medical Bulletin **53**(3): 451-465.

Xia, H., Q. Mao, et al. (2004). "RNAi suppresses polyglutamine-induced neurodegeneration in a model of spinocerebellar ataxia." Nat Med **10**(8): 816-820.

Xia, W., T. Yang, et al. (2009). "A Specific Enzyme-Linked Immunosorbent Assay for Measuring {beta}-Amyloid Protein Oligomers in Human Plasma and Brain Tissue of Patients With Alzheimer Disease." Arch Neurol **66**(2): 190-199.

Xu, J., N. Zhong, et al. (2005). "The Parkinson's disease-associated DJ-1 protein is a transcriptional co-activator that protects against neuronal apoptosis." Human Molecular Genetics **14**(9): 1231-1241.

Yabe, I., H. Sasaki, et al. (2001). "Clinical trial of acetazolamide in SCA6, with assessment using the Ataxia Rating Scale and body stabilometry." Acta Neurol Scand. **104**(1): 44-7.

Yong, V. W. and S. Rivest (2009). "Taking Advantage of the Systemic Immune System to Cure Brain Diseases." Cell **64**(1): 55-60.

Yu, X., J. Lin, et al. (2006). "Computational analysis of tissue-specific combinatorial gene regulation: predicting interaction between transcription factors in human tissues." Nucleic Acids Research **34**(17): 4925-4936.

Zeviani, M. and S. Di Donato (2004). "Mitochondrial disorders." Brain **127**(10): 2153-2172.

Zhang, L., M. Shimoji, et al. (2005). "Mitochondrial localization of the Parkinson's disease related protein DJ-1: implications for pathogenesis." Human Molecular Genetics **14**(14): 2063-2073.

Zhang, W., X. Xia, et al. (2006). "Dot1a-AF9 Complex Mediates Histone H3 Lys-79 Hypermethylation and Repression of ENaCα in an Aldosterone-sensitive Manner." The journal of biological chemistry **281**: 18059-18068.

Zhong, J., J. Deng, et al. (2005). "Insulin-like growth factor-I protects granule neurons from apoptosis and improves ataxia in weaver mice." J. Neurosci. Res. **80**: 481-490.

Zoghbi, H. Y. and H. T. Orr (2000). "Glutamine Repeats and Neurodegeneration." Annual Review of Neuroscience **23**(1): 217-247.

List of constructs

Name of construct	vector	tag
shRNA human Oxr1 #55074	pLKO.1-puro	
shRNA mouse Oxr1 #170719	pLKO.1-puro	
shRNA Ncoa7 #241622	pLKO.1-puro	
scrambled shRNA	pLKO.1-puro	
shRNA empty-GFP	pLKO.1-puro	_GFP
pCDNA3 empty		
hOxr1 FL-HA	pcDNA3	_HA
hOxr1 S-HA	pcDNA3	_HA
mOxr1 FL-HA	pcDNA3	_HA
mOxr1 S-HA	pcDNA3	_HA
pCX empty		
mOxr1 FL-HA	pCX	_HA
mOxr1 S-HA	pCX	_HA
HA-mOxr1 FL	pCX	HA_
HA-mOxr1 S	pCX	HA_
mOxr1 FL-HA-GFP	pCX	_HA _GFP
mOxr1 S-MYC	pCX	_MYC
mOxr1 FL E773A	pCX	_HA
mOxr1 S E773A	pCX	_HA
mOxr1 FL MLS-HA	pcDNA3	_HA
mOxr1 S MLS-HA	pcDNA3	_HA
pLenti6/V5-D-TOPO empty		
mOxr1 FL-HA	pLenti	_HA
mOxr1 S-HA	pLenti	_HA
pCAGGS-based vector IRES empty		_GFP
mOxr1 FL-HA	IRES	_HA
mOxr1 S-HA	IRES	_HA
mNcoa7 FL-HA	pcDNA3	_HA
mNcoa7 S-HA	pcDNA3	_HA
mNcoa7 FL-HA	pCX	_HA
mNcoa7 S-HA	pCX	_HA
mFUS wt-MYC	pCDNA3	_MYC
mFUS P525L	pCDNA3	_MYC
mFUS R521C	pCDNA3	_MYC
mTDP-43 wt-FLAG	pCDNA3	_3xFLAG
mTDP-43 A371G	pCDNA3	_3xFLAG
mTDP-43 D168G	pCDNA3	_3xFLAG
mTDP-43 Q331H	pCDNA3	_3xFLAG
mTDP-43 H337V	pCDNA3	_3xFLAG
pET22b (+)		

List of antibodies

antibody	manufacturer	species	applications		
			WB	IF	IP
8-oxo-dG 2E2	Trevigen	mouse		✓	
actin	Sigma	rabbit	✓		
BTB/POZ	abcam	rabbit			✓
Calbindin D28k	Swant	rabbit		✓	
CCT2	Cell signaling	rabbit			✓
Cdc2	abcam	rabbit			✓
Cdk4	abcam	rabbit			✓
CDKN2/p19ARF	abcam	rat			✓
Citron	Santa Cruz	mouse			✓
COXIV	abcam	mouse		✓	
DDX3 H114	Santa Cruz	rabbit			✓
Erk1/2	Cell Signaling	rabbit	✓	✓	
EWS C19	Santa Cruz	goat			✓
FLAG M2	Sigma	mouse	✓	✓	✓
FUS	Bethyl	rabbit	✓	✓	✓
GAPDH	abcam	mouse	✓		
HNE	Calbiochem	rabbit		✓	
Hsp40	abcam	rabbit			✓
IGF1	abcam	rabbit	✓	✓	
IGF1R	abcam	rabbit	✓	✓	
Myc 9E10	Sigma	mouse	✓	✓	✓
Myelin Basic Protein	abcam	rat	✓		
Nitro-tyrosine	Cell Signaling	rabbit		✓	
Nrf2	Santa Cruz	rabbit	✓		
P-AKT1/2/3	Santa Cruz	rabbit	✓	✓	
P-IGF1R	abcam	rabbit	✓	✓	✓
P-MAPK	Cell Signaling	rabbit	✓		
P-PKC	abcam	rabbit	✓	✓	
P-SAPK/JNK	Cell Signaling	rabbit	✓		
TARDBP	Proteintech	rabbit	✓	✓	✓

WB : western blot

IF : immuno-fluorescence

IP : immuno-precipitation

Genes deregulated in the *robotic* mouse and confirmed by qRT-PCR

Affy number	Gene	Fold change in *robotic*
	Channels and ion transporters	
1434008_at	**Scn4b**, Sodium channel type IV beta	4.0-4.2 DOWN
1448741_at	**Slc3a1**, Solute carrier family 3 member 1	3.6 UP
1455005_s_at	**Slc5a2**, Solute carrier family 5 member 1	3.6-5.2 UP
1454866_s_at	**Clic6**, Chloride intracellular channel 6	4.1-5.4 DOWN
	Insulin signaling pathway	
1437401_at	**Igf1**, Insulin-like growth factor 1	2.4-2.7 DOWN
1454671_at	**Insig1**, Insulin-induced gene 1	2.1-2.8 UP
1419017_at	**Corin**	4.1-4.5 DOWN
	Calcium signaling pathway	
1458836_at	**Calb1**, Calbindin-28K	2.9-3.0 UP
1419085_at	**Pcp2**, Purkinje cell protein 2 (L7)	2.0-3.4 UP
1450930_at	**Hpca**, Hippocalcin	4.8-5.1 DOWN
1451987_at	**Arrb2**, Arrestin beta 2	2.3-6.9 UP
	Cytosketon organization, biogenesis, and cell adhesion molecules	
1454979_at	**Diap1**, Diaphanous homolog 1	2.7-5.8 UP
1438628_x_at	**Cntn3**, Contactin 3	2.3-2.7 DOWN
	Hormones, neurotransmitters and their release through vesicle synaptic exocytosis	
1428664_at	**Vip**, Vasoactive intestinal polypeptide	8.7 UP
1422756_at	**Slc32a1**, Solute carrier family 32 member 1	2.3-2.5 DOWN
1420418_at	**Syt2**, Synaptotagmin II	2.1-2.2 DOWN
1441165_s_at	**Clstn2**, Calsyntenin 2	2.5-2.9 DOWN
1420667_at	**Doc2b**, Double C2 beta	2.1-3.0 DOWN
1443341_at	**Anxa4**, Annaxin A4	9.1 DOWN
	Transcription factors and chromatin remodeling	
1436600_at	**Tox3**, TOX high mobility group box family member 3	8.4 UP

Fold changes of key genes involved in the OS-response in bella cerebellum and brain compared to wild-type

Genes	Cerebellum	Brain
pgcla	0.73	1.10
nqo1	0.83	1.62
sod2	1.60	1.37
ho1	0.84	1.54
nrf2	0.93	1.52
gclm	1.23	0.56
keap1	1.19	1.08
gclc	0.79	0.97
dj1	1.40	1.29
gfap	1.21	0.92
catalase	1.50	0.36
ant	0.89	0.98
cyt c	1.07	0.85
cullin3	1.06	1.15
sod1	1.15	1.25
sod2	0.94	0.92
gpx	0.51	1.31